

**DELINEATING THE ROLES OF KINESIN AND DYNEIN MOTOR
PROTEINS DURING MITOTIC SPINDLE ASSEMBLY AND FUNCTION
IN THE FUNGAL PATHOGEN *CANDIDA ALBICANS***

by

Irsa Shoukat

A thesis submitted to the Department of Biomedical and Molecular Sciences
in conformity with the requirements for
the degree of Doctor of Philosophy

Queen's University

Kingston, Ontario, Canada

(December 2021)

Copyright ©Irsa Shoukat, 2021

Abstract

During cell division, cells must accurately orchestrate and execute DNA segregation to daughter cells. To do this, eukaryotes assemble a dynamic macromolecular structure called the mitotic spindle, which undergoes a series of conformational changes to attach, orient, and separate sister chromatids. These dynamic events depend on the correct localization and activation of structurally and functionally diverse teams of microtubule-associated motor proteins. Kinesins and dyneins are the main families of motors involved in orienting and moving the microtubule arrays that compose, or are attached to, the mitotic spindle. Many of these motor proteins' roles and molecular mechanisms have been extensively studied in several model systems. These studies have led to the broad perception that some motor functions have been evolutionarily conserved. One example is that bipolar spindle assembly ubiquitously requires kinesin-5 family members and thus these motors are essential for cell viability. However, we discovered that the human fungal pathogen, *Candida albicans*, relies heavily on the kinesin-14 motor, Kar3Cik1, for bipolar spindle assembly, rather than its kinesin-5, Kip1. This suggests that *C. albicans* uses force-producing motors differently than other eukaryotes and even related yeasts.

The studies detailed in this thesis's first two experimental chapters have delineated the roles of Kip1 and dynein (Dyn1) in *C. albicans* mitosis. Chapter 3 demonstrates that cells lacking Kip1 can undergo all mitotic processes, albeit with subpar integrity. Kip1-deficient cells have shorter metaphase spindles and longer and more numerous astral microtubules. Interestingly, Kip1 mutants are delayed in their entry into anaphase but execute anaphase at the same rate as wild-type cells. Furthermore, simultaneous loss of function of Kip1 and Kar3Cik1 is lethal, suggesting that *C. albicans* seems to diverge from the classic force-balance paradigm in maintaining spindle integrity. Chapter 4 provides evidence that Kip1 works collaboratively with Dyn1 in spindle elongation and that either motor can partially compensate for the loss of the other. The final experimental chapter, Chapter 5, investigates the curious phenotype that some spindles in Kip1 mutants disintegrate and form duplicated bipolar spindles within the same cell compartment. Evidence is provided that subsequent division of these spindles leads to the generation of random aneuploidies that can provide a growth advantage compared to wild-type cells when exposed to the antifungal drug fluconazole. Transcriptomic analysis of fluconazole-treated cells showed altered expression patterns of several genes involved in mitosis, including *KIP1*. This finding suggests that *C. albicans* cells may actively regulate mitotic kinesins, like Kip1, under stress to promote spindle errors that foster aneuploidy and act as a driver of adaptive genome plasticity.

Co-Authorship

Corey Frazer was instrumental in the development of *kip1* Δ/Δ mutant strains used in chapter 3. In addition, his methodology and experimental set-up for microscopy was implemented in chapter 3. Lastly, *kar3/cik1* Δ/Δ strains were engineered by him.

Future publication of Chapter 5 would acknowledge Dr. Michele Loewen and Dr. Simon Foote for their help in funding RNA sequencing and processing RNA sequencing data, respectively.

Acknowledgements

As this chapter in my life nears an end, the journey to get here would not have been easy without the support of many individuals. Such is the nature of scholarship; we stand on the backs of so many giants to reach our full potential. Indeed, it is remarkable to reflect that the success in completing a dissertation depends upon a whole array of relationships, support systems, and social networks. The final product, which obscures these background forces and factors, belies the truth: that we are only our best with the help of the people around us.

To my fellow Allingham lab and 6th floor mates – know that your discussions challenged me, your support grounded me, and your friendship balanced me. Because of you, my reach has spilled beyond academia, in hopes to always pursue truth and kindness. I will look back on our time spent together very fondly, especially all the heated (figuratively and literally) office talks and weekend ping pong escapades. Thank you for being such a positive force in my life.

I am also greatly appreciative of my friends who played a myriad of sports with me, experienced Kingston's finest cuisines, and for just being good company over the years. Without you, the last few years would have consisted of long periods of solitary work (with even longer periods of agony and frustration). Thank you for being an escape and a source of fun and laughter in my life.

I have had the extreme fortune of conversing with my brilliant thesis committee scholars. Many thanks to Drs. Andrew Craig and Graham Côté for letting me pursue my intellectual interests. Your mentoring guided this project to where it is, and I am indebted to your efforts in challenging and supporting me. I would also like to thank Dr. Corey Frazer who has been instrumental in my training as a fungal biologist. Corey, if not for you, this project would have never taken off and been as successful.

When I think about all the qualities that make a scientist (and person) admirable, I think of my PhD supervisor, Dr. John Allingham. John, I find it hard to adequately express my gratitude for all your efforts since I have known you (years that soon I will no longer be able count on my fingers). As my supervisor, you constantly set the bar high for each of us, which is a direct reflection of your passion for science and enthusiasm for pursuit of knowledge. Your generous mentorship and ongoing efforts to foster a stimulating and challenging research environment has provided me with foundational skills to think and communicate critically as an academic. And as you radiate academic rigor, scholarly generosity and intellectual depth, it is your personal warmth that continues to astound and inspire me. You have profoundly shaped the person I am today. Although our days of working together may be coming to an end, I am extremely honoured to gain a colleague and friend that shares my passion for all things caffeinated, soul-crushing music (best accompanied with Matt's voice), and the ever-growing obsession with playing racquet sports - a joy that is

worth all the long-term sustained injuries. It has been a privilege to be a part of your life – and a privilege to have and rely on your support as life joyously handed me good times and bitterly coughed out hard realities. Without you, the resilience and patience I now hold would be markedly immature. Know that you grace my life and the pages of this dissertation in immeasurable ways.

Last (though as far from least as one can possibly get), I must give thanks to my parents, brother and best friend. To my partner, my love – Russell, I owe you more than words can express, and more than any metric can measure. Life without you would be infinitely worse, so much so that I dare not contemplate it. To my brother, who is a true scientist, your dedication to academia is so powerfully motivating that I consistently fail to be as assiduous as you. To my Dad, whose patience has no boundaries. You are the rock of our family and your sacrifices (as you uprooted your life to move half-way around the world) to give us better opportunities are forever awe-inspiring and appreciated. And lastly, to my mom, to whom I dedicate this dissertation to. I have no words Mom - if only one day you get to read this and know that without you, I wouldn't have made it this far. Thank you for being a light in my life.

Table of Contents

Abstract.....	ii
Co-Authorship.....	iii
Acknowledgements.....	iv
List of Figures.....	ix
List of Tables.....	x
List of Movies.....	xi
List of Abbreviations.....	xii
Chapter 1 Introduction.....	1
Chapter 2 Literature Review.....	3
2.1 <i>C. albicans</i> as a model system to study mitosis.....	3
2.2 Earlier studies of mitosis.....	4
2.3 Microtubule structure and function.....	7
2.4 The mitotic spindle and the cell cycle in budding yeast.....	9
2.4.1 Kinesin motor proteins.....	14
2.4.2 Kinesin-5 motors.....	16
2.4.3 Kinesin-14 motors.....	21
2.4.4 Force-balance paradigm.....	22
2.4.5 Dynein motor proteins.....	26
2.4.6 Genome plasticity of <i>C. albicans</i>	29
2.4.7 Machinery in the chromosome segregation process in <i>C. albicans</i>	31
2.4.8 Aims of my thesis research.....	33
Chapter 3 Kinesin-5 is dispensable for bipolar spindle formation and elongation in <i>Candida albicans</i> , but simultaneous loss of kinesin-14 activity is lethal.....	35
3.1 Abstract.....	35
3.2 Introduction.....	36
3.3 Results.....	38
3.3.1 Localization of <i>C. albicans</i> Kip1 mirrors other yeast kinesin-5s.....	38
3.3.2 <i>C. albicans</i> forms bipolar spindles without kinesin-5.....	41
3.3.3 A subpopulation of <i>kip1</i> Δ/Δ cells have multiple spindles and show atypical cell cycle dynamics.....	48
3.3.4 Simultaneous loss of Kip1 and Kar3/Cik1 function is lethal.....	52
3.4 Discussion.....	54

3.5 Materials and Methods.....	58
3.5.1 Genetic Manipulations	58
3.5.2 <i>C. albicans</i> Transformation.....	65
3.5.3 <i>C. albicans</i> Cell Culture and Growth Assays.....	65
3.5.4 Light Microscopy.....	66
3.5.5 RNA Sequencing.....	66
Chapter 4 Dynein contributes to spindle elongation during anaphase in <i>Candida albicans</i>	68
4.1 Abstract.....	68
4.2 Introduction.....	69
4.3 Results.....	71
4.3.1 Dynein has overlapping functions with Kip1 in anaphase spindle elongation.....	71
4.3.2 Dynein localization on astral MTs increases in the absence of Kip1.....	73
4.3.3 The duration of anaphase is nearly tripled in <i>dyn1</i> Δ/Δ cells.....	78
4.3.4 MT polymerization forces facilitate <i>C. albicans</i> spindle positioning and elongation.....	81
4.4 Discussion.....	85
4.5 Materials and Methods.....	89
4.5.1 <i>C. albicans</i> Strains and Genetic Manipulations	89
4.5.2 <i>C. albicans</i> Transformation.....	93
4.5.3 <i>C. albicans</i> Growth Media and Chemical Reagents	93
4.5.4 Microscopic Imaging of Spindle and Nuclear Morphologies and Motor Localization	93
Chapter 5 <i>Candida albicans</i> may actively downregulate spindle-associated kinesins to promote aneuploidy as part of a stress adaptation mechanism.....	95
5.1 Abstract.....	95
5.2 Introduction.....	96
5.3 Results.....	98
5.3.1 <i>kip1</i> Δ/Δ mutants are less sensitive to FLC exposure compared to wild type	98
5.3.2 <i>kip1</i> Δ/Δ cell population is genetically heterogeneous.	102
5.3.3 Absence of Kip1 readily generates non-specific aneuploidies.....	104
5.3.4 Wild-type cells treated with FLC downregulate motor protein gene expression.....	109
5.3.5 Addition of FLC alters expression levels of many spindle-related proteins	112
5.3.6 <i>kip1</i> Δ/Δ mutants exhibit similar gene expression changes for spindle proteins as FLC-treated wild-type cells.....	115
5.4 Discussion.....	118
5.5 Materials and Methods.....	123

5.5.1 <i>C. albicans</i> Cell Culture and Growth Assays.....	123
5.5.2 Light Microscopy.....	125
5.5.3 Flow Cytometry	125
5.5.4 qPCR Ploidy Assay.....	126
5.5.5 RNA Sequencing.....	126
Chapter 6 General Discussion and Future Directions.....	128
6.1 <i>C. albicans</i> as a model system for studying mitotic motors	128
6.2 An apparent lack of force-balance	128
6.3 Kip1 and Dyn1 collaborate in spindle elongation.....	131
6.4 Can tuning motor activity induce tetraploidy?.....	133
6.5 Future studies to delineate the links between cell stress and spindle motor regulation	136
6.6 Significance of this research	137

List of Figures

Figure 2-1. Early drawings of mitotic events.....	6
Figure 2-2. MTs exhibit dynamic instability.	8
Figure 2-3. Spindle pole body embedded into the nuclear membrane.....	10
Figure 2-4. Budding yeast cell cycle.....	13
Figure 2-5. The mechanochemical cycle of processive and non-processive kinesins.	18
Figure 2-6. Kinesin-5 functions on MTs.....	20
Figure 2-7. Kinesin-14 and kinesin-5 motors crosslinking MTs.	24
Figure 2-8. Dynein function in budding yeast mitosis.	28
Figure 3-1. Kip1 exhibits similar localization to other kinesin-5s during the cell cycle.	40
Figure 3-2. Loss of Kip1 affects growth and viability.	43
Figure 3-3. <i>kip1</i> Δ/Δ cells form bipolar spindles but exhibit defects in spindle dynamics.	45
Figure 3-4. <i>kip1</i> Δ/Δ cells have longer and more numerous cytoplasmic MTs.	47
Figure 3-5. <i>kip1</i> Δ/Δ cells have abnormal number of spindles and SPBs.	49
Figure 3-6. A subpopulation of Kip1-inhibited cells display abnormal nuclear division.	51
Figure 3-7. Loss of kinesin-5 and kinesin-14 function is lethal.....	53
Figure 4-1. Simultaneous loss of Dyn1 and Kip1 function is lethal.	74
Figure 4-2. Dyn1 localization and abundance increases when Kip1 function is lost or inhibited.	77
Figure 4-3. Dyn1 mutants exhibit unusual anaphase dynamics.	79
Figure 4-4. <i>dyn1</i> Δ/Δ cells have longer and more numerous aMTs.....	83
Figure 5-1. <i>kip1</i> Δ/Δ mutants survive better in the presence of FLC compared to wild type.	101
Figure 5-2. Flow Cytometry analysis of <i>kip1</i> Δ/Δ mutants demonstrates aneuploid peaks.	103
Figure 5-3. Kip1 mutants exhibit non-specific aneuploidies.	108
Figure 5-4. Differential gene expression profiles of wild-type cells treated with FLC.	111
Figure 5-5. Differential gene expression profiles of wild-type cells vs <i>kip1</i> Δ/Δ	116
Figure 6-1. Hyphal defects in <i>kip1</i> Δ/Δ mutants.	134

List of Tables

Table 2-1. Specific functions of yeast kinesin-5 and -14 motors.....	25
Table 3-1. Names, genotypes, mating types, and sources of the strains used in this study	62
Table 3-2. Oligonucleotide primers used in strain construction	63
Table 4-1. Names, genotypes, mating types, and sources of the strains used in this study	91
Table 4-2. Oligonucleotide primers used in strain construction	92
Table 5-1. Downregulated genes related to spindle function when FLC is added to wild-type <i>C. albicans</i> cells	114
Table 5-2. Downregulated spindle component genes in <i>kip1</i> Δ/Δ	117
Table 5-3. Names, genotypes, mating types, and sources of the strains used in this study	124

List of Movies

Movie S1. Time-lapse of *kip1* Δ/Δ mutants exhibiting two fluorescent bars in one cell compartment.

Movie S2. Time-lapse of wild type cells exhibiting normal spindle and nuclear dynamics.

Movie S3. Time-lapse of ABT-treated wild type cells exhibiting aberrant spindle and nuclear dynamics.

List of Abbreviations

ABT	1-aminobenzotriazol
ADP	Adenosine Di-Phosphate
aMT	Astral Microtubule
APC/C	Anaphase Promoting Complex/Cyclosome
ARG	Arginine
ATP	Adenosine Tri-Phosphate
BF	Brightfield
BH	Benjamini and Hochberg Method
CGD	Candida Genome Database
CPC	Chromosomal Passenger Complex
DAPI	4',6-diamidino-2-phenylindole
DNA	Deoxyribonucleic Acid
DOX	Doxycycline
FBS	Fetal Bovine Serum
FLC	Fluconazole
GAL	Galactose
GDP	Guanosine Di-Phosphate
GFP	Green Fluorescent Protein
GO	Gene Ontology
GTP	Guanosine Tri-Phosphate
HIS	Histidine
i(5L)	Isochromosome of Left Arm of Chromosome 5
ipMT	Interpolar Microtubule
kMT	Kinetochore Microtubule
LEU	Leucine
LiAc	Lithium Acetate
MAL	Maltose
MAP	Microtubule-Associated Protein
MEN	Mitotic Exit Network
MT	Microtubule
MTL	Mating-Type Locus
NA	Numerical Aperture
NOC	Nocodazole
OD	Optical Density
ORF	Open Reading Frame
PBS	Phosphate Buffered Saline
PCR	Polymerase Chain Reaction
PEG	Polyethylene Glycol
RNA	Ribonucleic acid
SAC	Spindle Assembly Checkpoint
SAT1	Resistance gene for ClonNAT Nourseothricin
S.D.	Standard Deviation
SD	Synthetic Dropout
SDC	Supplemented Dropout Media (Complete)
SEM	Standard Error of the Mean
SPB	Spindle Pole Body
TAP	Tandem Affinity Purification

TET
TIRF
WGD
YPD
YPM
 γ -TuRC

Tetracycline
Total Internal Reflection Fluorescence
Whole Genome Duplication
Yeast Extract Peptone Dextrose
Yeast Extract Peptone Maltose
 γ -tubulin Ring Complex

Chapter 1

Introduction

“All things begin in order, so shall they end, and so shall they begin again; according to the ordainer of order and mystical mathematics of the city of heaven.” - Sir Thomas Browne, 1658.

For a cell to proliferate, it must duplicate and segregate its genetic material accurately and efficiently. Eukaryotes assemble a dynamic macromolecular machine composed of a self-assembling array of parallel and antiparallel microtubules (MTs), called a mitotic spindle, to accomplish this. As the spindle forms, it attaches and orients the cell's chromosomes in the cell midzone and then changes its structure again to segregate the sister chromatids into two daughter nuclei before cell division. The complexity of the spindle, along with the regulation of its various transitions during mitosis, can vary greatly depending on the organism, but many key elements are conserved across species. Spindle MTs are nucleated from two MT-organizing centres and arranged in a bipolar array in all eukaryotes. As cells transition through each phase of the mitotic cycle, MT-associated motor proteins help restructure these MT arrays into new configurations by converting energy from ATP binding and hydrolysis into mechanical forces that can move chromosomes. Mis-regulation of spindle restructuring can lead to chromosome segregation errors (e.g., aneuploidy), which can have severe consequences, including cell death, congenital disabilities, and cancer in higher eukaryotes. However, sometimes errors in mitotic spindle function can facilitate survival as specific aneuploidies can increase fitness. This has been observed in cancer cells and fungal pathogens, like *Candida albicans*, which leverage mistakes in

mitosis to facilitate cell survival under stressful growth environments like exposure to antifungal drugs. Therefore, gaining a better understanding of mitosis and the players that regulate mitotic spindle function is crucial. The work presented in this thesis aims to delineate the roles of mitotic motor proteins in chromosome segregation in *C. albicans*. This introduction briefly reviews the events of mitosis in the related budding yeast, *Saccharomyces cerevisiae*, the molecular machinery involved in separating chromosomes, and the causes and consequences of chromosome missegregation in the context of a fungal pathogen.

Chapter 2

Literature Review

2.1 *C. albicans* as a model system to study mitosis

Candida species inhabit environmental, human, and other mammalian sources[1]. In mammals, they are part of the microbial flora of the gastrointestinal and genitourinary tracts[2]. These mucosal surfaces are an important niche in the lifecycle of *Candida* species because the physical environment in this reservoir has optimal pH, oxygen levels, and nutrient levels[3]. There are only a small number of *Candida* species that are clinically important in humans. These include *Candida albicans*, *Candida auris*, *Candida glabrata*, *Candida tropicalis*, *Candida parapsilosis* and *Candida krusei*[1]. *C. albicans* is presently the most prevalent cause of human fungal infections. It can cause life-threatening complications in immunocompromised patients, including cancer patients, organ transplant recipients, individuals infected with HIV, and the elderly population. In healthy individuals, milder, superficial infections of the skin and mucosal membranes are more common and are often more persistent when the host microbiota is suppressed, for example after antibiotic use[4, 5]. To further exacerbate infection, *C. albicans* can also form debilitating biofilms on implanted medical devices, including, but not limited to, dental implants, catheters, heart valves, and artificial joints[6]. The main challenge in treating these infections is that *C. albicans* and other fungal pathogens share many biological processes with humans, and this greatly limits the ability to synthesize antifungals that lack human toxicity. It is thus an important goal to understand the biology of these opportunistic pathogens in order to identify new drug targets that will lead to better therapeutic outcomes.

Rapid advances in understanding *C. albicans* has been made possible by its similarity to the well-studied budding yeast, *Saccharomyces cerevisiae*, which diverged from *C. albicans* over 800 million years ago[7]. Although more than 80% of genes are similar in these distant cousins, and many fundamental biological processes are conserved, numerous other cellular mechanisms in *C. albicans* are still unknown. Fortunately, the completion of the genome sequence of *C. albicans* in 2004 made it possible to expand research in this pathogen[8]. Over the last two decades, substantial advances have been made in understanding *C. albicans* pathogenicity, genome structure and dynamics, the pattern of gene expression, drug resistance, biofilm formation, and host-parasite interactions[9]. Moreover, studies have highlighted that *C. albicans* genome displays a very high degree of plasticity, including gross chromosomal rearrangements, aneuploidy, and loss of heterozygosity[10-12]. Such differences aid in survival, growth and dissemination in their mammalian hosts and are less readily studied using *S. cerevisiae*[9]. The work in this thesis hopes to contribute to the growing knowledge of these abilities in *C. albicans* by studying its mitosis and mitotic motor proteins.

2.2 Earlier studies of mitosis

Initial work on mitosis began in 1870 by Friedrich Schneider, Eduard Strasburger, and Eduard Van Benedin, who looked at the structures and positions of chromosomes. These scientists concluded that “all cells come from cells” (**Figure 2-1**)[13-15]. At that time (1823), it was only possible to observe whole, fixed cells due to the difficulty in isolating dividing nuclei and the limited resolution (~ 1 μm) of achromatic lenses. The subsequent introduction of oil immersion lenses in 1878 further increased the resolution to 0.2 μm and allowed for more detailed sketches of mitosis. Around this time, Waław

Mayzel gave the first verbal description of the events of mitosis from live salamander larvae epidermal cells, which were later hand-drawn by Walther Flemming[16, 17]. These remarkably accurate drawings were the best early descriptions of the chronology of chromosome behaviour.

Although chromosomes were considered storage devices of genetic information as early as 1885 by August Weismann[18], there was no knowledge about the relationship between the thick (chromosomes) and thin (spindle) fibers that were seen in the fixed material of the nucleus. This was because spindle fibers were not observed in living cells, primarily due to the limitation in stains used to visualize cell components. In 1896, it was speculated that mitotic fibers existed when Lauterborn observed them in live diatom cells[19], however, it was not until the introduction of electron microscopy in 1950 that this was finally confirmed[20, 21]. The nuclear “fibers” in amoeba cells appeared as bundles of thinner fibers 15 nm wide and appeared tubular. Advances in fixative technologies for electron microscopy showed that these “microtubules” seemed to attach to specialized points at chromosome constriction sites[22]. As a result, the spindle's structural characterization was considered an organized assembly of MTs that somehow exerted forces on chromosomes. Since then, this model has served as the framework for almost all mitosis studies in eukaryotes[23].

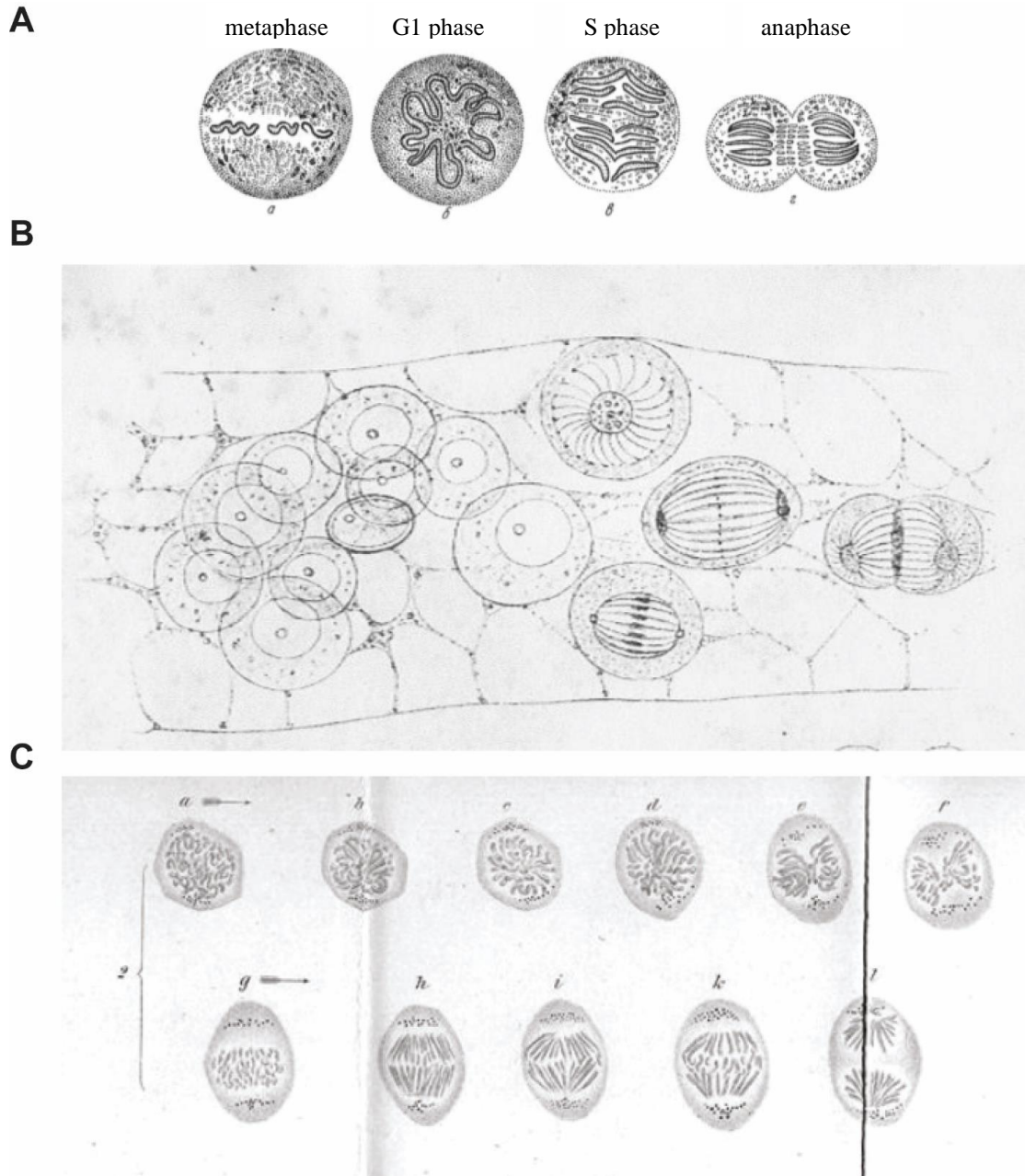


Figure 2-1. Early drawings of mitotic events. (A) Hand drawing by Schneider (1873) illustrating dividing nuclei. B. Drawing by van Benedin (1876) illustrating structures at the spindle poles of dividing cells. C. Drawing by Flemming (1878) illustrating chromosome segregation in living epidermal cells of a salamander larva[18].

2.3 Microtubule structure and function

There are two intrinsic properties of MTs that are important for the function of the spindle: their structural polarity and their intrinsic dynamic behavior. Their structural polarity is defined by the head-to-tail arrangement of α/β tubulin heterodimers in each of their thirteen protofilaments. These tubulin protofilaments associate laterally in a slightly staggered manner to form a helical tube that is flexible yet sturdy enough to be resistant to many of the physical forces that occur against or within cells[24]. Since the α/β tubulin heterodimers in each of the protofilaments have the same orientation, β -tubulin is exposed at one end of the MT, which is known as the “plus” end, while α -tubulin is at the opposite end, also known as the “minus” end. These differences in MT ends can be distinguished by MT-associated proteins (MAPs) so that they can function in different cellular locations according to the location of the plus and minus end of the MT. The polar structure of MTs is also intimately connected to their dynamic behaviour (**Figure 2-2**). Cellular MTs exhibit alternating periods of rapid growth and shrinkage, a process called dynamic instability[25]. The plus-end is typically the fast-growing end, while the minus-end is slower growing. Spontaneous nucleation of MT filaments does not occur readily because the assembly of α/β tubulin subunits to make short MT polymers is energetically unfavourable, and those that do form tend to disassemble quickly. To overcome this, cells use a pre-existing MT nucleation protein known as the γ -tubulin ring complex (γ -TuRC), which facilitates MT assembly at the minus-end[26]. γ -TuRC complexes are concentrated in organelles known as the centrosome or spindle pole body (SPB), which act as MT-organizing centers during cell division and serve as a cap for the MT minus-end[27]. As a result, the plus-end is the primary site of rapid MT assembly/disassembly control in the cell.

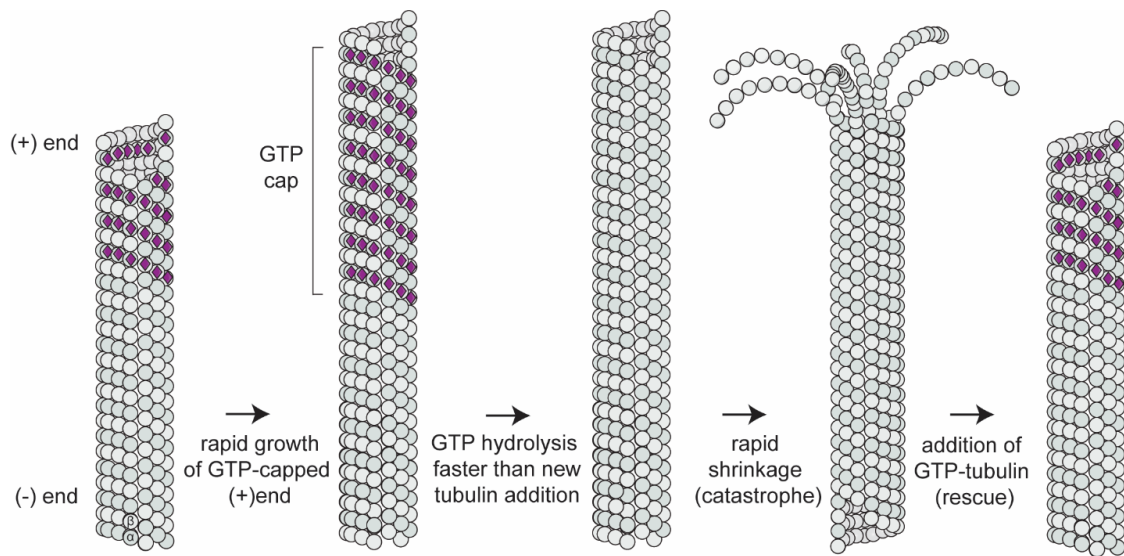


Figure 2-2. MTs exhibit dynamic instability. MTs are composed of polymers of $\alpha\beta$ -tubulin heterodimers. These polymers rapidly switch between phases of growth and shrinkage at the plus-ends due to the faster rate of subunit addition and GTP hydrolysis at this end compared to the minus end. Rapid MT growth occurs when GTP-bound tubulin dimers are added at a higher rate than GTP is hydrolyzed by the tubulins embedded in the MT lattice. This can lead to formation of a stable GTP-tubulin cap that prevents MT shortening. As tubulin subunits within the MT plus-end undergo GTP hydrolysis, the GTP-tubulin cap is lost because the resulting GDP-tubulin dimers form weaker MT lattice contacts and dissociate from the plus end. This change can produce a switch from rapid MT growth to rapid shrinkage. GTPs are purple diamonds. Figure adapted from The Cell Cycle[28].

2.4 The mitotic spindle and the cell cycle in budding yeast

Simpler eukaryotes such as budding yeasts have been ideal model organisms for studies of the function and regulation of the mitotic spindle, primarily because most of the proteins are conserved throughout metazoans. Additionally, budding yeast have the advantage of having a relatively simple and small spindle. A notable difference between yeasts and higher eukaryotes is that yeast undergo a closed mitosis, where the nucleus stays intact for the duration of mitosis and the SPB is embedded into the nuclear membrane. SPBs are a collection of approximately seventeen proteins that come together in layers (inner, central and outer plaques) that face both the nucleus and the cytoplasm (**Figure 2-3**)[29]. In early G1 phase, a satellite structure, a miniature version of the SPB, is assembled on the distal end of the cytoplasmic side of the central layer[30]. The satellite grows until it reaches maturity and can be separated from the original SPB. There are three types of MTs that are nucleated from SPBs: kinetochore MTs (kMTs), interpolar MTs (ipMTs) and cytoplasmic/astral MTs (aMTs)[31]. The cytoplasmic face of SPBs nucleates aMTs that extend towards the cell cortex to position the spindle. The nuclear face nucleates both ipMTs and kMTs (spindle MTs). In *C. albicans*, each SPB can nucleate two ipMTs which interdigitate with the ipMTs from the opposite SPB at the spindle midzone and provide structural integrity to the spindle[32, 33]. kMTs extend within the nucleus to attach kinetochores of sister chromatids, with one kMT per centromere (for a total of approximately thirty-two kMTs to couple all eight diploid chromosomes in *C. albicans*[33, 34]). The simplicity of such a spindle makes yeast like *C. albicans* an excellent system for studies of MT regulation in the cell cycle.

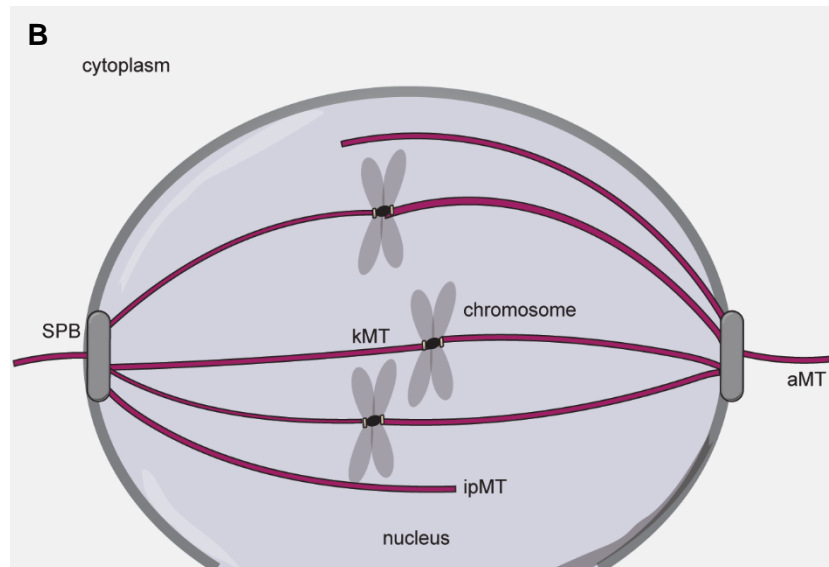
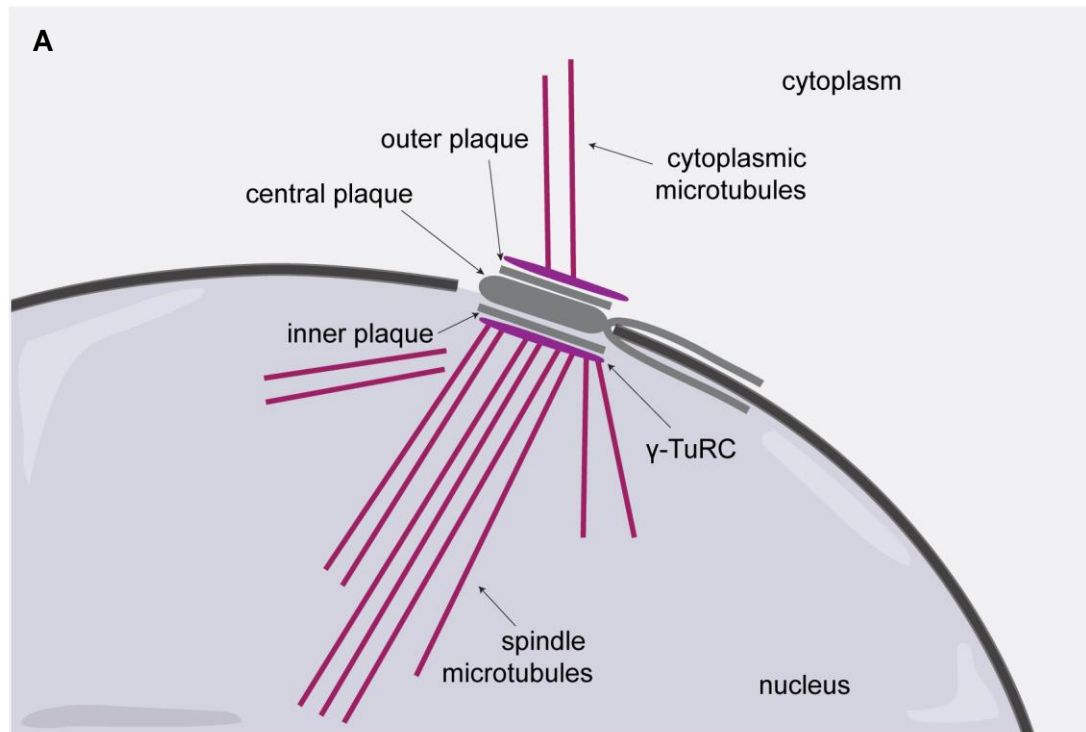


Figure 2-3. Spindle pole body embedded into the nuclear membrane. (A) The SPB is composed of three layers (plaques) where the inner and outer layers (plaques) nucleate MTs. (B) Cartoon representation of the mitotic spindle (not drawn to scale regarding number of chromosomes and MTs in *C. albicans*). Following mitotic spindle formation, three types of MTs emanate from the SPB: aMTs outside of the nucleus, kMTs attached to kinetochores of sister chromatids, ipMTs at the spindle midzone.

As its name suggests, budding yeast divide asymmetrically by forming a small round daughter cell that grows and separates from the larger mother cell, leaving each with one complete copy of the genome (**Figure 2-4**). At the end of the G1 period, the START checkpoint (also known as the G1-phase checkpoint) defines the entry into the cell cycle[35]. Bud emergence happens as the cell passes START and is coordinated with DNA replication and SPB duplication. At this point, each SPB has both a set of nuclear and astral MTs and begins preparations for mitosis by assembling the mitotic spindle - an indication that the cell is committed to dividing. Detection of DNA damage or inappropriate cell size will trigger the G1 checkpoint and induce cell cycle arrest before proceeding to START. After SPB duplication, the adjacent SPBs are pushed apart to form a bipolar spindle. As the spindle assembles and grows, the cell proceeds to G2/M, where kMTs undergo rapid cycles of growth and shrinkage to capture kinetochores and achieve kinetochore biorientation (i.e., each kinetochore from a sister chromatid is attached to a SPB)[36]. The *C. albicans* metaphase spindle has a length of $\sim 0.8 \mu\text{m}$ [33]. Also at this time, the nucleus is positioned and oriented toward the neck between the mother and bud compartments[37, 38]. A second checkpoint called “spindle assembly checkpoint” (SAC) monitors the assembly of the mitotic spindle including attachment and biorientation of kinetochores[35]. Budding yeast also possess a spindle alignment checkpoint, which blocks anaphase if the daughter nucleus is not properly positioned near or into the bud compartment, and a morphogenetic checkpoint that blocks mitosis if the bud is not properly formed[35]. As the cell progresses through mitosis, the daughter bud grows until it is slightly smaller than the mother cell. As such, bud size can be a useful indicator of cell cycle position[28].

In the final events of mitosis, the metaphase-to-anaphase transition marks the last major checkpoint and initiates a signaling cascade that activates the anaphase-promoting complex (APC). APC causes proteolytic destruction of proteins that hold sister chromatids together leading to stretching of the nucleus and elongation of the spindle to partition a set of chromosomes to each cell compartment[39, 40]. Lastly, exit from mitosis requires essential GTP-dependent kinases that initiate a signaling cascade to induce spindle disassembly, in which MT-stabilizing proteins detach from the spindle and MT-destabilizing proteins are activated to break the spindle at the midzone and promote shrinkage of the spindle halves[41, 42]. The actomyosin ring is assembled at the mother-bud neck and cytokinesis begins, physically separating the mother and daughter cells, paving way for both cells to initiate a new cell cycle.

All mitotic events require physical movements of spindle and nuclear material. Molecular motors are the main drivers of mitotic spindle restructuring and chromosome movement[43]. As such, much effort has been put toward understanding the roles of molecular motors in these processes. However, most of these studies come from model systems where mitosis is tightly regulated, and any errors in mitosis lead to cell arrest or even cell death. In recent years, emerging studies have implicated molecular motors as contributors to mitotic errors that appear in some cancer cells[44-48]. In fact, almost all mitotic motor families have been linked to tumor growth, and it has been shown that the expression levels of several motors are altered in many cancers[49].

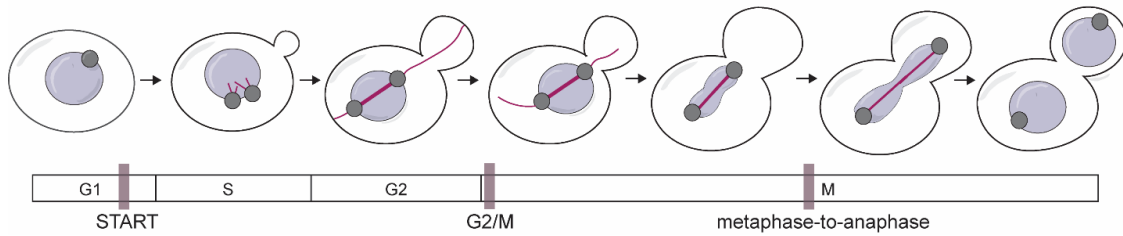


Figure 2-4. Budding yeast cell cycle. The cartoon shows a schematic of how a budding yeast cell progresses through the cell cycle and how the mitotic spindle looks like at each stage. The SPB is in grey, the nuclear envelope in purple, and the MTs are pink. Mitosis starts at G1 when the SPB duplicates and occurs during bud emergence. During S phase the SPBs start to separate to form a bipolar spindle and the DNA duplicates (not shown). During G2/M phase the spindle has reached a length of 0.8 μm . Following spindle assembly, the nucleus is oriented at the mother-bud junction. Chromosomes are then segregated and is followed by spindle disassembly.

The goal of my PhD thesis is to expand the knowledge on these motors, and to understand the mechanistic basis in which they may be involved in mitotic errors that lead to genome rearrangements. With this goal in mind, I focused on the human fungal pathogen *Candida albicans*. This budding yeast has a simple and small mitotic spindle, with a small complement of molecular motors in its genome. It also readily experiences chromosome segregation errors when faced with adversity, such as antifungal drugs. These attributes make *C. albicans* an excellent model system to study the roles of motors that mediate spindle assembly and chromosome segregation.

2.4.1 Kinesin motor proteins

Kinesins were first discovered thirty-five years ago as MT-based anterograde proteins from the axonal cytoplasmic extract from a giant squid[50]. Currently, the repertoire of the kinesin superfamily can be branched into fourteen subfamilies based on sequence, structure, and function[51, 52]. Aside from mitosis (and meiosis), kinesin motors are important in vesicle and organelle transport and flagellar and ciliary movement. The human genome encodes 45 kinesin genes from all 14 families, each of which have specialized functions. Fungi, however, only carry a subset (six in *C. albicans*) of these kinesin family members, including four mitotic motors from the kinesin-5, 7, 8, -14 families. Motors from the kinesin-5 and -14 family have particularly important roles in spindle assembly, maintenance, and elongation.

Kinesin motors typically contain four domains: a conserved motor domain, a ~12-residue neck linker, a less conserved α -helical coiled-coil region, and a tail domain with varying protein binding motifs[53] (**Figure 2-5**). The degree to which kinesins differ is due to the rearrangement of these four domains, and their ability to incorporate additional

domains/motifs. The relative position of the motor domain in the polypeptide sequence has been used previously to categorize these motors. Motors with motor domains on the N-terminal are usually MT plus-end directed, while C-terminal motors are MT minus-end directed. The function of kinesins with a motor domain located in the middle of the peptide sequence seems to be limited to MT-depolymerization[52].

The motor domain couples ATP binding and hydrolysis in its active site to generate movement along MT filaments. The hydrolysis state of ATP (ATP, ADP-Pi, ADP, or no nucleotide) determines the conformational change that re-orientates the neck-linker to generate motor domain movement and regulates MT affinity[54]. The α -helical coiled-coil region serves as a rigid linker between the motor domain, neck linker and the tail domain, and is also important for motor dimerization via coiled-coil formation. Dimerization coupled with allosteric communication between the two motor heads allows for processive movement along the MT track. Depending on the function of the kinesin, the degree of processivity can range by multiple orders of magnitude and can hydrolyze between 80-600 ATP molecules before dissociating from the MT[55]. Post-translational modifications, such as phosphorylation and acetylation, and modulation of other physical parameters can heavily influence kinesin activity[56].

One model of kinesin processivity is the asymmetric hand-over-hand “stepping” mechanism where both motor domains of dimeric kinesins coordinate their ATP activity and MT interactions such that one motor domain is always attached to the MT (**Figure 2-5A**). A “step” occurs when the “front motor head” is attached to the MT filament and binds ATP (**Figure 2-5A state 3**). This causes its neck linker to zipper against the side of the motor head, which in turn propels the “rear motor head” past the ATP-bound head and

toward the next MT binding site (**Figure 2-5A, state 4**). When ATP hydrolysis is completed and Pi is released, the former rear head binds tightly to the MT and becomes the new front motor head (**Figure 2-5A, state 2**)[57]. In this model, one motor is always bound to the MT because the rate of binding of the “free” motor head is simply much faster than the rate of release of the “bound” motor head[55]. In contrast, non-processive kinesins dissociate from the MT after just a few steps and use a powerstroke motion of their neck region to propel forward (**Figure 2-5B**)[58, 59].

2.4.2 Kinesin-5 motors

Kinesin-5 motors are conserved from fungi to humans. One of their defining characteristics is that they form bipolar homotetramers in which the two pairs of motor domains are oriented toward opposite ends of the molecule (**Figure 2-6A**). This structural organization allows one kinesin-5 complex to crosslink and simultaneously step along two adjacent MTs[60, 61]. When these MTs are in an antiparallel configuration, the plus-end directed motility of each motor pair results in bidirectional MT sliding. In most eukaryotes, kinesin-5 motors use that ability to help assemble the mitotic spindle. Briefly, during spindle assembly, kinesin-5 motors can crosslink MTs from adjacent SPBs, and by simultaneously walking on each MT, can generate force to facilitate SPB biorientation (**Figure 2-6B**). *In vitro* assays have shown that *Xenopus laevis* kinesin-5, Eg5, can crosslink antiparallel MTs to slide minus-ends away from one another following SPB duplication. Here, the observable sliding rate of Eg5 was $\sim 40 \text{ nms}^{-1}$; equivalent to spindle pole separation rates *in vivo*[62, 63]. It is therefore not surprising that loss or inhibition of kinesin-5 in these species prevents SPB separation, subsequently leading to cell death. Addition of monastrol, a kinesin-5 specific inhibitor, to *Xenopus* metaphase spindles prompted rapid centrosome

(SPB-equivalent in higher eukaryotes) collapse into monopoles[64, 65]. In *Drosophila melanogaster* embryos, injection of anti-kinesin-5 (KLP61F) antibodies resulted in collapsed monopoles and cells that failed to progress past metaphase[66]. Similarly, inhibition of kinesin-5 motors, Kip1 and Cin8, in *S. cerevisiae* resulted in rapid collapse of metaphase spindles where the previously separated SPBs were drawn back together[67-69]. Indeed, kinesin-5 motors have been investigated for many years in different systems and all have arrived at the same conclusion about motor function in spindle assembly[70-74]. However, in more recent years, studies in yeast have highlighted novel facets of this motor that may imply additional kinesin-5 functions during mitosis. In both budding and fission yeast, for example, kinesin-5 motors (*ScCin8*, *ScKip1* and *SpCut7*) contribute outward forces needed for spindle elongation during anaphase. Here, kinesin-5s crosslink and slide the antiparallel ends of ipMTs at the spindle midzone, increasing the spindle pole-to-pole distance in anaphase [75, 76]. In *S. cerevisiae*, the MT sliding and plus-end directed motility of Kip1 elongate the spindle up to five times its initial length[77, 78].

Interestingly, there are some exceptions to the essentiality of kinesin-5 motors. In *Caenorhabditis elegans*, *Physcomitrella patens*, and *Dictyostelium discoideum*, kinesin-5 activity acts as a braking mechanism to restrict spindle elongation [79-81]. For example, deletion of the kinesin-5 homolog in *D. discoideum* results in faster spindle elongation and premature separation of chromosomes[81]. It is apparent that these motors ubiquitously crosslink antiparallel MTs to elicit forces within the spindle. Therefore, it is surprising that kinesin-5s are often enriched near the spindle poles where most of the MTs are parallel[82-84]. A possible explanation is that role of kinesin-5 here is to contribute to SPB separation by increasing the probability that antiparallel MTs interact.

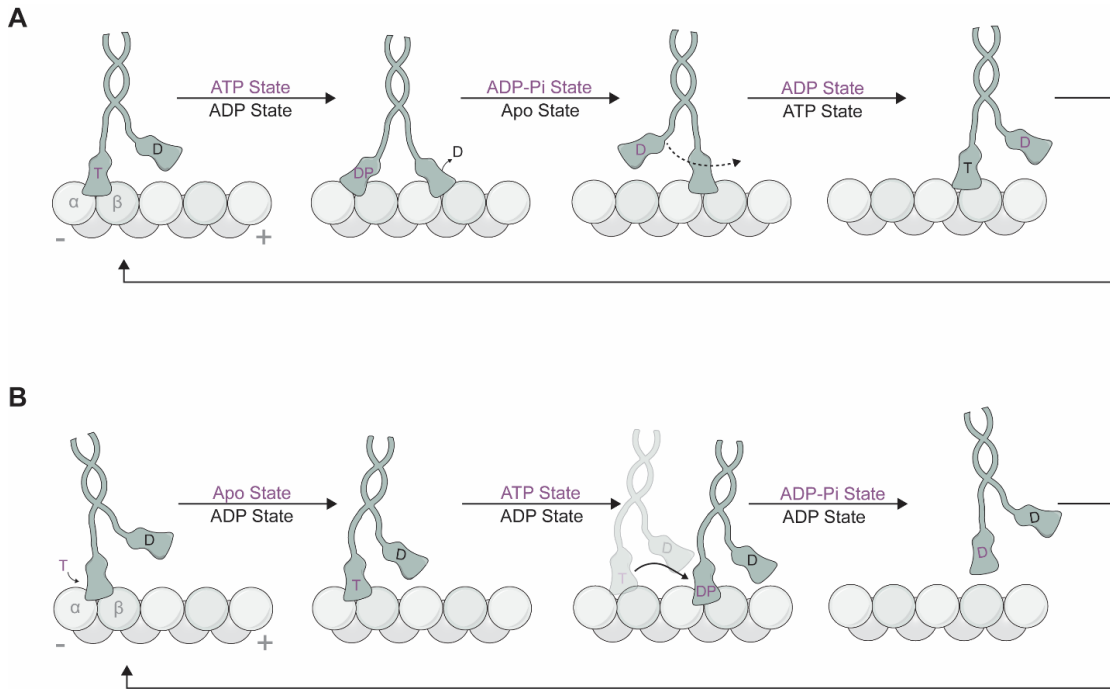


Figure 2-5. The mechanochemical cycle of processive and non-processive kinesins.

(A) The ATP-like state has high affinity for MTs while the ADP state has low affinity for MTs. As the ATP is hydrolyzed, the motor head takes a 8 nm step to become the new leading motor (B) The powerstroke cycle of a non-processive motor. In the ADP state, the neck is oriented toward the MT plus-end. In the ATP state, the neck rotates towards the MT minus-end, producing a powerstroke and displacement on the MT track.

Before a spindle is bipolar, the duplicated SPBs are adjacent to each other and nucleate MTs. MTs from each SPB can interdigitate and form antiparallel overlaps. Crosslinking motors, including kinesin-5 motors, can crosslink these antiparallel MTs. As they slide antiparallel MTs, they push apart adjacent SPBs into a bipolar array. An alternative explanation is that kinesin-5 contributes to MT cohesion/focusing at the spindle poles via parallel MT crosslinking[76, 85, 86]. In support of this type of activity, it has been shown that the *S. cerevisiae* kinesin-5 Cin8, can crosslink parallel kMTs, creating bundles that help establish and maintain spindle length[87].

These findings raise the question of how a plus-end directed motor becomes enriched near the spindle poles, where the MT minus ends reside. In *X. laevis* and mammalian cells, kinesin-5 is transported by minus-end directed dynein[88, 89]. In budding and fission yeast, several groups recently made the surprising discovery that some kinesin-5s exhibit bidirectional motility[90-94]. How this occurs mechanistically is not fully understood but seems to be related to differences in motor concentration. *In vitro* microscopy assays involving purified kinesin-5 motors and MTs show that individual motors move fast towards the minus end, whereas groups of motors move slowly in the plus-end direction[90, 92-95]. Changes in the ionic strength of these *in vitro* motility experiments also affected the directionality. At high salt concentration (close to physiological 200-300 mM NaCl), motors moved towards the minus-end, but as ionic strength was lowered, directionality switched to the plus-end[92-95]. This effect may be due to the strong impact ionic strength can have on the affinity with which motors interact with the MT[63, 93, 96, 97]. Further studies have shown that when motors engaged

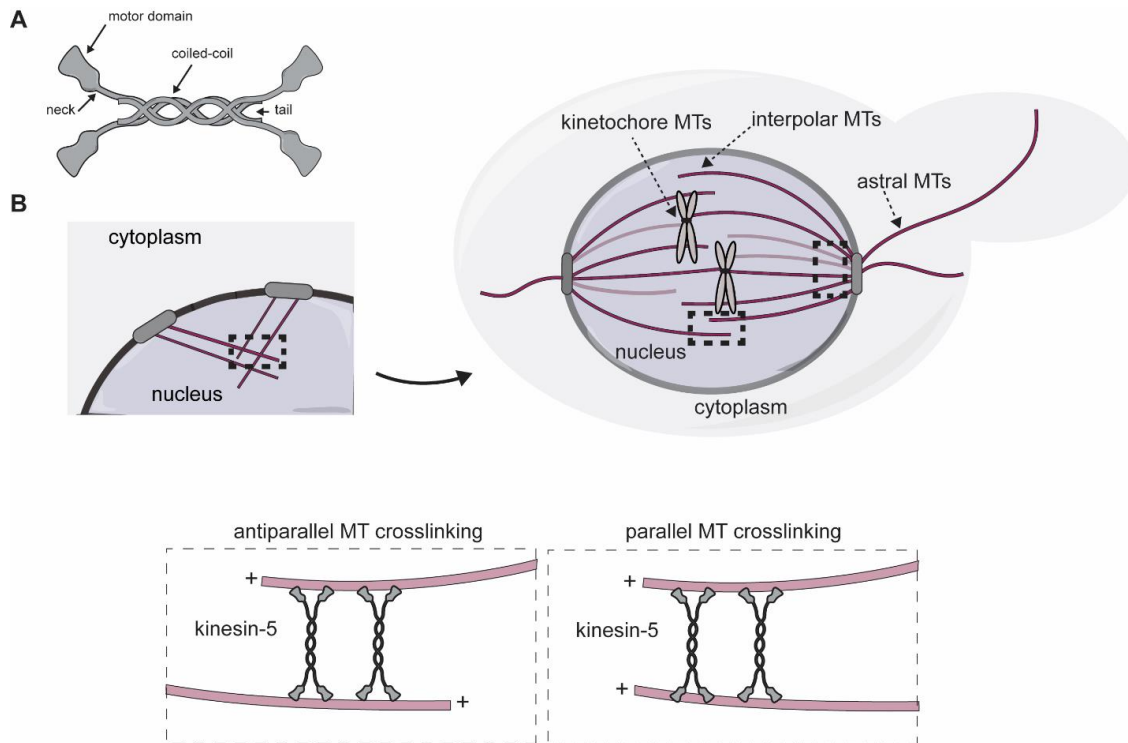


Figure 2-6. Kinesin-5 functions on MTs. (A) Cartoon illustration of a kinesin-5 homotetramer. (B) Kinesin-5 motors function within the mitotic spindle and are localized to spindle poles and midzone. During spindle assembly, kinesin-5 motors crosslink antiparallel MTs. Thereafter, their plus-end directed motility pushes spindle poles apart. Following bipolar spindle assembly, they can crosslink parallel MTs at the spindle poles and antiparallel ipMTs at the spindle midzone.

antiparallel MTs, they predominantly moved to the plus-end and became less processive. Based on these observations, researchers have proposed that the bidirectional motility of yeast kinesin-5s is essential to transition from a monopolar to a bipolar configuration. In support of this, computational studies of spindle assembly showed that when *SpCut7* motors were limited to only plus-end directed motility, the simulations were incapable of generating a stable bipolar spindle[98].

2.4.3 Kinesin-14 motors

Kinesin-14 motors are the only kinesin family members that possess a C-terminal motor domain. This structural configuration gives them a unique motile mechanism that involves slow, non-processive motility via a lever-arm swinging action directed toward the MT minus end. The functional form of most of kinesin-14s is a homodimer, but some yeast kinesin-14s are heterodimers, where one subunit is catalytically inactive[99-101]. Like kinesin-5s, kinesin-14 motors can crosslink MTs, but they do this using a second MT binding site in their N-terminal tail domain[102-104]. These features endow them with the capacity to mediate MT-organizing functions, such as crosslinking parallel MTs and focusing the spindle poles, sliding antiparallel MTs in a direction that produces inward spindle forces, and MT nucleation[104-107]. By efficiently organizing MTs and providing inward force, they play an important role in the assembly and maintenance of a functional spindle midzone[107]. More recent studies suggest that this facilitates engagement of the kinesin-5 family members with ipMTs, which exert outwardly directed MT sliding forces that are required for maintaining spindle length in metaphase and spindle elongation in anaphase (**Figure 2-7**)[108, 109]. In *S. cerevisiae*, loss of kinesin-14 functions results in compromised spindle organization where cells display unbundled MTs at the spindle poles,

have unusually long cytoplasmic MTs, shorter spindle lengths, and in some cases, multipolar spindles[110-112]. Studies in our lab have characterized the *C. albicans* homolog of this kinesin, *CaKar3Cik1*[113]. Loss of either Kar3 or Cik1 results in cell cycle arrest, as well as filamentation and karyogamy defects. Intriguingly, examination of spindle structure in the absence of either protein shows a monopolar spindle or two dissociated half-spindles, which is unprecedented for Kar3 and Cik1 homologues in budding yeast.

2.4.4 Force-balance paradigm

The bipolar spindle apparatus assembly and maintenance requires coordination of antagonistic forces from MT force generators. The “force-balance model” explaining this mechanism originated in the early 90’s in budding yeast. Since then, accumulating evidence from studies of different organisms reveals that a ‘tug-of-war’ takes place between kinesin-14 and kinesin-5 motors on antiparallel MTs to maintain the correct spindle organization that is needed to properly segregate chromosomes[67, 68, 72, 114]. One form of antagonism involves the use of MT plus-end-directed outward forces by kinesin-5 motors to drive poleward flux and pole separation, while minus-end-directed kinesin-14s produce inward forces to bring spindle poles together, shortening the spindle. Proper coordination of these two activities is required for the correct assembly of the spindle and control of its length[104, 115]. In budding yeast, the spindle length in metaphase (following spindle assembly and chromosome attachment) is constant as Cin8 and Kip1 act to elongate the spindle, while Kar3 acts antagonistically to shorten spindles[114, 116]. Tipping this balance by up- or down-regulating subsets of motors can drive specific mitotic movements[109, 114]. Improper forces on the spindle, by removal

or inhibition of a force-producing motor can have fatal consequences, including chromosome segregation defects or spindle collapse[117, 118].

For almost all eukaryotes in which kinesin-5 and -14 have been studied, the individual activities of these motors are essential. However, in many systems, simultaneous loss of kinesin-14 and kinesin-5 together restores viability of cells that lacked activity of only one motor family[68, 109, 114, 119]. In *Schizosaccharomyces pombe*, loss of its two kinesin-14 motors (Pkl1 and Klp2) and kinesin-5 (Cut7) restores a nearly normal spindle phenotype. In these cells, pushing forces generated by MT growth and MT bundling proteins are sufficient to promote spindle pole separation and spindle assembly[120-123]. Although functional, these nearly normal spindles are shorter and more disorganized, and their MT minus ends are unfocused and often extend past the opposite spindle pole[107, 124]. Also important to note is that most eukaryotes encode more than one kinesin-5 or -14 family member in their genome. For example, *S. cerevisiae* has two kinesin-5 motors and assembles two functionally distinct kinesin-14 motors by pairing the Kar3 protein with two different non-catalytic kinesin-like binding partners. Conversely, *S. pombe* has one kinesin-5 and two kinesin-14 motors. Sometimes these duplicate family members display functional redundancies, but they typically have distinct roles within the spindle. This is outlined in **Table 2-1**. Interestingly, *C. albicans* only encodes for one kinesin-5 and -14 motor. The unique functions of these kinesins are one of the primary foci of this thesis.

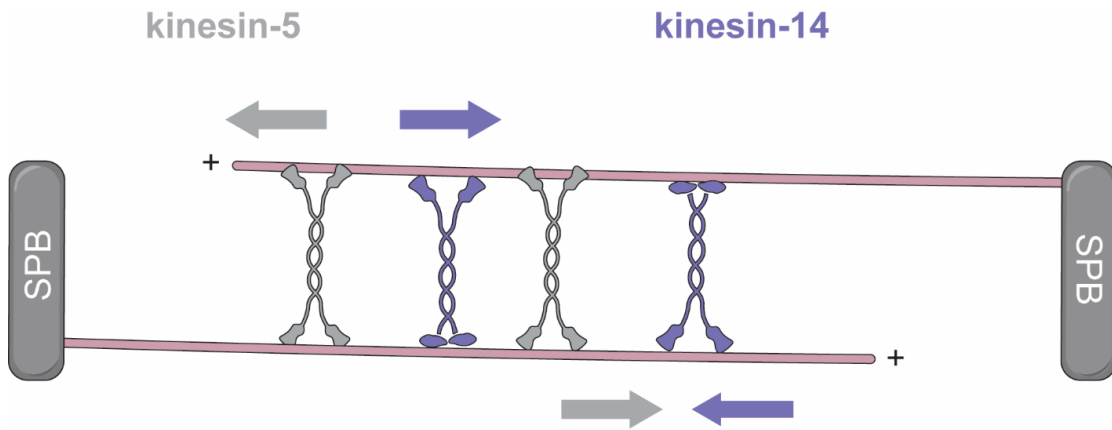


Figure 2-7. Kinesin-14 and kinesin-5 motors crosslinking MTs. The minus-end directed kinesin-14 (purple) and the plus-end directed kinesin-5 (grey) motors collectively exert opposing forces on MTs, thus establishing the “push-pull” model[67, 68, 72, 114].

Table 2-1. Specific functions of yeast kinesin-5 and -14 motors

			Localization	Directionality	Function	kinesin-5, -14 Δ
<i>S. cerevisiae</i>	kinesin-5	Cin8	SPB	Bidirectional	Spindle assembly/ kinetochore congression (kMT length regulation/Ndc80 attachment to kinetochores/ initial fast phase of anaphase B	<i>cin8</i> Δ = viable <i>kip1</i> Δ = viable
		Kip1	Spindle MTs (midzone)	Bidirectional	Spindle assembly/ crosslinking and sliding apart ipMTs in anaphase/slow phase of anaphase B	<i>cin8</i> Δ <i>kip1</i> Δ = inviable
	kinesin-14	Kar3/Cik1	SPB and spindle MTs	Minus-end	Mating(karyogamy)/control metaphase length/ align spindle MTs/ depolymerase	<i>kar3cik1</i> Δ = viable <i>kar3vik1</i> Δ = viable
		Kar3/Vik1	SPB	Minus-end	Vik1 is required for Kar3 SPB localization/potential depolymerization of MTs at SPB	<i>cin8</i> Δ <i>kip1</i> = viable Δ <i>kar3cik1</i> Δ
<i>S. pombe</i>	kinesin-5	Cut7	SPB	Bidirectional	Spindle assembly/outward force production/chromosome congression	<i>cut7</i> Δ = inviable <i>klp2</i> Δ = viable <i>plk1</i> Δ = viable
	kinesin-14	Klp2	Spindle MTs (midzone)	Minus-end	Crosslink and slide MTs, mediate MT nucleation at SPB, inward force production	<i>cut7</i> Δ <i>plk1</i> Δ = viable <i>cut7</i> Δ <i>klp2</i> Δ = inviable
		Plk1	SPB	Minus-end	Karyogamy/ maintenance of spindle (generates inward force at midzone)/ kinetochore-associated to promote net MT shortening	<i>cut7</i> Δ <i>klp2</i> Δ = viable <i>plk1</i> Δ

2.4.5 Dynein motor proteins

Dynein has also been proposed to counteract the activity of kinesin-5 motors on the mitotic spindle. Similar to kinesin motors, dynein molecules also use the MT track to fulfill their functions in intracellular transport, ciliary movement, and mitotic spindle organization. There are two categories of dynein motors: axonemal dyneins, which help with the movement of cilia and flagella, and cytoplasmic dynein which are important for cargo transport, chromosome segregation and spindle organization. Cytoplasmic dynein (with its binding partner dynactin) is present in all eukaryotes and is the only dynein member present in yeast species. In budding and fission yeast, dynein motors do not enter the nucleus and thus perform functions solely using aMTs[125, 126]. In contrast, because the nuclear envelope breaks down in metazoans, dynein has acquired additional functions in chromosome congression and alignment[127]. For the purposes of this thesis, dynein function will largely focus on studies from yeast.

The main role of dynein in budding and fission yeast (including *C. albicans*) is to position the nucleus using aMTs so that chromosome segregation occurs across the mother-bud neck[128-130] (**Figure 2-8**). Dynein mutants fail to move the spindle to the bud neck, and cells proceed with anaphase entirely in the mother cell. Depending on the location of the nucleus, this can sometimes be resolved using a different pathway (Kar9 pathway) implicated in nuclear movement[125]. Mechanistically, dynein is a minus-end directed motor, but localization studies show that it accumulates mostly at the cytoplasmic MT plus-ends. A plausible explanation for the translocation of dynein to MT plus ends is by kinesin-7, Kip2, which also transports other proteins to plus ends[131]. From here, dynein is off-loaded onto the cell cortex where it can form lateral contacts with aMTs. Since the aMT

minus-ends are attached to the SPB, and the SPB is imbedded in the nuclear envelope, dynein-mediated tugging on the aMT allows for nuclear movement. In this regard, dynein is also able to generate pulling forces on the nucleus after it has been positioned at the bud-neck and contribute to spindle pole separation during anaphase. Additional roles of dynein have been postulated in higher eukaryotes such as pole separation during spindle assembly[119, 132, 133] and anaphase spindle elongation by pulling on aMTs[134-136]. As a result, dynein is also an important motor that contributes to spindle force-balance[134].

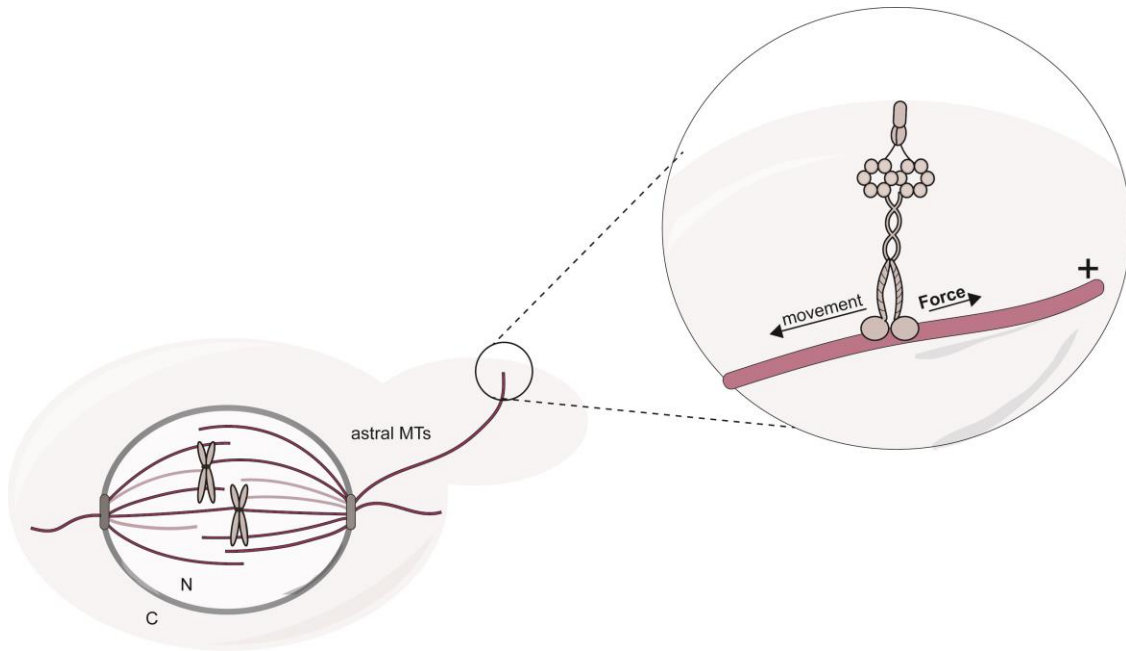


Figure 2-8. Dynein function in budding yeast mitosis. Cartoon representation of dynein motor localized to the cell cortex of budding yeast. Here, the dynein motor can tether aMTs and pull on the nucleus/spindle to position and orient the spindle at the mother-bud neck.

2.4.6 Genome plasticity of *C. albicans*

Euploidy is a genome state where cells exhibit a karyotype that is an exact multiple of the haploid genome content. Divergence from euploidy, such as the gain or loss of one or more chromosomes, is termed aneuploidy[137]. There are many ways a cell can acquire aneuploidy during mitosis; improper attachment of chromosomes, defects in cell cycle checkpoints that allow mitotic progression before chromosomes are attached and bioriented, tetraploidy, and/or endoreplication[138-140]. Across species, aneuploidy is known to have diverse consequences on organism fitness, viability and reproduction[141, 142]. While most cells may not tolerate aneuploidy well, others, like cancer cells can leverage aneuploidy as a fast and reversible strategy to overcome stress conditions or maintain rapid growth[143, 144]. Gain or loss of specific chromosomes can provide genetic variation that allows cells to adapt during changing environments or selective pressures. This same strategy is also often employed by *C. albicans* (and other fungal pathogens) as a means of adaptation when exposed to stresses like antifungal drugs[11, 145, 146]. In *C. albicans*, chromosomal loss and/or gain can arise from genome rearrangements, isochromosome formation, and segmental duplication[11, 147-151]. These forms of genetic diversity mainly arise through somatic events since *C. albicans* undergoes clonal (asexual) reproduction, however, *C. albicans* can also generate diversity through its unique parasexual cycle[152].

One mechanism of aneuploidy generation in *C. albicans* arises through structural rearrangements of repetitive DNA regions[153]. By their very nature, repetitive loci often serve as hotspots for genetic recombination events and do not require perfect sequence identity for recombination to occur. *C. albicans* genome sequencing has identified

hundreds of novel multicopy repeats that can undergo both inter- and intra-locus recombination events, which can either promote or restrict sequence evolution[154]. Additional repetitive elements, including expanded gene families and centromeric repeats, also facilitate recombination via a non-conventional, long-range DNA double-strand break (DSB) repair mechanisms[153]. Furthermore, *C. albicans* centromeres are typically flanked by repeat regions and act as common breakpoints for isochromosome formation. A recent study unveiled that a double-strand break near the inverted repeat sequence on the centromere of chromosome 5 will copy the entire arm of the broken chromosome, resulting in the development of a homozygous isochromosome[153].

Another mechanism that generates aneuploidy in *C. albicans* is through the formation of a tetraploid intermediate[155]. Tetraploidy can arise via endoreduplication, cell fusion, and/or cytokinesis failure. Tetraploidy is observed when *C. albicans* strains that are homozygous for the mating-type locus (MTL) mate, resulting in nuclear fusion and tetraploid DNA. Cells then undergo concerted chromosome loss and obtain a near diploid state, with aneuploids prevalent[156-158]. Another mechanism of tetraploidy generation in *C. albicans* cells is through cytokinesis failure when exposed to the antifungal fluconazole (FLC). FLC inhibits lanosterol α -14 demethylase enzyme, Erg11, and impacts production of ergosterol, a key cell membrane component. When exposed to FLC, a subpopulation of cells exhibits abnormal synchronization of chromosomal and cytoplasmic division, where mother and daughter cells fail to physically separate following chromosome segregation (i.e., Cytokinesis failure). Initiation of the next cell cycle still ensues resulting in populations of cells composed of multimeric chains (“trimeras”) of mother, daughter and granddaughter cells linked together by a common cytoplasm[155].

These binucleate trimers undergo coordinated nuclear division yielding four daughter nuclei, two of which experience mitotic collapse and form a tetraploid cell with extra spindle components. Defective nuclear divisions of these multi-spindle nuclei can result in aneuploid progeny and drug-resistant phenotypes. Appearance of trimers was also observed in FLC-treated *C. glabrata* cells, but not *S. cerevisiae*, suggesting that aneuploidy may be a property of pathogenic fungi in general[155].

A balance between genome plasticity and stability is required to maintain DNA integrity and help cells survive in fluctuating or unpredictable environments. Aneuploidy allows for the increase (or decrease) in gene dosage, influencing cell circuitry and stress response pathways[159, 160]. This can confer resistance to antifungal drugs for pathogenic fungi. For example, *C. albicans* acquires resistance to FLC by accumulating extra copies of drug-resistance genes through isochromosome of the left arm of chromosome 5 (i(5L))[145, 148]. Remarkably, the gene encoding Lanosterol 14-alpha-demethylase (*ERG11*) and a transcriptional regulator of efflux pumps, *TAC1*, are both located on this isochromosome[161]. Additional aneuploidies that confer FLC resistance are loss of one copy of chromosome 4 and gain of one copy of chromosome 3[162], although how this aneuploidy confers resistance is less clear.

2.4.7 Machinery in the chromosome segregation process in *C. albicans*

Given the proclivity of *C. albicans* to experience aneuploidy, it is prudent to investigate the machinery it uses to perform the chromosome segregation process. As outlined earlier, the accuracy of chromosome segregation relies on the correct organization of MTs into a bipolar structure, proper chromosome attachment, and segregation into their respective cellular compartments – all of which require functions of molecular motors like

kinesins and dynein. In many eukaryotes, defects in any of these processes can lead to chromosome segregation errors and aneuploidy. One example of how kinesins are implicated in chromosome movement is evident in studies from *S. cerevisiae* and *C. albicans* [33]. In both species, kinesin-5 motors mediate length-dependant kMT disassembly to drive chromosome congression to properly align chromosomes at the spindle midzone. kMT length regulation proposes that kMTs grow in a length-dependant manner where short MTs grow efficiently by net tubulin addition at the spindle poles and long kMTs undergo net shortening at the spindle midzone, most likely through catastrophe [33, 163]. First, kinesin-5 motors bind to kMTs, move to their plus ends, and upon arrival at a growing plus-end, promote net kMT plus-end disassembly[163]. Since there are more binding sites on long kMTs, it is likely that more kinesin-5 motors accumulate at these plus-ends to undergo kMT catastrophe. In *C. albicans* cells lacking Kip1, spindles had disorganized and longer kMTs suggesting that chromosomes were not properly congressed at the spindle midzone.

Improper chromosome congression can result in kMTs of varying lengths and thus affect the tension of kMT fibers across the spindle. Further, improper chromosome congression can increase mechanical stress on the MT-kinetochore attachment site leading to disruption of the kinetochore structure and disengagement of the kinetochore to the kMT[164-166]. If this is not resolved before anaphase, it could result in chromosome detachment, leading to aneuploidy. As such, proper chromosome congression is important to prevent mitotic errors from occurring. The importance of kinesin-5's in chromosome congression suggests that changes or alterations in their activity may serve as a way for

cells to control chromosome segregation (i.e., generate chromosome missegregation errors).

Aside from kMT length regulation by Kip1 in *C. albicans*, additional studies reveal that loss of Kip1 function interferes with normal mitotic progression and an aberrant spindle morphology[167]. Inhibition or deletion of Kip1 revealed that some cells formed multiple spindle poles that accumulate near each other. While inhibition of Kip1 was lethal due to an inability to move SPBs apart, the Kip1-null mutant was viable. These studies indicate that Kip1 is a non-essential motor in *C. albicans*.

The kinesin-14, Kar3, was also previously studied in *C. albicans*. Loss of Kar3 led to defects in nuclear congression in mating and a slow growth phenotype in vegetatively dividing cells. The slow growth was due to a delayed cell cycle progression as these cells exhibited unstable or aberrant mitotic spindles[168]. Additional studies emphasized that deletion of Kar3 or its partner protein, Cik1, resulted in a dramatic bipolar spindle formation defect[113] and increased polarized growth. Spindle assembly is normally observed after loss of kinesin-5 in other systems. This unique phenotype highlights divergence in how motor proteins regulate spindle structure and function in *C. albicans*.

2.4.8 Aims of my thesis research

Aside from the studies mentioned above, few groups have focused on kinesin motor functions in *C. albicans* mitosis. The first aim of this thesis was to determine the role of kinesin-5 in mitosis and its relationship to kinesin-14. A key finding of these studies was that Kip1 was not required for bipolar spindle assembly or anaphase B spindle elongation. Therefore, the second aim of this thesis was to study mitotic functions of the motor that could most likely be compensating for Kip1 loss, such as cytoplasmic dynein (Dyn1).

Lastly, because it was discovered in studies related to the first aim that inhibition or deletion of *C. albicans* Kip1 caused errors in spindle and nuclear dynamics that resembled FLC-treated cells, the final aim of this thesis explored the involvement of Kip1 in FLC stress response.

Chapter 3

Kinesin-5 is dispensable for bipolar spindle formation and elongation in *Candida albicans*, but simultaneous loss of kinesin-14 activity is lethal

Shoukat, I., Frazer, C., & Allingham, J. S. (2019). Kinesin-5 Is Dispensable for Bipolar Spindle Formation and Elongation in *Candida albicans*, but Simultaneous Loss of Kinesin-14 Activity Is Lethal. *mSphere*, 4(6), e00610-19. <https://doi.org/10.1128/mSphere.00610-19>

3.1 Abstract

Mitotic spindles assume a bipolar architecture through the concerted actions of MTs, motors, and crosslinking proteins. In most eukaryotes, kinesin-5 motors are essential to this process, and cells will fail to form a bipolar spindle without kinesin-5 activity. Remarkably, inactivation of kinesin-14 motors can rescue this kinesin-5 deficiency by re-establishing the balance of antagonistic forces needed to drive spindle pole separation and spindle assembly. We show that the yeast form of the opportunistic fungus *C. albicans* assembles bipolar spindles in the absence of its sole kinesin-5, Kip1, even though this motor exhibits stereotypical cell cycle-dependent localization patterns within the mitotic spindle. However, cells lacking Kip1 function have shorter metaphase spindles, and longer and more numerous aMTs. They also show defective hyphal development. Interestingly, a small population of Kip1-deficient spindles break apart and reform two bipolar spindles in a single nucleus. These spindles then separate, dividing the nucleus, and then elongate simultaneously in the mother and bud, or across the bud neck, resulting in multinucleate cells. These data suggest that kinesin-5-independent mechanisms drive assembly and elongation of the mitotic spindle in *C. albicans*, and that Kip1 is important for bipolar

spindle integrity. We also found that simultaneous loss of kinesin-5 and kinesin-14 (Kar3Cik1) activity is lethal. This implies a divergence from the antagonistic force paradigm that has been ascribed to these motors, which could be linked to the high mitotic error rate that *C. albicans* experiences, and often exploits, as a generator of diversity.

3.2 Introduction

The mitotic spindle is a highly dynamic MT-based structure that undergoes a distinct set of morphological changes in order to correctly attach, orient, and then separate sister chromatids in the dividing cell. Kinesin motor proteins play major roles in shaping and organizing MTs within the spindle over the course of cell division. Early in mitosis, evolutionarily conserved kinesin-5 proteins crosslink the overlapping plus ends of interpolar MTs from newly duplicated centrosomes (spindle pole bodies, SPBs in yeast), and then slide them apart via plus end-directed motility to establish spindle bipolarity[63, 66, 69, 83, 169-172]. Genetic or chemical inhibition of kinesin-5 activity produces monopolar spindles or inward collapse of pre-anaphase spindles, usually leading to cell death[64, 68, 173]. This spindle defect arises from loss of outward forces needed to counterbalance the inward forces supplied by MT minus-end directed kinesin-14 motors, which pull spindle poles together[68, 114, 119]. In many organisms, a nearly normal spindle phenotype can be restored by inactivating or depleting cells of kinesin-5 and kinesin-14 simultaneously because this force imbalance is eliminated[68, 72, 114, 115, 174]. In this experimental scenario, pushing forces generated by MT growth are sufficient to promote spindle pole separation and bipolar spindle assembly[120-123].

This interplay of motor and MT forces has been studied extensively in the model yeasts *Saccharomyces cerevisiae* and *Schizosaccharomyces pombe*[68, 120, 121, 123, 135,

175]. *S. cerevisiae* encodes two kinesin-5 homologs, *ScKip1* and *ScCin8*, that have overlapping, but non-equivalent functions during mitosis[69, 169], while *S. pombe* encodes a single kinesin-5, named *SpCut7*[176]. All three of these proteins form homotetramers that exhibit bidirectional motility, and all of them function in bipolar spindle assembly and crosslink parallel MTs to help focus kinetochore clusters[87, 90, 93-95, 177]. They are also important for stabilizing the overlapping array of MTs at the anaphase spindle midzone, and for promoting and regulating timely anaphase spindle elongation[77, 120, 134, 135, 178-180]. In both yeast species, loss or inhibition of kinesin-5 function is lethal. However, simultaneous inactivation of their kinesin-14 motors (*ScKar3Cik1* and *ScKar3Vik1* in *S. cerevisiae* or *Pkl1* and *Klp2* in *S. pombe*) neutralizes kinesin-5 deficiency[67, 111, 181, 182], highlighting the importance of keeping inward and outward forces acting on the spindle in balance. In contrast to the lethality of kinesin-5 loss, bipolar spindles are able to form in the absence of kinesin-14 activity, but are either short and disorganized, or their MT minus ends are unfocused and extend past the opposite spindle pole[107, 124]. Our studies of the homologous motors in the opportunistic fungus *C. albicans* indicate that these phenotypes, and the opposing relationship of kinesin-5 and kinesin-14 proteins in spindle regulation, are not as highly conserved among eukaryotes as previously thought.

C. albicans is a close relative of *S. cerevisiae* and *S. pombe*, but it encodes only one kinesin-5 and one kinesin-14 motor, named *Kip1* and *Kar3*, respectively, the latter of which forms a heterodimer with a non-catalytic kinesin-like protein *Cik1*[113]. *C. albicans* is viable without *Kip1*[167], and cells lacking *Kar3Cik1* activity often arrest with a monopolar spindle or two dissociated half-spindles[113]. Through further investigation of these unconventional phenotypes, we found that *Kip1* is not needed for bipolar spindle

assembly or nuclear division, even though it exhibits the same cell cycle-dependent localization as its homologs in budding yeast. However, *kip1* Δ/Δ spindles are shorter and intermittently disassemble prior to cell division. When spindle disassembly occurs, two or more independent bipolar spindles emerge that either segregate between the mother and daughter cells or elongate across the bud neck. Each bring portions of the nucleus with them, which are further subdivided when the spindles undergo anaphase. Rather than neutralizing these kinesin-5 deficiencies, we found that simultaneous loss of kinesin-14 activity is lethal. These results imply that *C. albicans* Kip1 and Kar3Cik1 have mostly overlapping rather than antagonistic functions in bipolar spindle assembly, and that their combined loss cannot be compensated for by MT polymerization forces or other spindle-associated factors.

3.3 Results

3.3.1 Localization of *C. albicans* Kip1 mirrors other yeast kinesin-5s

Like many mitotic proteins, the localization and function of kinesin-5 motors changes throughout the cell cycle. During spindle assembly, *S. cerevisiae* Kip1 and Cin8, as well as *S. pombe* Cut7, are enriched at the minus ends of nuclear MTs, toward the spindle poles[91, 94, 183]. Here, they are thought to capture MTs emanating from neighboring SPBs to establish antiparallel MT interactions and provide outward sliding forces to support SPB separation[63, 90, 93-95, 176, 177, 184]. Persistence of kinesin-5 near spindle poles in metaphase has been attributed to their interaction with kinetochores, or to kMTs, where they could crosslink parallel kMTs and regulate their assembly dynamics to help achieve chromosome congression[87, 163, 185]. Upon anaphase onset, kinesin-5 motors relocate toward the plus-ends of ipMTs, which overlap in an antiparallel array in the spindle

midzone. Here, their MT crosslinking and plus end-directed motility help stabilize and elongate the spindle, fully separating the two opposing SPBs, leading to final chromosome segregation[77, 120, 134, 135, 178-180]. Recent studies suggest that this cell cycle-dependent redistribution of yeast kinesin-5s in the spindle is enabled by their capacity for bidirectional motility[90, 92-95, 98].

The discovery that *C. albicans* is viable without Kip1[167] suggests that its localization and/or function may be different from other yeast kinesin-5s. However, when we imaged fields of unsynchronized cells expressing GFP-labelled Kip1 and mCherry-labelled tubulin (Tub2) we observed similar cell cycle-dependent motor localization patterns within the mitotic spindle as seen in other yeasts. In small-budded early mitotic cells, Kip1 localized near one end of monopolar spindles (in which SPBs are adjacent) (**Figure 3-1A, row 1**) and was found at both poles after SPB separation and bipolar spindle assembly (**Figure 3-1A, row 2**). In cells that were entering anaphase, Kip1-GFP fluorescence was dispersed along the length of the spindle. In late anaphase cells, Kip1 accumulated at the spindle midzone. These same localization patterns were seen when we imaged individual cells expressing Kip1-mScarlet and Tub2-Neon over the course of mitosis by time-lapse microscopy, although photobleaching affected the ability to detect Kip1 at later time points (**Figure 3-1B**). To determine whether midzone clustering of Kip1 requires overlapping arrays of antiparallel ipMTs in this region, we imaged Kip1-GFP in fields of unsynchronized cells lacking kinesin-14 activity (*cik1Δ/Δ*). In other yeast, kinesin-14 is important for organizing antiparallel ipMT interactions in the midzone so that kinesin-5 motors can properly crosslink and slide antiparallel spindle MTs[107, 124, 186]. Without kinesin-14 activity, Kip1 remains exclusively near the poles of bipolar spindles

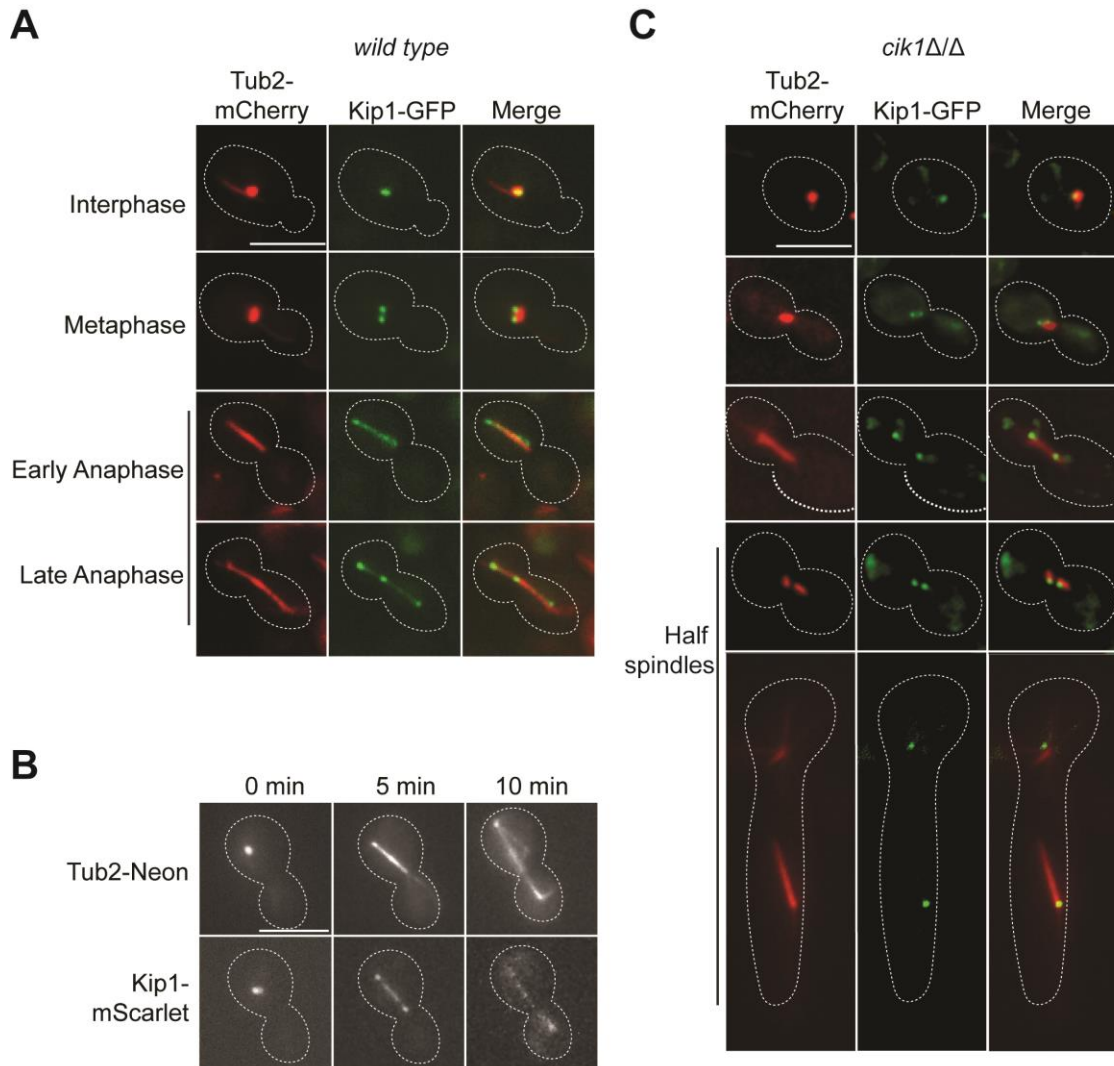


Figure 3-1. Kip1 exhibits similar localization to other kinesin-5s during the cell cycle.

(A) Images of wild type cells expressing Tub2-mCherry and Kip1-GFP (strain CF338). Representative cells from different stages of mitosis were selected. (B) Individual frames from time-lapse microscopy of cells expressing GAL-Tub2-mNeonGreen and Kip1-mScarlet (strain CF443). (C) Images of *cik1Δ/Δ* cells expressing GAL-Tub2-mCherry and Kip1-GFP (CF340). All cells were obtained from logarithmically growing, unsynchronized cultures in SDC-Sucrose medium at 30°C. Scale bars, 5 μm.

and to one pole of dissociated half-spindles, presumably due to paucity of antiparallel ipMT overlaps (**Figure 3-1C**).

3.3.2 *C. albicans* forms bipolar spindles without kinesin-5

To understand the role of Kip1 in mitosis, we used PCR- and CRISPR-based gene targeting to generate two independent homozygous *KIP1* deletion strains. Wary that Kip1 could be essential for cell growth[187], we also engineered a conditional *KIP1* gene expression strain using the tetracycline-regulatable (TR) promoter system, which enables tight repression of *KIP1* in the presence of doxycycline (DOX)[188, 189]. Transformants of each strain were screened by PCR to confirm the intended gene modification (data not shown). We further used RNAseq analysis to confirm absence of *KIP1* expression in the gene deletion strains (**Supplemental Table 1**, BioProject accession no. PRJNA579546). The RNAseq data showed that there were no changes in expression of any other molecular motors or MT-associated proteins (MAPs) to suggest the presence of compensatory mechanisms from such proteins.

In dilution spot assays, all Kip1-depleted strains displayed modest sensitivity to higher temperature but were otherwise viable (**Figure 3-2A**). However, in liquid culture, cells lacking Kip1 activity proliferated slower than wild-type and contained a mixture of blastoconidia and cells with long extensions resembling pseudohyphae (**Figure 3-2B and C**). Upon further visual inspection and quantification of *kip1* Δ/Δ by microscopy, we observed this hyperpolarized morphology in approximately 30% of the cells (**Figure 3-2C**). These elongated cells indicate a delay in cell cycle progression or a cell cycle arrest and could mask a slower proliferation rate on solid growth media by giving *kip1* Δ/Δ dilution spots a similar appearance to wild-type. We also found that loss of Kip1 affected

filamentous growth under hypha-inducing conditions. Kip1-depleted colonies formed a smaller halo of invasive growth on Spider media (**Figure 3-2D**), and cells grown in serum produced shorter germ tubes and fewer septa (**Figure 3-2E and F**). When we added a wild type copy of *KIP1* back into the *kip1* Δ/Δ strain at the native locus, normal cell growth rate and cell morphology were restored (**Figure 3-2B, C, and D**), confirming that these defects were a direct consequence of *KIP1* loss.

Expecting that the slow growth phenotype of Kip1-depleted cells was caused by errors in mitotic spindle assembly, we imaged fields of unsynchronized wild-type and *kip1* Δ/Δ blastoconidia expressing Tub2-mCherry and Spc98-GFP (a component of the spindle pole body) and examined their spindle structures. We found that most of the spindles in budded *kip1* Δ/Δ cells (~92%) formed a stereotypical bipolar spindle structure (**Figure 3-3A**). However, nearly twice as many *kip1* Δ/Δ cells had metaphase spindles (53.5%) compared to wild type (28.9%) (**Figure 3-3B**), and the mean length of *kip1* Δ/Δ metaphase spindles was significantly shorter (*kip1* Δ/Δ = 0.68 ± 0.01 μm versus wild type = 0.93 ± 0.01 μm) (**Figure 3-3C**). When we tracked progression of the mitotic phases by time-lapse microscopy, we observed that *kip1* Δ/Δ cells took an average of 117.1 ± 7.8 min to initiate anaphase after a spindle had formed, whereas wild type required only 80.0 ± 5.2 min on average (**Figure 3-3D and E**). In contrast, when *kip1* Δ/Δ spindles did eventually elongate, there was no difference in the duration of anaphase compared to wild type (**Figure 3-3F**). These data show that *C. albicans* is not solely dependent on kinesin-5 activity for bipolar spindle assembly or late anaphase spindle elongation, but that Kip1 is important for timely separation of spindle poles after spindle assembly.

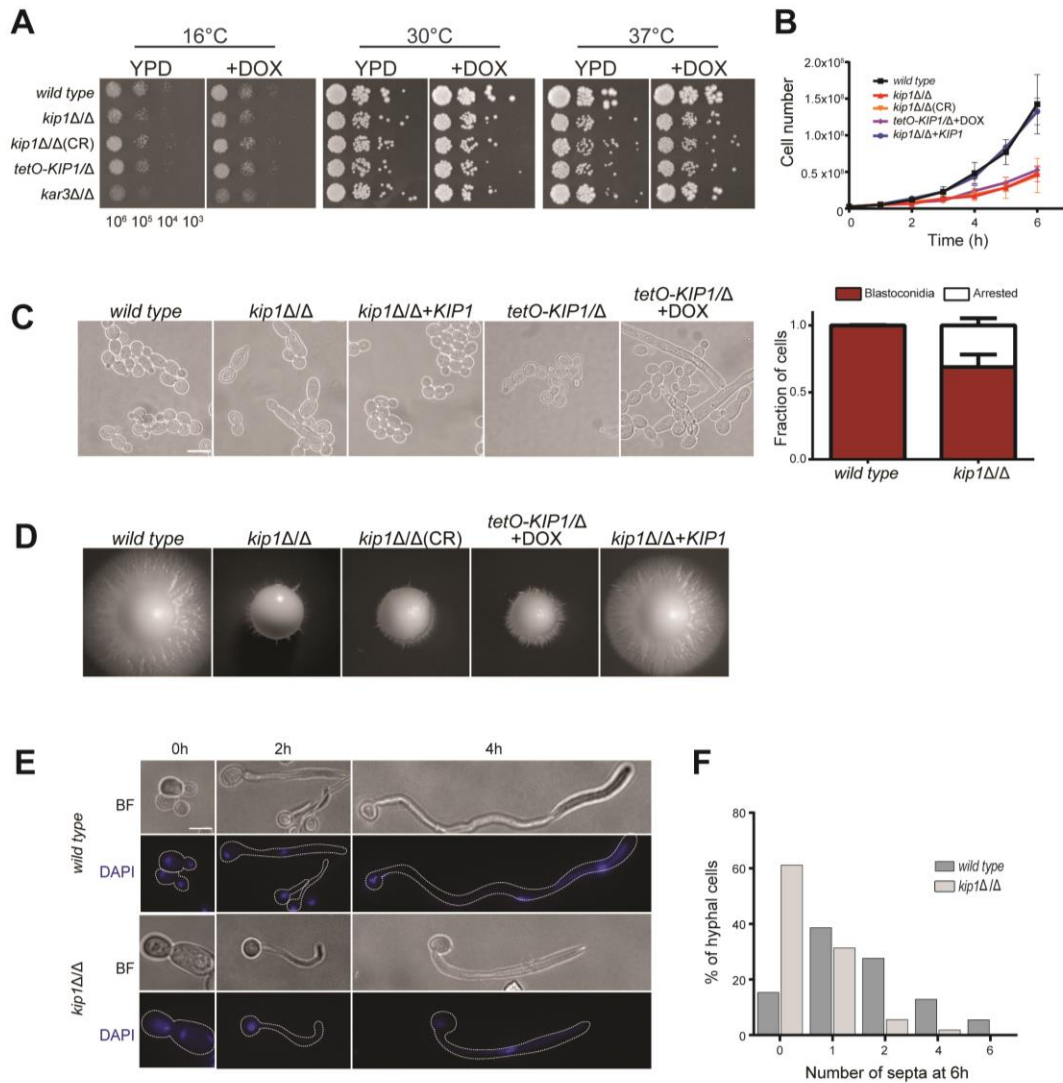


Figure 3-2. Loss of Kip1 affects growth and viability. (A) Spot assay of the various mutant *KIP1* strains (*kip1Δ/Δ*, strain CF311; *kip1Δ/Δ(CR)* strain CF429; *tetO-KIP1/Δ*, strain CF436) to assess cell growth. Cells were serially diluted to the specified concentrations and 5 μ L droplets were plated on YPD with or without DOX (10 μ g/mL). Plates were incubated for 2 days at the indicated temperatures. (B) Cell growth assay of the independent *KIP1* strains, including a *KIP1* add-back strain (CF354). Cells in SDC media were diluted to 2.5×10^6 cells per mL, incubated at 30°C and counted every hour with a hemocytometer. Data points represent an average of three independent experiments, +/- SEM. (C) Cells were grown in SDC and bright field images were collected. The graph

shows the proportion of normal looking blastoconidia and arrested cells observed in these bright field images. Data represents the average of three independent experiments +/- SEM. N>3000 cells per strain. (D) Assessment of hyphal growth on various *KIP1* null strains. Wild type and each *KIP1* mutant were plated onto Spider media and incubated for 5 days at 30°C before imaging. (E) Bright field (BF) and fluorescence images of wild type and *kip1Δ/Δ* cell cultures. Cells were diluted 1:50 into fresh YPD media supplemented with 10% FBS and incubated at 37°C to induce hyphae. Cells were removed from the cultures at the indicated time points, and then fixed and stained with DAPI before imaging. (F) Cells were induced to form hyphae using the same conditions in (E), and then fixed and stained with calcofluor white before imaging. The number of septa per hyphae was quantified and graphed.

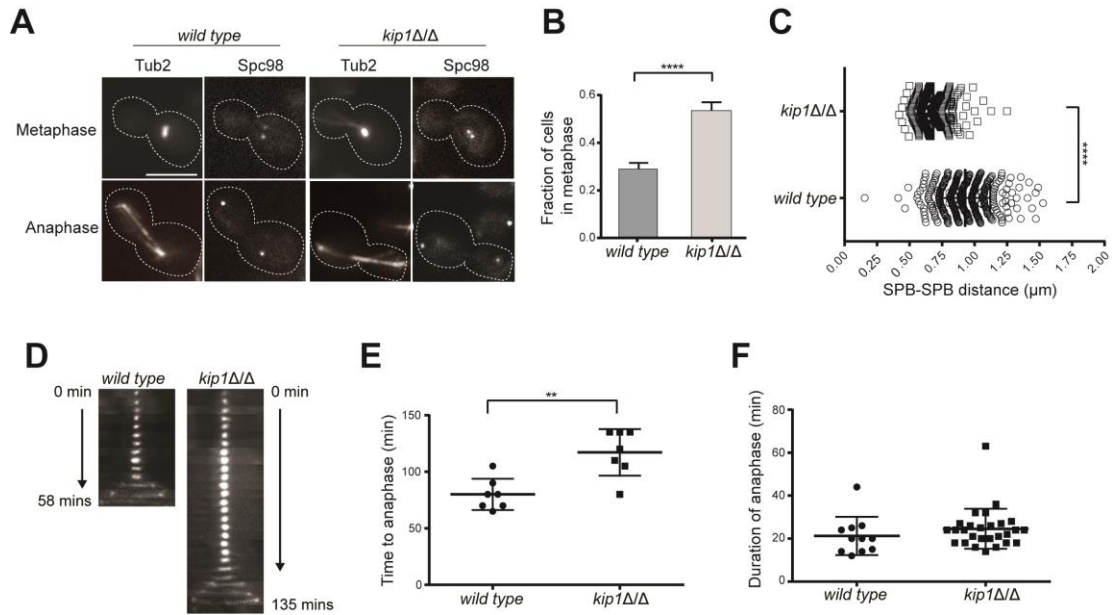


Figure 3-3. *kip1Δ/Δ* cells form bipolar spindles but exhibit defects in spindle dynamics. (A) Static images of wild type (CF363) and *kip1Δ/Δ* (CF368) cells expressing Tub2-mCherry and Spc98-GFP in SDC-Sucrose at 30°C. Scale bars, 5 μm. (B) Quantification of nuclear MT structures observed in Tub2-GFP-labelled wild type (CF289) and *kip1Δ/Δ* (CF226) cells. The proportions of cells with metaphase spindles in *kip1Δ/Δ* cells were significantly different from that of wild type cells ($p < 0.0001$ Student's test). Data represent mean values for three independent replicates of >1000 cells for each genotype, +/- SEM. (C) The distance between SPBs in blastoconidia with a bipolar spindle was measured in logarithmically growing cells (wild type (CF363) $n=357$, *kip1Δ/Δ* (CF368) $n=367$), +/- SEM, ($p < 0.0001$ Student's test). (D) Kymograph of wild type and *kip1Δ/Δ* cells using time-lapse microscopy. (E) Quantification of wild type and *kip1Δ/Δ* cells using time-lapse microscopy ($n = 7$) ($p = 0.0019$ Student's test). (F) Quantification of wild type and *kip1Δ/Δ* cells using time-lapse microscopy to analyze the duration of anaphase. Long (2 to 4 h) time-lapse series were captured with 150 ms exposures to measure the length of time between emergence of the bud until the end of anaphase for Tub2-GFP ($n = 11$) and Tub2-GFP *kip1Δ/Δ* ($n = 28$) cells ($p > 0.3$ Student's test).

Interestingly, *kip1* Δ/Δ spindles had longer and more numerous astral MTs than wild-type (**Figure 3-4A-C**). In many eukaryotes, including *C. albicans*, the plus ends of astral MTs strike the cell cortex, where they are captured by the minus-end-directed MT motor protein dynein[190-192]. When this happens, dynein can draw the MT, and the attached SPB, toward the cortical contact site to facilitate proper spindle positioning, elongation and/or migration[126, 193]. In *S. cerevisiae*, this activity of dynein assists Cin8 and Kip1 in anaphase spindle elongation, and simultaneous loss of dynein and Cin8 activity is lethal[134, 135]. We found *dyn1* Δ/Δ strain to be non-viable in the presence of the Kip1-specific inhibitor aminobenzothiazole (ABT), suggesting that Kip1 and dynein also have overlapping functions in *C. albicans* (**Figure 3-4D**). Perhaps the longer and more numerous astral MTs in *kip1* Δ/Δ are an adaptation to Kip1 loss that provides more opportunities for MT capture and pulling events by dynein, which could promote both anaphase spindle elongation and SPB separation during spindle assembly.

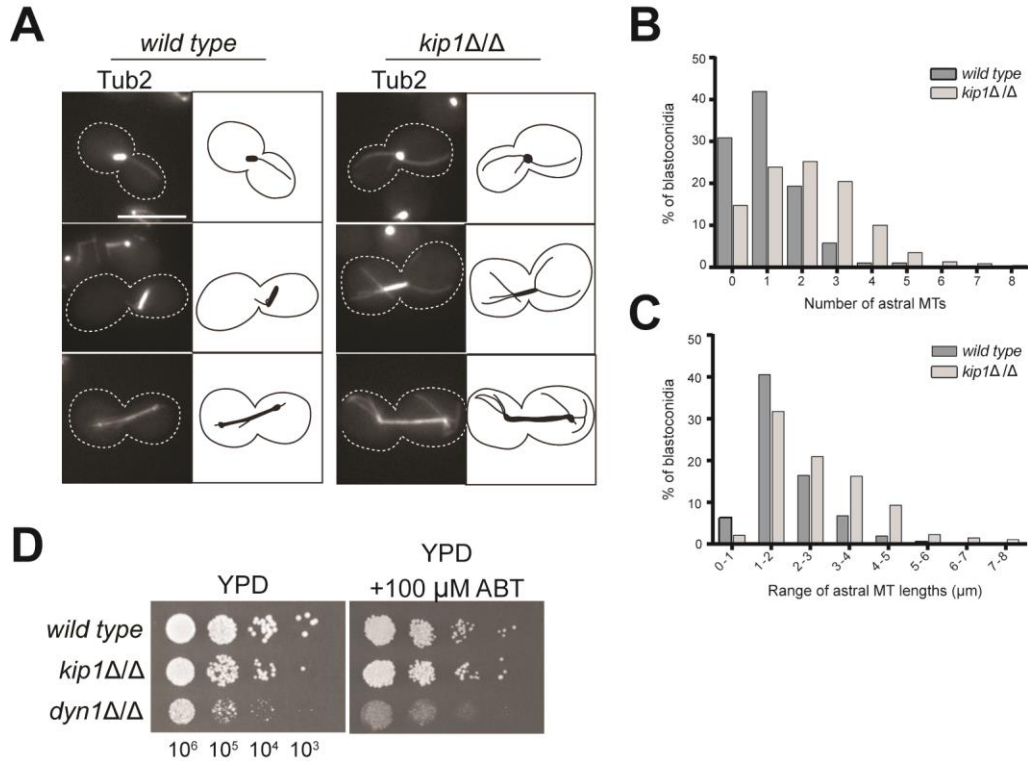


Figure 3-4. *kip1Δ/Δ* cells have longer and more numerous cytoplasmic MTs. (A) Representative images of wild type and *kip1Δ/Δ* cells expressing Tub2-GFP are shown beside cartoon representations of each cell to illustrate the difference in astral MT number and length. (B) The number of astral MTs in wild type (CF289) and *kip1Δ/Δ* (CF226) expressing Tub2-GFP was counted in cells with visible spindles. (C). For cells in (B) that contained aMTs, aMT length was determined by measuring the distance between the metaphase spindle pole and the plus end. These lengths were organized into bins of the size ranges indicated. (D) Wild type (CF027), *kip1Δ/Δ* (CF311), and *dyn1Δ/Δ* (CF358) cells were serially diluted to the indicated concentrations and 5 μL droplets were plated on solid YPD media and YPD+100 μM ABT, and incubated for 2 days at 25°C.

3.3.3 A subpopulation of *kip1* Δ/Δ cells have multiple spindles and show atypical cell cycle dynamics

Similar to previous findings by Chua *et al.*[167], we observed that a significant proportion (~12%) of *kip1* Δ/Δ blastoconidia, and all *kip1* Δ/Δ cells with a hyper-elongated morphology, contained multiple spindles (**Figure 3-5A and B**). In some cases, monopolar and bipolar spindles were simultaneously visible within the same budding cell (**Figure 3-5A, row 3**). To determine how these extra spindles formed, we collected time-lapse images of *kip1* Δ/Δ blastoconidia expressing Tub2-GFP. All of the multi-spindle blastoconidia that we tracked (n = 20) formed two short “bars” of tubulin fluorescence in the mother cell as the new bud began to emerge. Once a new bud formed, we observed two different multi-spindle configurations. In 65% of the cells we imaged, one of the tubulin structures traversed the bud neck, while the other remained in the mother compartment (**Figure 3-5C, row 2, t=6 min**). Each short fluorescent bar then elongated simultaneously, suggesting that they had formed distinct bipolar spindles. However, both spindles broke apart or disintegrated once the cell divided (**Figure 3-5C, row 3, t=36 min** and **Movie S1**). This phenotype suggests that Kip1 activity is important for anaphase spindle stability. In a smaller cohort of cells (45%), one or both of the spindles elongated across the bud neck and appeared to complete anaphase (not shown). Both of these multi-spindle phenotypes were recapitulated in wild-type cells treated with ABT (**Figure 3-5D**).

We were intrigued by this spindle defect because a subpopulation of wild-type *C. albicans* cells exposed to the antifungal agent fluconazole (FLC) display abnormal numbers of spindles as well. In the presence of FLC, DNA replication and nuclear division proceed ahead of bud emergence and completion of cytokinesis, respectively. Harrison *et al.* showed that forming tetraploid with extra spindle components [155]. Therefore, we next

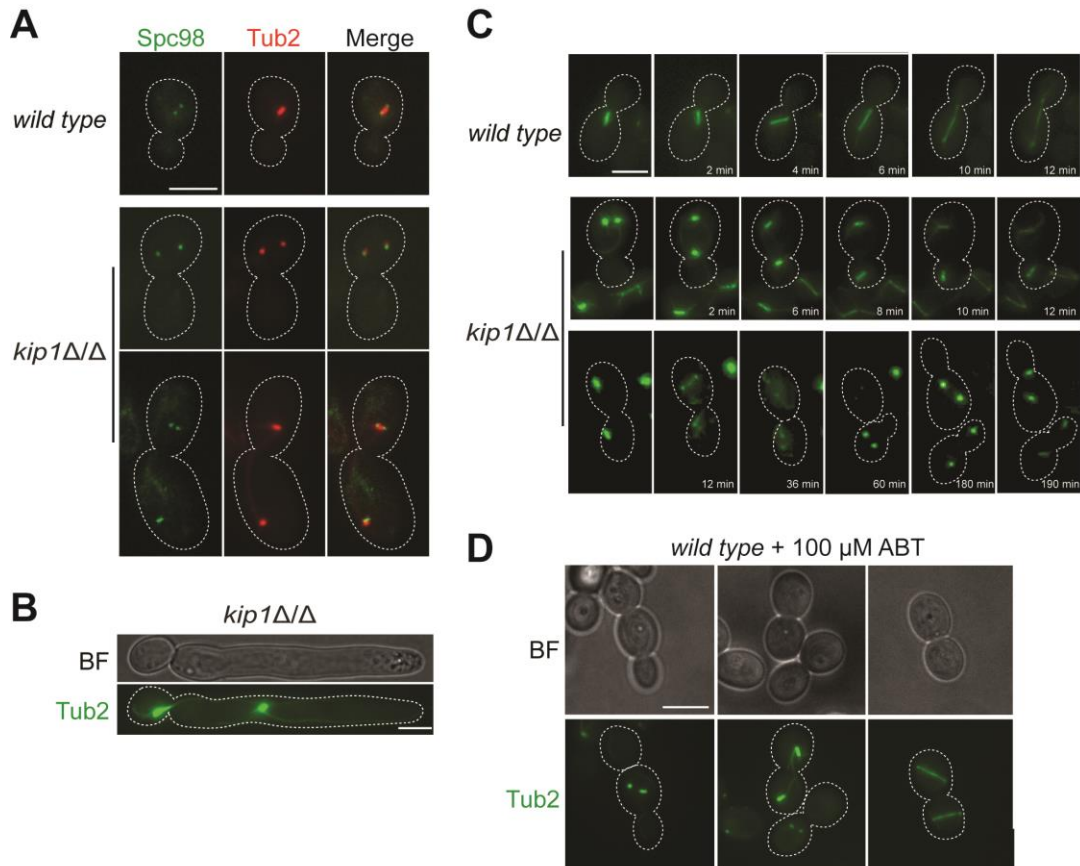


Figure 3-5. *kip1Δ/Δ* cells have abnormal number of spindles and SPBs. (A) Wild type (CF363) and *kip1Δ/Δ* (CF368) cells expressing Tub2-mCherry and Spc98-GFP and were grown in SDC-Sucrose at 30°C. Top row shows a normal metaphase spindle in wild type. Middle row shows two monopolar spindles in the mother compartment of *kip1Δ/Δ*. Bottom row shows a *kip1Δ/Δ* cell with one monopolar and one bipolar spindle. (B) Tub2-GFP labelled *kip1Δ/Δ* (CF226) arrested cells display multiple spindles. (C) Time-lapse of wild type (CF289) and *kip1Δ/Δ* (CF226) cells expressing Tub2-GFP. Two examples of *kip1Δ/Δ* spindle dynamics are shown (Rows 2 and 3). (D) Inhibition of Kip1 by ABT phenocopies *kip1Δ/Δ* cells. Tub2-GFP wild type cells (CF289) were incubated with 100 μM ABT for 2 hours and imaged. Scale bar, 5 μm.

used time-lapse microscopy to track nucleolar segregation (using Nop1-mScarlet) in ABT-treated wild-type cells that formed multiple spindles. While the “no drug” condition showed stereotypical nuclear and spindle dynamics that were well-coordinated with bud emergence and growth (**Figure 3-6, rows 1 and 2, Movie S2**), ABT-treated cells contained one large patch of Nop1-mScarlet fluorescence and two separate bars of Tub2-GFP when the bud emerged (**Figure 3-6, row 4, Movie S3**). This indicates that a bipolar spindle had already formed and broken apart before bud evagination. As bud growth continued, the Nop1 patch divided and migrated with each spindle. When these spindles were segregated to the mother and daughter cell (**cell #1, 65% of the cells imaged**), two smaller nuclear fragments were visible in each compartment after spindle elongation (four Nop1-mScarlet patches in total, **cell #1, t=95 min**). However, within 20 minutes, each pair of Nop1 patches coalesced as a result of mitotic collapse. When the spindles elongated across the neck (**cell #2, 45% of the cells imaged**), each spindle divided a Nop1-mScarlet patch into two different pieces, again resulting in four separate nuclear fragments (**cell #2, t=45 min**). Here, the two Nop1 foci in each compartment were produced from different anaphase spindles. As the time-lapse continued, these Nop1 foci appeared to merge into one (**Figure 3-6, cell #2, t=75 min**). These results suggest that the extra spindles seen in *kip1Δ/Δ* and ABT-treated wild-type cells could have formed in nuclei that experienced mitotic collapse, or after merging of nuclear fragments from two distinct spindles that completed anaphase.

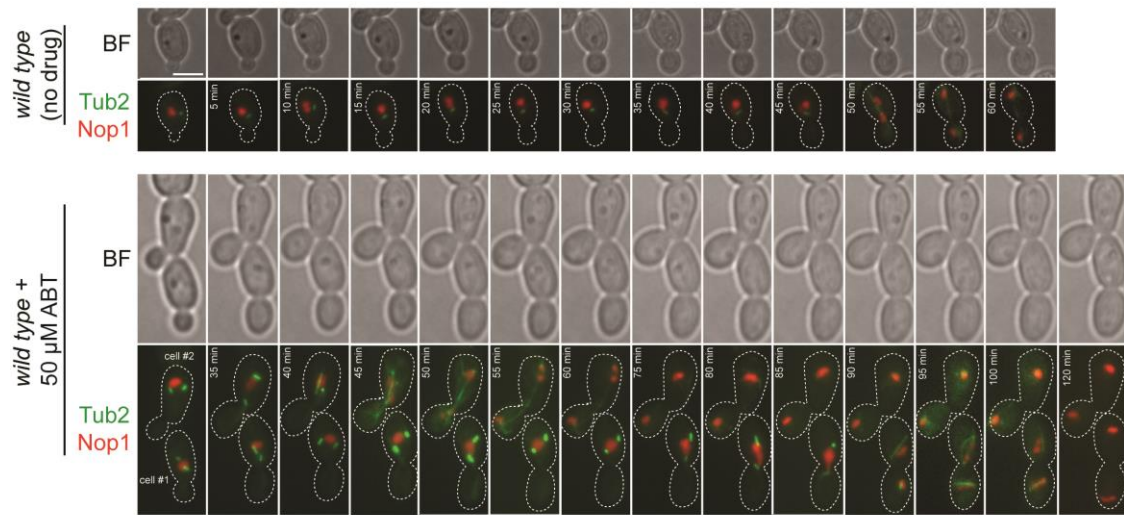


Figure 3-6. A subpopulation of Kip1-inhibited cells display abnormal nuclear division. (A) Time-lapse microscopy of wild type cells expressing Nop1-mScarlet and Tub2-GFP (CF417) (“no drug” condition). (B) Wild type cells expressing Nop1-mScarlet and Tub2-GFP were incubated with 50 μ M ABT for 3 h and imaged every 5 mins. Exposure times were 150 ms. Scale bars, 5 μ m.

3.3.4 Simultaneous loss of Kip1 and Kar3/Cik1 function is lethal

In many of the eukaryotic systems, inactivation of kinesin-14 rescues the lethal spindle defects arising from inhibition or loss of kinesin-5 activity and spindles recover the ability to complete a relatively normal mitotic cycle[67, 72, 104, 108, 109, 114, 115, 119, 174, 182, 194-196]. This has been rationalized as a restoration of force-balance in the spindle, where compensatory spindle forces are provided by MT polymerization and crosslinking proteins[120, 180, 197]. In spite of repeated attempts, we were unable to obtain a *kip1* Δ/Δ *kar3* Δ/Δ strain by traditional methods (data not shown), suggesting they are synthetically lethal. To confirm this, we constructed a *KIP1*-knockout strain containing only one functional copy of *KAR3* that is under the control of the maltose inducible Mal2 promoter. Indeed, when we deactivated the Mal2 promoter by culturing this strain on glucose (YPD media), cell growth was arrested, demonstrating that simultaneous loss of Kar3 and Kip1 is lethal (**Figure 3-7A**). We also observed that *kar3* Δ/Δ and *cik1* Δ/Δ cells were not viable in the presence of ABT (**Figure 3-7B**). To visualize events leading to cell death by loss of Kip1 and Kar3 function, we imaged Tub2-GFP fluorescence in *kar3* Δ/Δ cells treated with 100 μ M ABT by time-lapse microscopy every 15 mins to avoid photobleaching. After 165 mins of imaging, we observed a short anaphase spindle that did not elongate further. Within three hours, spindle structures disappeared, and cells showed no tubulin fluorescence (**Figure 3-7C**). These results demonstrate that kinesin-5- and kinesin-14 have more functional overlap in *C. albicans* than in other organisms.

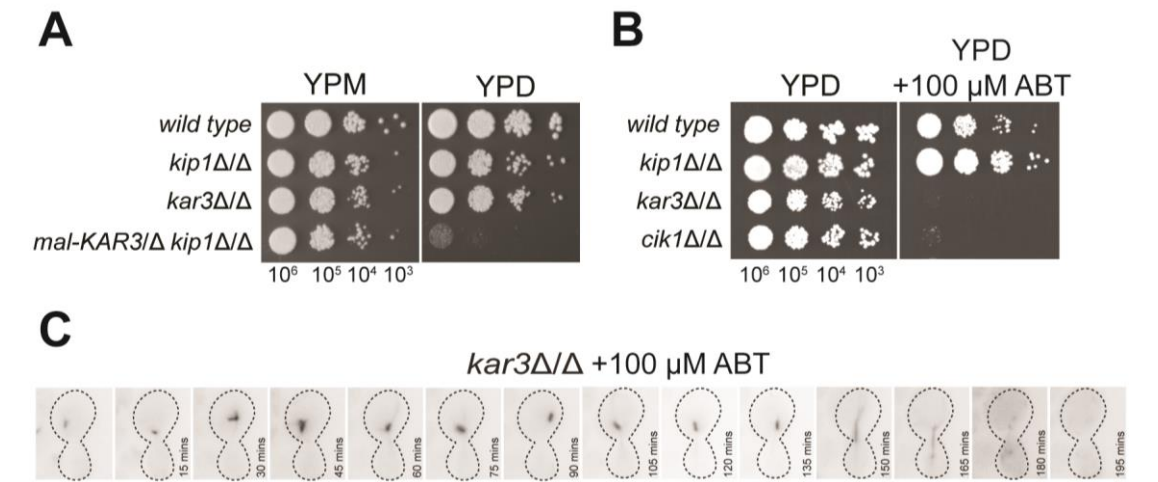


Figure 3-7. Loss of kinesin-5 and kinesin-14 function is lethal. (A) Wild type (CF027), *kip1Δ/Δ* (CF311), *kar3Δ/Δ* (CF024) and *mal-KAR3/Δ kip1Δ/Δ* (CF396) cells were plated on YPM or YPD. Cells were serially diluted to the indicated concentrations and 5 μ L droplets were plated and incubated for 2 days at 25°C. (B) The genotypes indicated in (A), in addition to *cik1Δ/Δ* (CF016), were plated on YPD or YPD+100 μ M ABT and were plated as in (A). (C) Time-lapse microscopy of ABT-treated *kar3Δ/Δ* cells (CF172). Cells were imaged every 15 mins with a 150 ms exposure time to avoid photobleaching. Between 165 to 180 mins, the short anaphase spindle breaks down and disappears.

3.4 Discussion

In nearly every type of eukaryotic system studied, kinesin-5 activity is needed to push newly duplicated centrosomes or SPBs apart to establish spindle bipolarity[69, 83, 169, 170, 172, 176]. Kinesin-5s also crosslink and bundle parallel and antiparallel spindle MTs, and are the major providers for outward forces during anaphase spindle elongation[63, 69, 83, 169, 170, 172, 176, 198]. Without them, most cells exhibit mono-astral spindles and are non-viable[64, 68, 169, 173]. In contrast, our genetic data demonstrates that the sole kinesin-5 gene in *C. albicans* is not essential in diploid cells. Perhaps the recent finding that *KIP1* is an essential gene in a haploid isolate of *C. albicans*[187] is an indication that *KIP1* mutants exhibit a form of ploidy-specific lethality, which is shared by other yeast genes involved in mitotic spindle stability[199]. An alternative explanation for this discrepancy is that there are differences in protein expression between the haploid and diploid proteomes[200]. Our results further show that kinesin-5 is dispensable for spindle assembly and anaphase spindle elongation in *C. albicans*. The only other organisms reported to complete mitosis without kinesin-5 activity are *C. elegans* and *D. discoideum*[79, 81, 201]. Although their mechanisms for kinesin-5-independent bipolar spindle assembly and elongation are not yet known, it has been suggested that cytoplasmic dynein-mediated astral MT pulling forces are involved. We propose that dynein may also fulfill these roles in *C. albicans* in the absence of kinesin-5 activity for several reasons. In earlier studies, *C. albicans* cells lacking the heavy chain of cytoplasmic dynein or the p150^{Glued} subunit of dynactin exhibited spindle position, orientation, and elongation defects, and dramatically slowed nuclear dynamics[130, 202]. In the filament-forming fungus *Ustilago maydis*, it was shown that stationary dynein motors capture and pull on

the plus ends of astral MTs that emanate from SPBs, drawing the attached SPB toward the cortical contact site[136]. In our studies, astral MTs were much longer and more numerous in *kip1Δ/Δ* cells, which could increase the frequency of these MT capture and dynein-mediated pulling events for SPB separation and spindle elongation. We also found *dyn1Δ/Δ* mutants to be non-viable in the presence of the inhibitor ABT, suggesting that Kip1 and dynein have overlapping functions. Our future studies aim to better understand this putative intersection of dynein and Kip1 functions. We will also investigate the alternative possibility that Kip1 has a direct role in limiting the number and length of astral MTs, based on recent evidence that kinesin-5s can act as length-dependent MT depolymerases at kinetochores[33, 163, 203].

Although *kip1Δ/Δ* cells readily assembled metaphase spindles, these spindles were shorter and delayed in transitioning to anaphase relative to wild-type cells. This suggests a role for Kip1 in maintenance of the bipolar spindle prior to anaphase, which is an important kinesin-5 function in other fungi and in *Xenopus* and *Drosophila*[83, 170, 184, 204]. The redistribution of Kip1-GFP fluorescence along the spindle in early anaphase supports such a role. The metaphase-to-anaphase delay in *kip1Δ/Δ* cells may also explain their slower growth rate in liquid cultures. Our observation that *kip1Δ/Δ* spindles sometimes broke apart and then re-assembled two new bipolar spindles also supports this function and implies that Kip1 is acting as a MT crosslinker within the spindle. An alternative explanation for these short, unstable spindles is that Kip1 regulates kMT dynamics, which is important for congression of bioriented sister chromosomes in metaphase. Indeed, *S. cerevisiae*'s Cin8 is important for kinetochore clustering/positioning near the SPBs by crosslinking kMTs and promoting the disassembly of long kMTs[87,

163]. In *S. pombe*, Cut7 is recruited to the kinetochores by a SAC protein, Mad1, to promote chromosome gliding towards the spindle equator[177]. Recent EM reconstructions of *C. albicans* *KIP1/kip1* Δ spindles show disorganized kMTs[33], suggesting that chromosomes are not properly congressed at the spindle equator during metaphase. Without proper chromosome congression, mitotic errors are more likely to occur. Perhaps the short bipolar spindles we observed in *kip1* Δ/Δ cells are indicative of attempts to correct erroneous kMT attachments[33], and that spindle disassembly occurs when they are not corrected. If these cells initiate DNA replication and attempt mitosis again, this could explain the extra spindles and nucleoli observed in a subpopulation of *C. albicans* *kip1* Δ/Δ cells. Further work will be needed to uncover whether or not these defects in nuclear dynamics lead to an increase in the prevalence of aneuploid cells.

Surprisingly, Kip1 loss did not extend the duration of anaphase relative to wild-type, even though Kip1-GFP accumulated at the midzone of late anaphase spindles; a site where it could exert outward MT sliding forces for spindle elongation. This is unique from other fungi and *Drosophila* embryos, which rely on kinesin-5 to crosslink overlapping antiparallel MTs in the spindle midzone and drive anaphase B spindle elongation via plus-end-directed motility[66, 77, 109, 120, 134, 135, 178-180]. While we suspect that dynein provides pulling forces on the spindle to assist in anaphase spindle elongation in the absence of Kip1, it is also possible that other kinesins or MT crosslinking components within the spindle are involved. In fission yeast, kinesin-6 provides additional MT-sliding forces to kinesin-5 at the spindle midzone for anaphase spindle elongation and dynein is not involved[120, 197]. Although *C. albicans* has no kinesin-6 homolog in its genome, it encodes five other kinesin-like proteins in addition to Kip1. Therefore, we have begun to

generate strains lacking different combinations of these proteins in order to identify new collaborative roles of kinesins in mitosis.

By simultaneously disrupting kinesin-5 and kinesin-14 activity, we found that *C. albicans* displays a puzzling exception to the widely-regarded spindle force-balance model[67, 115, 195, 205]. Rather than providing antagonistic spindle forces, Kip1 and Kar3Cik1 may cooperate to focus and stabilize parallel and antiparallel interactions in certain areas of the spindle. In this regard, loss of both kinesins may reduce the number of MT crosslinking factors to an intolerable level that cannot support cell viability. Our previous finding that Kar3Cik1-depleted cells often arrest with two monopolar half-spindles that become pulled apart before assembling a bipolar spindle, supports this idea[113]. Combined with Kip1 loss, MTs may not be well-tethered at SPBs or fail to focus kinetochores, resulting in disorganized spindle structures that quickly break down.

C. albicans is a close relative of the model yeasts *S. pombe* and *S. cerevisiae* but is also an opportunistic fungal pathogen. An assortment of fitness attributes promote its pathogenicity[206], most of which arise by rapid genetic diversification within a population in response to stressful growth conditions as a means of adaptation[10, 146]. Research has shown that aneuploidy accounts for much of this diversity[11, 145, 207], and recent findings suggest that aneuploidies could be induced or enabled by altered activity of mitotic kinesin motors under stress[98, 124, 208-210]. As specific aneuploidies can confer resistance to antifungal drugs through altered gene copy numbers, it could be advantageous for *C. albicans* cells to regulate mitotic kinesins as a way to control aneuploidy occurrence. We are currently conducting studies to delineate the putative contributions of *C. albicans*

kinesins to mitotic defects of cells under stress, and to identify stress-specific regulatory factors that change kinesin activity to promote aneuploidy.

3.5 Materials and Methods

3.5.1 Genetic Manipulations

A list of *C. albicans* strains used in this study is presented in **Table 3-1**. The oligonucleotides used in strain construction are listed in **Table 3-2**. Gene disruption of the *C. albicans KIP1* open reading frame (*Candida* Genome Database: *orf19.8331*; *NCBI* Gene ID: 3645256) was conducted by PCR-based gene targeting and CRISPR-Cas9 methods (CRISPR toolkit kindly provided by Aaron Hernday)[211]. PCR amplification was used to generate disruption cassettes where a selectable marker was flanked by approximately 50 bp of *C. albicans* genomic sequence immediately 5' and 3' of the *KIP1* coding region. Disruption of *KIP1* in a wild type strain (CF027) was conducted sequentially. First a *kip1::LEU2⁺* cassette was amplified from *pSN40*[212] using primers P118 and P119 and transformed into strain CF027. Correct *kip1::LEU2⁺* cassette integration was confirmed using primer pairs P120/P13 and P121/P14 for the upstream and downstream junctions, respectively. To disrupt the second *KIP1* allele, a *kip1::HIS1⁺* cassette was amplified from *pSN52*[212] using primer pair P118/P119 and transformed to create strain CF311. Integration of the disruption cassette at the correct location was confirmed by PCR amplification across the junctions of integration using primers P120/P11 and P121/P12 for the upstream and downstream regions, respectively. CRISPR-Cas9-mediated *kip1* deletion was conducted as previously described[211] using custom gRNA primer P247 and double stranded donor DNA formed using primers P248/P249 to create the strain CF429[211]. To regulate the expression of *KIP1*, the tetracycline-repressible transactivator, the tetO

promoter, and the NAT flipper cassette were PCR amplified from pLC605 (kindly provided by Leah Cowen) using primers P240/P241. The PCR amplified product was transformed into the heterozygous *KIP1* strain to create strain CF436. Correct integration at the *KIP1* locus was verified using primer pairs P120 and P242.

To demonstrate that mutant phenotypes are solely a result of loss of *KIP1*, add-back strains were created to re-introduce a wild type copy of each gene. *KIP1* (+/-1000bp upstream/downstream) gene was cloned into *pCip10*-based integration plasmids bearing the *ARG4*⁺ selectable marker using primers P128/P129[113, 213]. The integration plasmid was digested at a unique restriction site (*PmlI*) to add back to the endogenous *KIP1* region into CF311 to create CF354. Confirmation of integration of *pCip10-ARG4*⁺ vector was done using P121/P170.

A strain lacking both Kip1 and Kar3Cik1 function was created by deleting both copies of *KIP1*, one copy of *KAR3*, and by placing the remaining functional *KAR3* copy under control of a maltose promoter as follows: one copy of the *KAR3* ORF was disrupted using *kar3::HIS1*⁺ knockout cassette amplified using primers P199/P200, transformed into CF027 and confirmed using primers P201/P11 and P202/P12 for the upstream and downstream junctions, respectively. *ARG:MAL:KAR3* cassette was amplified using primer pair P212/P213 from pFA-ARG4-MALp[214] and transformed in *kar3Δ::HIS1*⁺ to create CF411 (not shown). Integration of the cassette was confirmed using primers P201 and P16. *KIP1* was disrupted using *LEU2* (see above) and the *SAT1* Nourseothreicin resistance marker to create the strain CF396. Correct *kip1::SAT1* integration was confirmed with primer pairs P128/P17 and P129/P18.

Fluorescent tagging of *KIP1*⁺ in wild type cells was accomplished using the method described by Gerami-Nejad *et al.* (2001)[215] and using long-tailed primers P137 and P187 and the plasmid *pGFP-SAT1* as a template to create an integration cassette bearing approximately 50 base pairs of *KIP1*⁺ ORF immediately before the stop codon, and of sequence 3' to the ORF. This cassette was transformed into wild type (CF027) to create strain *KIP1-GFP-SAT1*^R. Correct integration was confirmed by PCR using the primer pair P69 and P169. The same integration cassette was also transformed in *cik1*Δ/Δ to create strain CF308 (not shown). *KIP1-mScarlet* was amplified using pSFS2A-mScarlet plasmid pRB897 (kindly provided by Richard Bennett) using primers P284/P285 and transformed into CF421 (pGal1-Tub2-mNeonGreen) to create CF443. Integration was confirmed using primers P254 and P121.

Strains expressing fluorescently labelled β-tubulin were constructed using the plasmids pGal1-Tub2-GFP-SatR::NEUT5L, pGal1-Tub2-mCherry-Arg4::NEUT5L, or pGal1-Tub2-mNeonGreen-Arg4::NEUT5L using the previously described method[113] and adapted to further include sequence of the neutral NEUT5L locus which was linearized using the restriction enzyme *KpnI*. pGal-Tub2-GFP was transformed into CF027 and CF311 to create CF289 and CF226, respectively. pGal-Tub2-mCherry was transformed into wild type, *kip1*Δ/Δ and *cik1*Δ/Δ strains to create CF363, CF368, and CF340 respectively. pGal-Tub2-mCherry was transformed into *KIP1-GFP* to create strain CF338. Correct integration for pGal vectors was confirmed by PCR using primers P16 (or P17- depending on SAT/ARG markers) and P107. To visualize the nucleus, the nucleolar protein Nop1 was fluorescently labelled using pScarlet. The integration cassette was PCR-amplified using primers P243/P244 and transformed into CF289 to create CF417. Correct

integration was confirmed by PCR using primers P254 and P246. To visualize spindle pole body structures, strains expressing *SPC98-GFP* were constructed as previously described[113].

Table 3-1. Names, genotypes, mating types, and sources of the strains used in this study

Strain	Genotype (Brief)	Genotype (Full)	Mating type	Source/parent
CF027	Wild type	<i>his1⁻/his1⁻ leu2⁻/leu2⁻ arg4⁻/arg4⁻</i>	<i>α/α</i>	RBY1133 ^[168]
CF16	<i>cik1Δ/Δ</i>	<i>cik1Δ::LEU2⁺/cik1Δ::HIS1⁺</i>	<i>α/α</i>	Frazer <i>et al.</i> [113]
CF024	<i>kar3Δ/Δ</i>	<i>kar3Δ::LEU2⁺/kar3Δ::HIS1⁺</i>	<i>α/α</i>	RSY11 ^[168]
CF311	<i>kip1Δ/Δ</i>	<i>kip1Δ::LEU2⁺/kip1Δ::HIS1⁺</i>	<i>α/α</i>	CF236 (This study)
CF429	<i>kip1Δ/Δ</i> (CR)	<i>kip1Δ::gRNA</i>	<i>α/α</i>	AHY940[211]
CF436	<i>tetO-KIP1/kip1Δ</i>	<i>tetO-KIP1/kip1Δ::LEU2⁺</i>	<i>α/α</i>	CF236
CF354	<i>kip1Δ/Δ/ KIP1⁺</i>	<i>kip1Δ::HIS1⁺/kip1Δ::LEU2⁺::KIP1-ARG4⁺</i>	<i>α/α</i>	CF311 (This study)
CF338	<i>pGAL-TUB2-mCherry KIP1-GFP</i>	<i>NEUT5L::[pGAL-TUB2-mCherry-SAT1^R]/NEUT5L⁺, KIP1-GFP-ARG4⁺</i>	<i>α/α</i>	CF306 (This study)
CF443	<i>pGAL-TUB2- mNeonGreen KIP1-mScarlet</i>	<i>NEUT5L::[pGAL-TUB2-mNeonGreen- ARG4⁺]/NEUT5L, KIP1-mScarlet-SAT1^R</i>	<i>α/α</i>	CF421 (This study)
CF340	<i>pGAL-TUB2-mCherry KIP1-GFP cik1Δ/Δ</i>	<i>NEUT5L::[pGAL-TUB2-mCherry-SAT1^R]/NEUT5L⁺, KIP1-GFP-ARG4⁺, cik1Δ::LEU2⁺/cik1Δ::HIS1⁺</i>	<i>α/α</i>	CF308 (This study)
CF289	<i>pGAL-TUB2-GFP</i>	<i>NEUT5L::[pGAL-TUB2-GFP-SAT1^R]/NEUT5L</i>	<i>α/α</i>	CF027
CF226	<i>pGAL-TUB2-GFP kip1Δ/Δ</i>	<i>NEUTL5::[pGAL-TUB2-GFP-SAT1^R]/NEUTL5, kip1Δ::ARG4⁺/kip1Δ::LEU2⁺</i>	<i>α/α</i>	CF311 (This study)
CF363	<i>pGAL-TUB2-mCherry SPC98-GFP</i>	<i>NEUTL5::[pGAL-TUB2-mCherry-ARG4^R]/NEUTL5, SPC98-GFP-SAT1^R</i>	<i>α/α</i>	CF156 (This study)
CF368	<i>pGAL-TUB2-mCherry SPC98-GFP kip1Δ/Δ</i>	<i>NEUT5L::[pGAL-TUB2-mCherry-ARG4⁺]/NEUT5L, SPC98-GFP-SAT1^R, kip1Δ::HIS1⁺/kip1Δ::LEU2⁺</i>	<i>α/α</i>	CF286 (This study)
CF163	<i>TUB2-RFP SPC98-GFP cik1Δ/Δ</i>	<i>TUB2-RFP-ARG4, SPC98-GFP-SAT1^R, cik1Δ::LEU2⁺/cik1Δ::HIS1⁺</i>	<i>α/α</i>	Frazer <i>et al.</i> [113]
CF417	<i>pGAL-TUB2-GFP NOP1-mScarlet</i>	<i>NEUT5L::[pGAL-TUB2-GFP-ARG4⁺]/NEUT5L, NOP1-mScarlet-SAT1^R</i>	<i>α/α</i>	CF405 (This study)
CF411	<i>kar3Δ/KAR3-MAL</i>	<i>kar3Δ::HIS1⁺/KAR3-MAL-ARG4⁺</i>	<i>α/α</i>	CF408 (This study)
CF396	<i>kar3Δ/KAR3-MAL kip1Δ/Δ</i>	<i>kar3Δ::HIS1⁺/KAR3-MAL-ARG4⁺, kip1Δ::LEU2⁺/kip1Δ:: SAT1^R</i>	<i>α/α</i>	CF388 (This study)
CF358	<i>dynΔ/Δ</i>	<i>dynΔ::URA3⁺/dynΔ::HIS1⁺, Hhf1-GFP-Arg</i>	<i>α/α</i>	Martin <i>et al.</i> [130]
CF172	<i>pGAL-TUB2-GFP kar3Δ/Δ</i>	<i>NEUTL5::[pGAL-TUB2-GFP-SAT1^R]/NEUTL5, kar3Δ::HIS14⁺/kar3Δ::LEU2⁺</i>	<i>α/α</i>	Frazer <i>et al.</i> [113]

^a Strains are in the *white* phase unless otherwise noted

^b All strains are derived from SN152 (Nobel and Johnson 2005). Full genotype at auxotrophic markers: *his1::hisG/his1::hisG leu2::hisG/leu2::hisG arg4::hisG/arg4::hisG ura3::imm434::URA3/ura3::imm434 iro1::IRO1/iro1::imm434*.

Table 3-2. Oligonucleotide primers used in strain construction

Primer	Name	Sequence (5' to 3')
P118	Long homologous tail knockout primer <i>KIP1::HIS1/LEU2/ARG4</i> 5'	GTTGTTGTTGTTTTTCATTCTTCATCTTGTGATTTTCAGTTAAA TTAATACTCATAGCAGCATTATCATCA ACCAGTGTGATGGATATCTGC
P119	Long homologous tail knockout primer <i>KIP1::HIS1/LEU2/ARG4</i> 3'	AAATAAACCTCACAATTAATTAACATGTACTGAACAAAT GGAGTAAAACAAATATTGGTCTAATTATA AGCTCGGATCCACTAGTAACG
P120	-500bp <i>KIP1</i> check 5'	CGCACAAGACCTGGCACAAGAGAA
P121	+500bp <i>KIP1</i> check 3'	ATGGGCCAATGGGATCACATGG
P11	<i>HIS1</i> check right 3'	AACACAACCTGCACAATCTGGC
P12	<i>HIS1</i> check left 5'	ATTAGATACGTTGGTGGTTCAGTT
P13	<i>LEU2</i> check left 3'	AGAATTCCTCAACTTTGTCTGTTC
P14	<i>LEU2</i> check right 5'	AAACTTTGAACCCGGCTGCG
P247	<i>KIP1</i> gRNA for Fragment B stitching	CGTAAACTATTTTTAATTTGCGAAGTAATACTGCTTGTGGG TTTTAGAGCTAGAAATAGC
P248	<i>KIP1</i> Donor DNA with mini AT 5'	ATTCTTCATCTTGTGATTTTCAGTTAAATTAATACTCATAGC AGCggGACCAATATTTGTTTTACTCCATTTGTTTCAGTACATG TTTAATTAATTGT
P249	<i>KIP1</i> Donor DNA with mini AT 3'	ACAATTAATTAACATGTACTGAACAAATGGAGTAAAACA AATATTGGTcGCTGCTATGAGTATTAATTTAACTGAAAT CACAAGATGAAGAAT
P240	<i>KIP1 tet-O-SAT^R</i> Flipper 5'	ATTCATTCAATCAATCAGAGTAGTTTTAATATCTTCTTATA GTGGCCTGCATATAGTTCAATCACGAC GGAAACAGCTATGACCATG
P241	<i>KIP1 tet-O-SAT^R</i> Flipper 3'	GAGATTTAGCAGCAATCTCTTGAGAGTTCCTTCCTCGACAT CTAACAACTTGGATATTGA CCGCGG CGACTATTATATTGTATG
P242	<i>tet-O</i> check 3'	AGTTATTGAATCTATTACTCAATCG
P170	<i>KIP1</i> ORF confirmation primer 3'	CTTCATTCACTATATTCCAACCTGTGATTG
P128	<i>KIP1</i> into pClp10 (MluI) primer 5'	GGACCGACGCGTCACAGAGAGAGAGAGAGAGAAAGA GAATGAG
P129	<i>KIP1</i> into pClp10 (KpnI) primer 3'	GGACCG GGTACCCATCATCAACATAATCAACCACATCACCCACA
P199	Long homologous tail knockout primer <i>KAR3::HIS1/LEU2/ARG4</i> 5'	TCAAAAAGTTGCCAGACAGGTTTTTACAATTTTGAAACT ACAATCCAATAGTCAATCGTGCACAAGTA ACCAGTGTGATGGATATCTGC
P200	Long homologous tail knockout primer <i>KAR3::HIS1⁺/LEU2⁺/ARG4⁺</i> 3'	TATATCTGAGCCAATATTTAAATAGATTCTTGTATATAAGT CATGTATGTAAACTATTAACGTAGTAAT AGCTCGGATCCACTAGTAACG
P201	-1000bp <i>KAR3</i> check 5'	GTCCCAACTTCTCCTTATTGACTTCTT
P202	+1000bp <i>KAR3</i> check 3'	GTTGCCTAAAATTCCTAAGGACCT

P212	<i>ARG4-MAL-KAR3</i> long homologous primer 5'	AAAGAAAACTTGCCCATCTCATCGAGAGTCTAATTTCTT ACGCGGGAAGTAGAAAAAAAAAACTGAA <i>GAAGCTTCGTACGCTGCAGGTC</i>
P213	<i>ARG4-MAL-KAR3</i> long homologous primer 3'	CCACCTAAAAGATTTGATGGTTGTGACACATTTAGAAATT TATGTTTAGTATTTTCGTCACAT CAT <i>TGTAGTTGATTATTAGTTAAACCAC</i>
P16	<i>ARG4</i> check left 3'	TTCCATTTAGAGAACTCATCATATTT
P17	<i>SAT1^R</i> check left 3'	CATACCACCGTCCATTTTGAATG
P18	<i>SAT1^R</i> check right 5'	TGATGAAGACTCTGCTTGCTATG
P137	<i>KIP1-GFP-ARG4</i> or <i>SAT1^R</i> long-tailed primer (C-term) 5'	TTCTACCACGACCAATAATAATAAAAAAGAGAAAAATATTA CAAACAATGGACAATTTATTAGGTTGGTTCTAAAGGTG <i>AAGAATTATT</i>
P187	<i>KIP1-GFP-ARG4</i> or <i>SAT1^R</i> long-tailed primer (C-term) 3'	CATATATTATATATTAATATTATTAAGAGTTTTTGGAAATA TGGAAGTATAATGAGGAGGACCACCTTTGATTGTAATAGT <i>AATAATTA</i>
P69	<i>GFP</i> sequencing/left junction check 3'	GATCTGGGTATCTAGCAAAAC
P169	<i>KIP1</i> ORF confirmation primer 5'	GCACAAGTCAATCTACTGGAAACAT
P284	<i>KIP1-mScarlet</i> localization long-tail 5'	TGTTGTTGTTTTTCATTCTTCATCTTGTGATTTTCAGTTAAATT AATACTCATAGCAGCATTATCATCA <i>GACTACTATAGGGCGAATTGGG</i>
P285	<i>KIP1-mScarlet</i> localization long-tail 3'	AAATAAACCTCACAAATTAATAAACATGTACTGAACAAAT GGAGTAAAACAAATATTGGTCTAATTATA <i>CAAAAGCTGGAGCTCCACCGC</i>
P254	<i>mScarlet</i> check 5'	GTAGATATTTGGCTGATTTCAAAAC
P108	<i>SPC98-GFP-SAT1^R</i> long-tailed primer for pGFP-Sat1 5'	TTTGAAAAATGATTTGAATAGAGATTATAATTTAAAGGAT CTTAGTAAGTTGTT GGTGGTGGT <i>TCTAAAGGTGAAGAATTACTCTGG</i>
P109	<i>SPC98-GFP-SAT1^R</i> long-tailed primer for pGFP-SAT1 3'	TGAGCTTTACAGAGATCTGTTCGTAATCATAGATTTCCCC ACTTGTCTGTAATCGACGAAATTG <i>AGGACCACCTTTGATTGTAATAG</i>
P110	<i>SPC98-GFP</i> integration check 3'	GCAGCGTCCACCTTTGTAAAAGTG
P107	<i>pGAL-TUB2-GFP/mCherry/mNeonGreen</i> downstream check 3'	TATTATCTATATTGTCAAGCCAAGACAAGCCCATT
P243	<i>NOPI-mScarlet</i> long-tail 5'	ACCTTATGAAAGAGACCATTGTATTGTTGTTGGTAGATAC ATGAGAAGCGGAATAAAAGAAA GGTGGTAGTGGTATGGTTTCTAAAG
P244	<i>NOPI-mScarlet</i> long-tail 3'	AAGGTCAAAGTGCCATCAAAGGTGTGTTATTGGGTTTCATT ATCAAATATTTGGTGACAA <i>GGCGGCCGCTCTAGAAGTAGTGATC</i>
P246	<i>NOPI</i> check 3'	CGATTGAACATGTTAAACAAAGC

Bold and italic: portion of primer homologous to plasmid template

underline: restriction enzyme cut site.

3.5.2 *C. albicans* Transformation

Disruption cassettes, fluorescent tags, and complementation plasmids were transformed into *C. albicans* using the lithium acetate/PolyEthylene Glycol (PEG)/heat shock method as previously described with minor modifications[216]. Incubation of cells with transforming DNA in lithium acetate/PEG solution was carried out for two hours at 30°C with rotation. Heat-shock was conducted at 43°C for 30 minutes. Transformations involving selection using the *SATI* gene were accompanied by a four-hour incubation in YPD (1% yeast extract, 2 % peptone and 2 % glucose) at 30°C to allow expression of the ClonNAT resistance gene before plating on selection media.

3.5.3 *C. albicans* Cell Culture and Growth Assays

Strains were maintained on YPD plates. YPD was supplemented with 200 µg/mL Nourseothricin (CloneNat, Werner BioAgents) for selection of positive *SATI* gene integration. Selection for auxotrophic markers was conducted using synthetic dropout (SD) media containing 0.66 % yeast nitrogen base, 0.2 % yeast dropout mix lacking uracil, arginine, leucine and histidine, 2 % glucose, 200 mg/L uridine and supplemented with 200 mg/L histidine, leucine and/or arginine where required. Experimental cultures were grown to mid-logarithmic phase in completely supplemented dropout media (SDC) unless otherwise indicated. In order to assess the generation time, logarithmically growing cells were diluted to 2.5×10^6 cells/mL in fresh medium and the density was measured hourly using a hemocytometer. To create dilutions for spot assays, logarithmically growing cells were diluted to 1.0×10^6 cells/mL in PBS. Serial dilutions of 10^5 , 10^4 , and 10^3 cells/mL were made. Five µL of cell culture dilutions were pipetted for each spot and plates were incubated at 30°C for two days, unless otherwise indicated.

3.5.4 Light Microscopy

Microscopy for static images was conducted using a Zeiss Axio Observer epifluorescence microscope with a 100X (1.40 NA) oil objective, AxioCam hRM camera controlled by Axiovision software. Time-lapse imaging was conducted using the Olympus IX83 with a 100X oil objective (1.4 NA), Andor Zyla 4.2 Plus camera controlled by the cellSens software. For time-lapse and static imaging, logarithmically growing cells were immobilized between an agarose pad and a glass coverslip, as previously described[113]. For time-lapses, images were captured in five Z-slices, 0.8 μm apart. Image stacks and pole-pole distances were analyzed with ImageJ (NIH). Graphs were calculated and displayed using Graphpad Software; figures were compiled in Adobe Photoshop and Adobe Illustrator. We thank Drs. Shetuan Zhang and Peter Davies for the use of microscopy facilities.

3.5.5 RNA Sequencing

Logarithmically growing yeast cells were harvested and centrifuged at 4,000 g for 10 min at 4°C. Cell pellets were flash frozen in liquid nitrogen and genomic DNA-free total RNA was extracted from each pellet by grinding the fungal mass to a fine powder and resuspending in 1 ml TRIzol (Ambion) solution and using the RNeasy mini spin columns (Qiagen) following the manufacturer's protocol. RNA quantification was carried out spectrophotometrically at 260 nm and 280 nm and RNA integrity was evaluated by NanoDrop2000 (Thermo Scientific). Total RNA (1 μg /sample) was shipped to the National Research Council of Canada, DNA Sequencing Technologies Facility (Saskatoon, Canada) where further quality check was performed using a BioAnalyzer followed by short cDNA fragment synthesis using TruSeq Stranded RNALT kit, and finally sequenced on an

Illumina HiSeq 2500 platform according to the manufacturer's guidelines (Illumina, USA). The DESeq2 based SARTools (v1.5.1) pipeline as previously described[217] was adopted for differential analysis of mapped *C. albicans* Assembly 22 RNAseq count data. The Benjamini-Hochberg p -value adjustment was performed[218, 219] and the false discovery rate was set at $p < 0.05$. We thank Dr. Michèle Loewen and Simon Foote for RNA sequencing collection and analysis.

Chapter 4

Dynein contributes to spindle elongation during anaphase in *Candida albicans*

4.1 Abstract

Budding yeast must position the mitotic spindle at the mother-bud junction during anaphase to provide a complete set of chromosomes to the daughter cell. Pushing and pulling forces on astral MTs from cortex-bound dyneins are critical for spindle positioning. Certain higher eukaryotes and filamentous fungi employ dynein to accelerate spindle elongation during anaphase. This dynein role is less apparent in yeast, where intra-spindle pushing forces from kinesin-5 motors are the main drivers of spindle elongation. However, our previous studies showed that spindle elongation could occur in *C. albicans* without a functional kinesin-5. Here, evidence is provided that *C. albicans* dynein, Dyn1, collaborates with kinesin-5, Kip1, to facilitate spindle elongation by pulling on SPB-bound astral MTs. Simultaneous loss of both motors is lethal and stems from an inability to initiate spindle elongation. Either motor can partially compensate for the loss of the other. Cells lacking Kip1 appear to rely on external pulling forces from an elevated abundance of Dyn1 motors and astral MTs. Dyn1-depleted cells rely on Kip1 pushing forces within the spindle and increased numbers of astral MTs that can assist in nuclear positioning and spindle elongation. The importance of astral MT dynamics in cells depleted of either motor is supported by the lethal effects of *dyn1Δ/Δ* mutant cell exposure to temperatures that destabilize astral MTs or the addition of MT-destabilizing drugs. Altogether, these results

demonstrate that *C. albicans* spindle elongation involves cooperative forces between Kip1 and Dyn1 to ensure timely and accurate separation of chromosomes during cell division.

4.2 Introduction

Mitotic chromosome segregation involves the equal partitioning of genetic information to daughter cells before cell division. This process depends on the assembly of a bipolar MT-based structure called the mitotic spindle, which must then form stable attachments to chromosomes, test that these connections were made correctly, and then separate sister chromatids to opposite ends of the dividing cell. All these activities require the help of teams of MT-binding motor proteins that apply directional forces on and within the spindle[220-222]. Spindle assembly and function also rely on a fine-tuned balance of forces from MT polymerization/depolymerization events that are regulated by other MT-associated proteins[220-222].

Physical separation of disjoined sister chromatids occurs during anaphase. In most eukaryotes, sister chromatids are first pulled towards the poles by depolymerizing the MTs bound to chromosomes, while overall spindle length is maintained. This process is referred to as anaphase A. In anaphase B, overlapping ipMTs in the spindle midzone slide apart, causing the two opposing spindle poles to separate and the disjoined chromatids to move toward their respective cellular compartments[223, 224]. Surprisingly, a universal mechanism explaining the origins of all forces required for anaphase B is still lacking as research continues to uncover more organism-specific spindle elongation force-producers and regulatory processes thereof[225]. In general, though, the major spindle forces of anaphase B typically include (i) ipMT sliding by spindle motors, (ii) ipMT braking by MT crosslinkers, (iii) pulling of aMTs from the cell cortex by dynein, and (iv) ipMT dynamics

by MT plus-end polymerization/depolymerization and MT minus-end depolymerization manifesting as poleward flux[62, 201, 222, 226-234]. Different combinations of these components generate distinct anaphase B mechanisms in different cell types.

In *C. albicans*, MTs are attached directly to the SPBs and are stabilized, resulting in the absence of MT flux[40]. In addition, anaphase A is not observed at the start of anaphase. Instead, chromosome segregation happens in anaphase B, where ipMT sliding by motor proteins in the cell midzone elongate the spindle, contemporaneously pulling each sister chromatid poleward[77]. Here, MT midzone-localized plus-end directed kinesin-5 motors crosslink antiparallel ipMTs and slide them outward, past each other[63, 77, 82, 135, 227, 233-235]. What remains unclear is the extent to which kinesin-5 pushing forces are required in spindle elongation. Recent studies have shown that alternative or complementary mechanisms by motors located at the cell cortex may also contribute forces for anaphase spindle elongation[136, 228, 236, 237]. For example, laser-mediated MT surgery experiments revealed that external forces are applied on the spindle via aMTs emanating from the spindle poles[228, 236, 238]. Here, dynein motors near the cell cortex bind these aMTs and apply pulling forces on the spindle[116, 193, 239-241]. In *C. elegans* and filamentous fungi, these dynein-mediated pulling events generate the primary spindle elongation force, while their kinesin-5 proteins are mainly employed to constrain the rate of spindle elongation[136, 228].

Previous studies in *C. albicans* showed dynein, Dyn1, to be important in nuclear positioning, but its role in spindle elongation was not defined[130]. Therefore, we studied the mitotic spindle phenotypes of cells depleted of Dyn1 as well as cells that lacked both Dyn1 and Kip1 activity. We observed that cells lacking Dyn1 could form anaphase spindles

but often failed to orient the spindle across the mother-bud junction. Dyn1-depleted cells that succeeded in segregating their nuclei to mother and daughter cells appeared to rely on Kip1 and polymerization of increased numbers of aMTs for compensatory forces. Conversely, cells lacking Kip1 contained an elevated abundance of dynein motors on aMTs. In the absence of both Dyn1 and Kip1 activity, cells arrested with a pre-anaphase spindle. Based on these findings, we propose that Kip1, Dyn1, and MT dynamics provide cooperative but spatially distinct spindle forces during anaphase.

4.3 Results

4.3.1 Dynein has overlapping functions with Kip1 in anaphase spindle elongation

In previous studies, we demonstrated that in wild-type *C. albicans*, the duration of anaphase lasts approximately 20 minutes[242]. We also showed that bipolar spindles can form and elongate in the absence of Kip1 but are ~25% shorter. *kip1* Δ/Δ spindles also had drastically longer and more numerous aMTs attached to their poles[242]. A possible explanation for these observations is that *kip1* Δ/Δ cells rely on Dyn1 motors distributed near the cell cortex to bind these aMTs and pull on them to elongate the spindle, thereby compensating for the loss of intra-spindle pushing forces from Kip1. If this is the case, Kip1 and Dyn1 likely function together during anaphase in wild-type cells. To investigate this putative functional overlap between Kip1 and Dyn1 in spindle elongation, we studied the growth and mitotic spindle phenotype of cells in which the activity of one or both motors was perturbed.

On solid YPD media, growth of *dyn1* Δ/Δ cells at 30 °C was reduced compared to wild-type but was comparable to cells lacking either *KIP1* (null mutants obtained by homologous recombination, CRISPR-based targeting (CR), and a TET-Off expression

system) or the kinesin-14 *KAR3* (**Figure 4-1A**). On YPD media supplemented with 100 μM of the Kip1-specific inhibitor ABT[167], *dyn1 Δ/Δ* cells were not viable. Similar growth defects were observed when *dyn1 Δ/Δ* cells were grown in liquid cultures supplemented with 100 μM ABT (**Figure 4-1B**). To identify cell cycle defects that could explain the death phenotype of ABT-treated *dyn1 Δ/Δ* cells, we generated wild type and *dyn1 Δ/Δ* cells that expressed β -tubulin fused to green fluorescent protein (Tub2-GFP) and mScarlet-labeled nucleolar protein (Nop1-mScarlet), allowing us to track morphologic changes in their mitotic spindle and nucleus, respectively, during progression through mitosis. To avoid lethality, we first grew these cells in ABT-free media and then added 50 μM ABT for three hours before imaging them by time-lapse fluorescence microscopy. **Figure 4-1C** shows that, following incubation with ABT, *dyn1 Δ/Δ* cells contained a single spot of nuclear fluorescence and a short, pre-anaphase spindle that persisted in the mother cell for the entire time-lapse (over 200 minutes) (**Figure 4-1C, row 4**). In comparison, untreated wild-type cells completed anaphase within 20 minutes. Suspecting that ABT addition prevented anaphase initiation, we added increasing concentrations of ABT to unsynchronized cell populations of *dyn1 Δ/Δ* mutants and compared the lengths of their spindles to those of wild-type and *dyn1 Δ/Δ* cells that were not exposed to ABT. We observed that, as ABT concentration increased, the average spindle lengths in *dyn1 Δ/Δ* cells decreased (mean lengths: wild type = 2.26 μm , *dyn1 Δ/Δ* = 2.54 μm , *dyn1 Δ/Δ* + 75 μM ABT = 1.4 μm , *dyn1 Δ/Δ* + 100 μM ABT = 1.0 μm ; $p < 0.05$) and that very few ABT-treated *dyn1 Δ/Δ* cells had spindles longer than 3 μm (**Figure 4-1D**). These data show that cells lacking both Kip1 and Dyn1 activity cannot enter anaphase, suggesting that both motors contribute forces for spindle elongation.

4.3.2 Dynein localization on astral MTs increases in the absence of Kip1

To further investigate the involvement of Dyn1 in anaphase spindle elongation in *C. albicans*, we constructed a Dyn1-mNeonGreen-labeled strain by inserting the coding sequence of the fluorescent protein mNeonGreen in frame with the 3' end of the chromosomal gene for dynein heavy chain *DYN1* (Dyn1-mNeonGreen). We engineered this strain to co-express a Tub2-mScarlet fusion protein, allowing us to compare Dyn1 localization in relation to the mitotic spindle and aMTs. In 70% of cells with small buds and metaphase spindles, Dyn1-mNeonGreen fluorescence was prominent on the plus ends of aMTs that extended towards or into the bud (**Figure 4-2A, wild type panel, row 1**). This asymmetric localization of Dyn1 has been observed in other *C. albicans* studies and in *S. cerevisiae* and helps with spindle positioning and orientation, ensuring that the daughter SPB enters the bud during cell division[202, 240, 243]. In 82% of cells with long anaphase spindles, in which the daughter SPB had moved into the bud, two to four Dyn1-mNeonGreen spots were visible at the plus ends of aMTs from both SPBs (**Figure 4-2A, wild type panel, rows 2 and 3**). In these cells, Dyn1-mNeonGreen was usually localized near the cortex of the mother and daughter compartments.

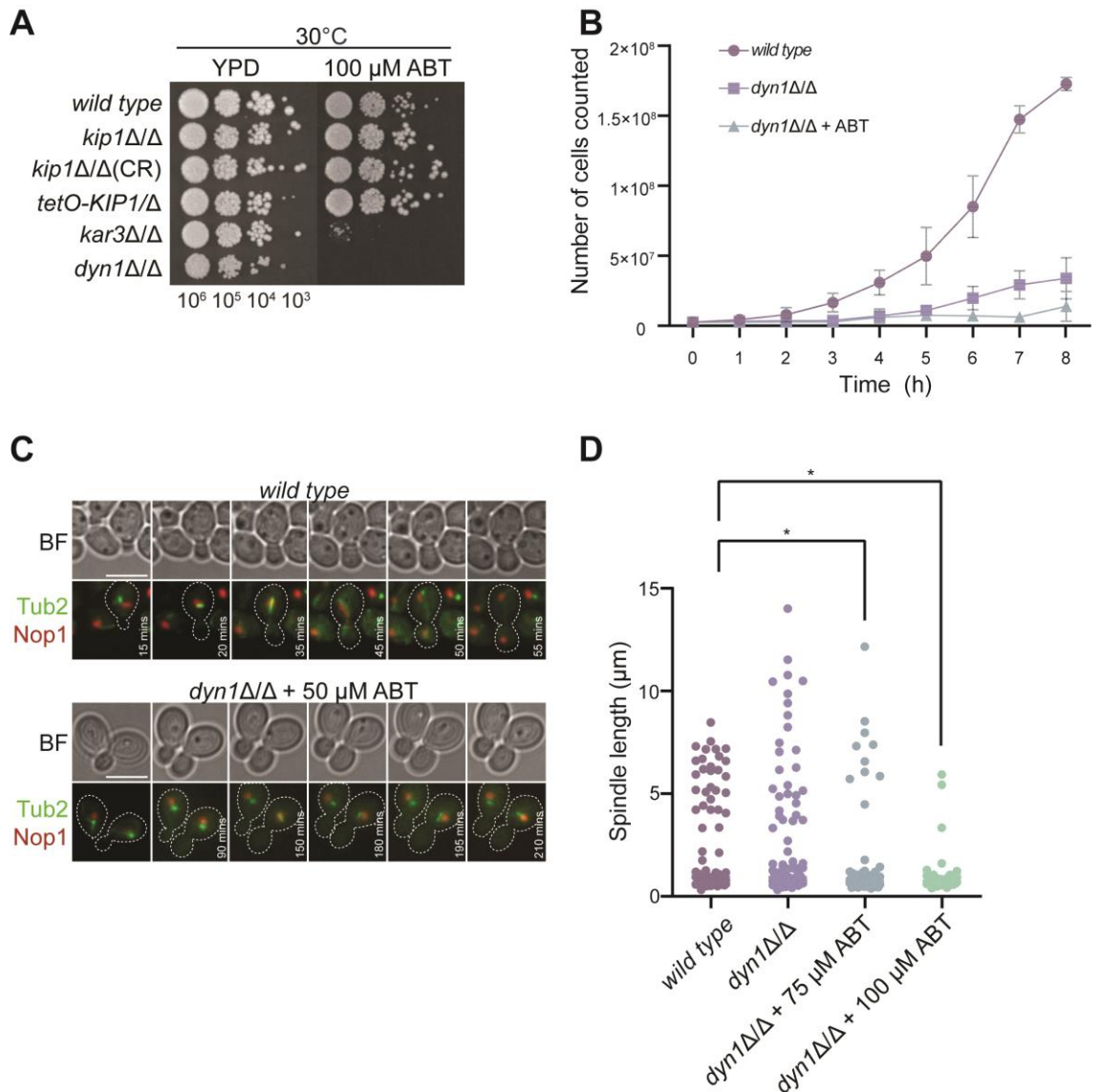


Figure 4-1. Simultaneous loss of Dyn1 and Kip1 function is lethal. (A) Wild type (CF027), *kip1Δ/Δ* (CF311, CRISPR-targeted null strain CF429, TET-Off expression strain CF436), *kar3Δ/Δ* (CF024) *dyn1Δ/Δ* (CF495) cells were plated on YPD or YPD + 100 μM ABT. Cells were serially diluted to the indicated concentrations and 5 μL drops were plated and incubated for 2 days at 30°C. (B) Cell growth assay of wild type (CF027), *kip1Δ/Δ* (CF311) and *dyn1Δ/Δ* (CF495) with and without 100 μM ABT. Strains in YPD media were diluted 2.5 x 10⁶ cells per mL, incubated at 30°C, and counted every hour using a hemocytometer. Data points represent an average from three independent experiments +/-

standard deviation (SD). (C) Time-lapse microscopy of wild type and *dyn1Δ/Δ* cells expressing Nop1-mScarlet and Tub2-GFP (CF417, CF486). 50 μM of ABT was added to *dyn1Δ/Δ* cells and incubated for 3 h before imaging. Images were collected every 5 mins with exposure times of 150 ms for both fluorescent tags. Scale bar, 5 μm. (D) Quantification of all spindle lengths observed in unsynchronized cell populations of wild type (CF405) (n=101), *dyn1Δ/Δ* (CF542) (n=101), *dyn1Δ/Δ* + 75 μM ABT (n=101), and *dyn1Δ/Δ* + 100 μM ABT (n=50) cells. Cells were grown to mid-logarithmic phase in SDC (supplemented with sucrose and galactose) and ABT was then added and incubated for 1 h (* $p < 0.05$).

If Dyn1 provides pulling forces on the aMTs of each SPB for anaphase spindle elongation, we speculated that the abundance of Dyn1 motors on these MTs would have to increase if Kip1 pushing forces from within the spindle were eliminated or inhibited. To investigate this possibility, we examined the location and abundance of Dyn1-mNeonGreen in *kip1* Δ/Δ and ABT-treated wild-type cells. Compared to wild-type cells, *kip1* Δ/Δ mutants usually exhibited two or three more fluorescent Dyn1 foci in both the mother and daughter cell, regardless of the cell cycle phase (**Figure 4-2A and B**) (average number of dots: wild type = 2, *kip1* Δ/Δ = 6, ABT-treated wild type = 2). Moreover, there was a 1.2-fold increase in the overall Dyn1-mNeonGreen fluorescence intensity in ABT-treated wild-type cells compared to untreated cells (average Dyn1 intensity: wild type = 95.6 (n = 30), *kip1* Δ/Δ = 77.2 (n = 30), ABT-treated wild type = 113.7 (n = 30)) (**Figure 4-2A and C**). We speculate that this small increase in Dyn1 fluorescence with ABT treatment is an indication that even more Dyn1 is needed to compensate for ABT's inhibitory effect on Kip1. Rather than eliminating pushing forces by Kip1 motors within the spindle, ABT-inhibited Kip1 motors could form a rigor-like complex with the MT[167]. Thus, a considerable increase in pulling forces from cortical Dyn1 may be required to break apart a rigid bipolar spindle stabilized by ipMT-locked Kip1 motors.

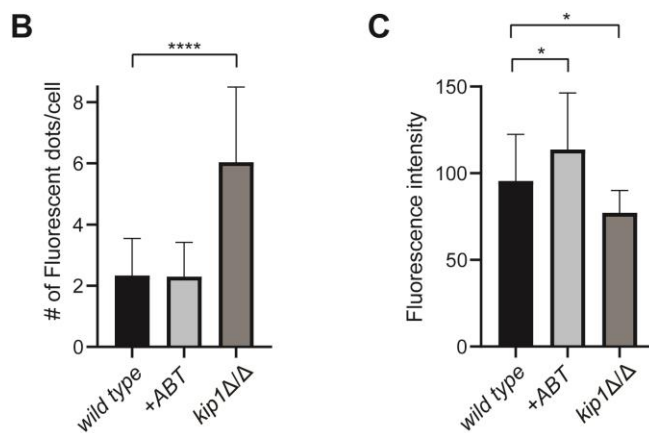
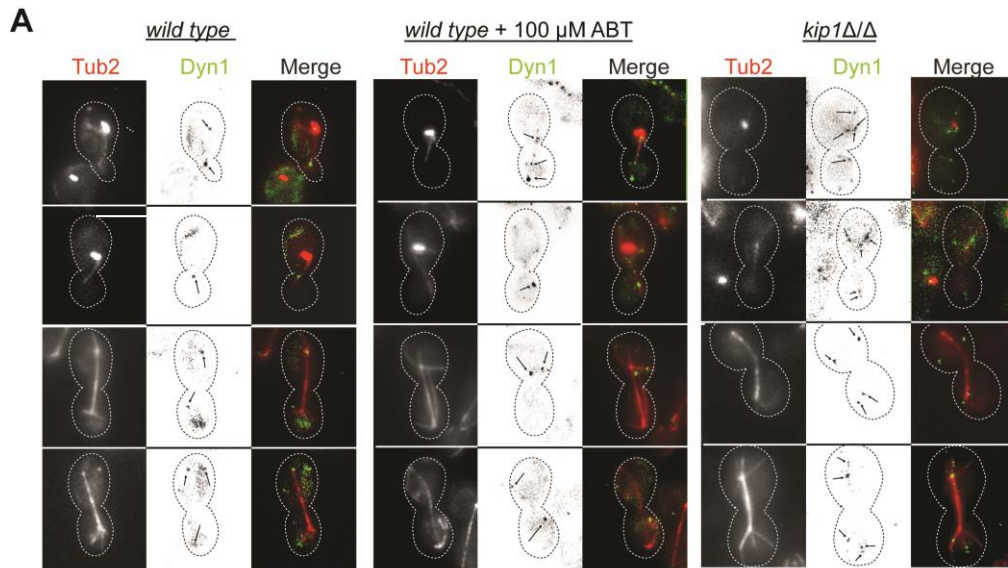


Figure 4-2. Dyn1 localization and abundance increases when Kip1 function is lost or inhibited. (A) Images of wild type and *kip1Δ/Δ* cells expressing Tub2-mScarlet and Dyn1-mNeonGreen (strains CF546, CF543). For Kip1 inhibition in wild type cells, 100 μM of ABT was added and incubated for 3 h. Representative cells at different stages of mitosis were selected. All cells were obtained from logarithmically growing, unsynchronized cultures in SDC-sucrose medium at 30°C. Scale bars, 5 μm. (B) The number of Dyn1 fluorescent patches in cell types from (A) was counted and graphed (wild type n = 30, *kip1Δ/Δ* n = 30, ABT-treated wild type n = 30, $p < 0.0001$). (C) Quantification of Dyn1 fluorescence intensity in all three cell types from (A). Dyn1 fluorescence intensity was measured against background using ImageJ Software ($p < 0.05$).

4.3.3 The duration of anaphase is nearly tripled in *dyn1* Δ/Δ cells

To understand how Dyn1 contributes to spindle elongation in *C. albicans*, we tracked spindle dynamics and nuclear segregation in dividing *dyn1* Δ/Δ cells using time-lapse imaging of Tub2-GFP and Nop1-mScarlet fluorescence, respectively. We found that most cells formed normal-looking bipolar spindles that elongated and separated the Nop1-mScarlet fluorescence into two distinct foci. However, the duration of anaphase in wild-type cells was significantly lower than *dyn1* Δ/Δ cells (average anaphase time in wild type = 21.3 mins (n = 11); *dyn1* Δ/Δ = 49.5 mins (n = 34), $p < 0001$) (**Figure 4-3A**). When we made kymographs of the wild-type and *dyn1* Δ/Δ spindles, beginning from bipolar spindle appearance and ending at late anaphase, we found that 60% of *dyn1* Δ/Δ cells remained in anaphase for an average of 60.8 mins before the spindle disassembled (**Figure 4-3B**). Just over half of these cells (~60%) underwent anaphase spindle elongation within the mother cell (**Figure 4-3C and E**). The rest (~40%) succeeded in elongating the spindle across the mother-bud junction (**Figure 4-3D, cell 2, and Figure 4-3E**). Thus, even the *dyn1* Δ/Δ cells that succeeded in moving the daughter SPB into the bud were delayed in spindle disassembly (**Figure 4-3F**). Another curious finding was that many *dyn1* Δ/Δ anaphase spindles showed signs of buckling (bending), especially when these spindles were trapped in the mother cell compartment (**Figure 4-3D, cell 1**). These data demonstrate that *dyn1* Δ/Δ cells have difficulty positioning the spindle for entry into the mother-bud junction and that Kip1 provides the bulk of the force for spindle elongation. We suspect that the spindle buckling events in *dyn1* Δ/Δ cells result from an inability of intra-spindle pushing forces from Kip1 to overcome the compression forces on the spindle when Dyn1 is absent[244].

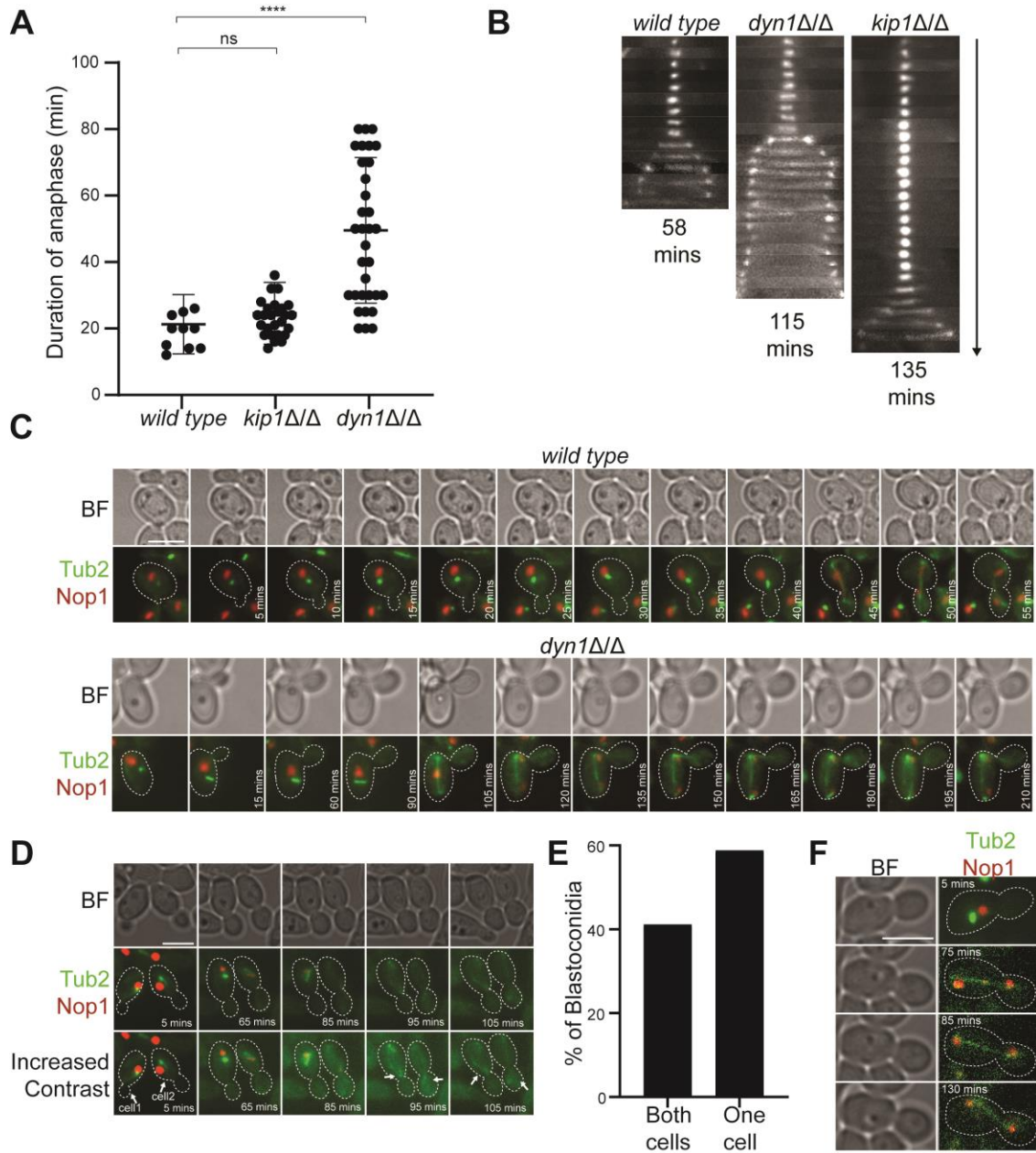


Figure 4-3. Dyn1 mutants exhibit unusual anaphase dynamics. (A and B) Quantification of wild type, *kip1Δ/Δ*, and *dyn1Δ/Δ* cells using time-lapse microscopy to analyze the duration of anaphase. Long (2 to 4 h) time-lapse series were captured with 150-ms exposures to measure the length of time from start to the end of anaphase for Tub2-GFP ($n = 11$), Tub2-GFP *kip1Δ/Δ* ($n = 28$), and Tub2-GFP *dyn1Δ/Δ* ($n = 34$) ($p < 0001$). Representative kymograph is illustrated in (B) for all three strains. (C and D) Time-lapse microscopy of wild type and *dyn1Δ/Δ* cells expressing Nop1-mScarlet and Tub2-GFP

(CF417, CF486). Images in the lower panel of *dyn1* Δ/Δ of (C) illustrate anaphase events occurring in the mother cell only. Images in (D) represent two scenarios of anaphase events in *dyn1* Δ/Δ cells. Cell 1 indicates anaphase occurring between the mother-bud neck. Cell 2 shows ‘buckling’ of the anaphase spindle. Images were collected every 5 mins with exposure times of 150 ms for both fluorescent tags. Scale bar, 5 μm . (E) Quantification of anaphase events in *dyn1* Δ/Δ cells occurring across mother-bud junction or solely in the mother cell. (F) Time-lapse microscopy of *dyn1* Δ/Δ cells expressing Nop1-mScarlet and Tub2-GFP (CF486). Spindle disassembly is not initiated even after the spindle has elongated into the bud.

4.3.4 MT polymerization forces facilitate *C. albicans* spindle positioning and elongation

Previous studies in *S. pombe* showed that MT polymerization-derived pushing forces are sufficient to promote spindle pole separation and assembly of a bipolar spindle in the absence of molecular motors[120, 121, 221]. Similar results have been observed in higher eukaryotes, signifying an evolutionary conservation of MT-based forces within the spindle[245, 246]. A curious phenotype of our *dyn1Δ/Δ* cells was that they formed longer and more numerous aMTs than wild-type cells (mean aMT lengths: wild type = 2.2 μm ± 1.25 SD, *dyn1Δ/Δ* = 3.9 μm ± 2.8 SD; mean aMT number: wild type = 1 aMT ± 1 SD, *dyn1Δ/Δ* = 4 ± 2 SD), suggesting that *C. albicans* may use MT polymerization forces in addition to motor-derived forces for spindle morphogenesis and chromosome segregation (**Figure 4-4A,B, and C**). Moreover, aMT dynamics could provide pushing forces to orient the spindle without dynein[222]. To investigate this possibility, we studied *dyn1Δ/Δ* cell growth under two different MT polymerization-disrupting conditions: (1) Nocodazole treatment and (2) cold temperature (8°C). As expected, when we incubated liquid cultures of unsynchronized wild-type and *dyn1Δ/Δ* cells with 50 μM nocodazole for six hours and then obtained snapshots of the spindles in these cell populations by fluorescence microscopy, we found that both strains formed normal-looking mitotic spindles but lacked aMTs (**Figure 4-4D**). In a dilution spot assay of cells grown on solid YPD media supplemented with 100 μM Nocodazole, *dyn1Δ/Δ* cells showed the most substantial growth defect (**Figure 4-4E**). Likewise, *dyn1Δ/Δ* cells were much more sensitive to Nocodazole compared to wild-type and *kip1Δ/Δ* cells when grown in liquid cultures (**Figure 4-4F**).

Similar growth defects were observed when wild type, *kip1Δ/Δ*, *kar3Δ/Δ*, and *dyn1Δ/Δ* cells were spotted on YPD plates and grown at a cold temperature (8°C) (**Figure 4-4G**). At this temperature, MT polymerization kinetics are dramatically slower, and MTs are less stable (Polymerization rates (μm/min): 10°C = 0.62 ± 0.16 , 30° = 1.15 ± 0.07 ; Depolymerization rates (μm/min): 10°C = 0.57 ± 0.16 , 30° = 1.94 ± 0.15 [247]). These results suggest that *C. albicans* uses MT polymerization forces to help in spindle positioning, and that these cells can employ these MT forces when faced with a motor-derived force deficit or imbalance.

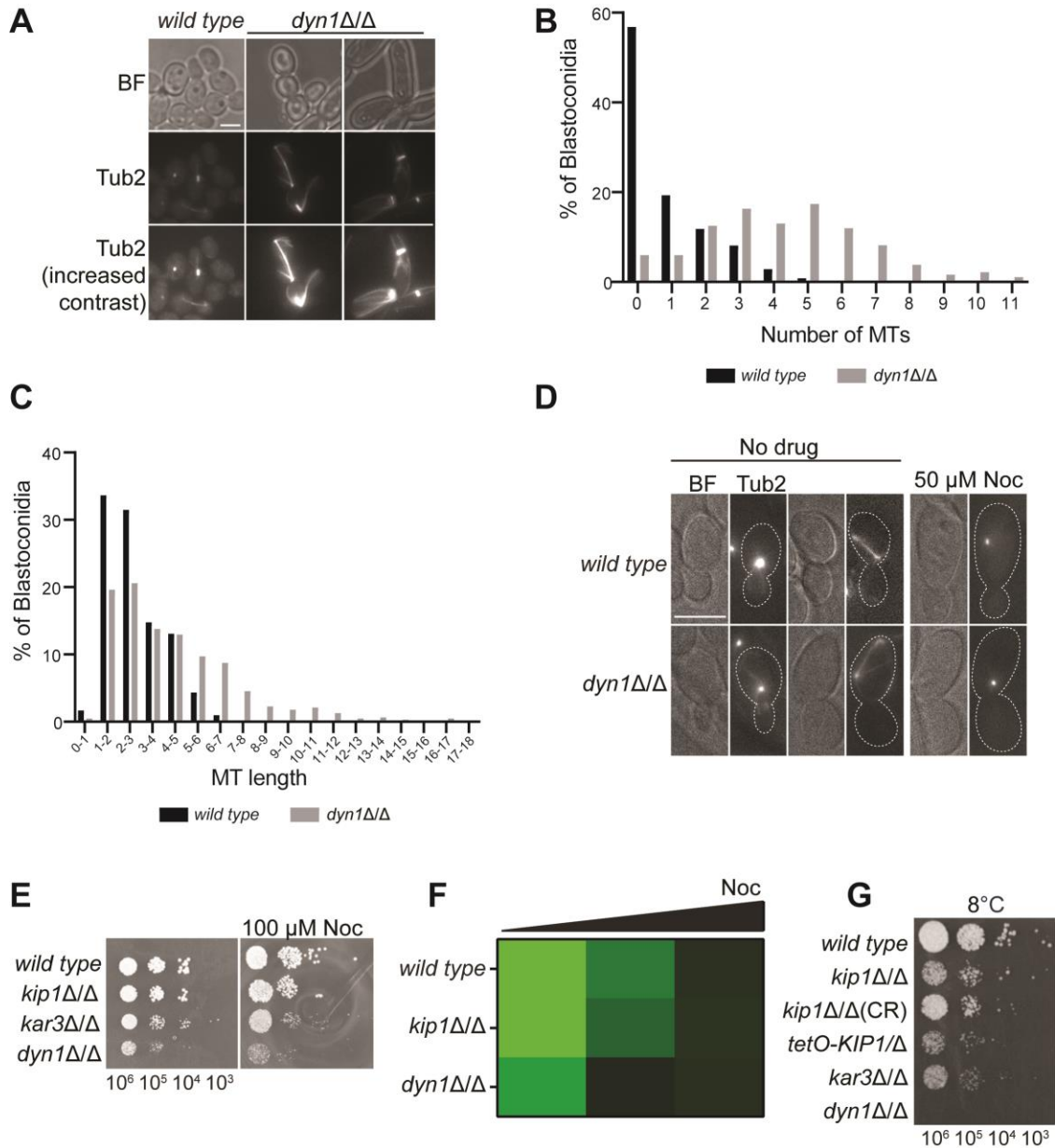


Figure 4-4. *dyn1Δ/Δ* cells have longer and more numerous aMTs. (A) Representative images of wild type and *dyn1Δ/Δ* cells expressing Tub2-GFP are shown. (B) The number of aMTs in wild type (CF405) and *dyn1Δ/Δ* (CF488) expressing Tub2-GFP was counted in cells with visible spindles. (C) For cells in panel B that contained aMTs, aMT length was determined by measuring the distance between the metaphase spindle pole and the plus end. These lengths were organized into bins of the size ranges indicated. (D) Static images of wild type (CF405) and *dyn1Δ/Δ* cells (CF488) expressing Tub2-GFP in SDC-sucrose and galactose. 50 μM of Nocodazole was added and cells were incubated for 6 h

and imaged. Scale bar, 5 μm . (E) Wild type (CF027), *kip1* Δ/Δ (CF311), *kar3* Δ/Δ (CF024) *dyn1* Δ/Δ (CF495) cells were plated on YPD or YPD + 100 μM Nocodazole. Cells were serially diluted to the indicated concentrations and 3 μL drops were plated and incubated for 2 days at 30°C. (F) Growth of wild type (CF027), *kip1* Δ/Δ (CF311) and *dyn1* Δ/Δ (CF495) with increasing concentrations of Nocodazole (100-250 μM). Strains in YPD media were diluted 0.2 optical density (OD) cells per mL, incubated at 30°C, and OD was measured every hour. Color scale for relative growth goes from green: no/low growth inhibition to black: complete growth inhibition. (G) Wild type (CF027), *kip1* Δ/Δ (CF311, CF429, CF436), *kar3* Δ/Δ (CF024) *dyn1* Δ/Δ (CF495) cells were plated on YPD. Cells were serially diluted to the indicated concentrations and 5 μL drops were plated and incubated for 25 days at 8°C.

4.4 Discussion

It is well-established that pulling forces on the plus ends of SPB-bound aMTs by cortical Dyn1 motors are critical for proper mitotic spindle orientation and nuclear migration in *C. albicans*[130, 202]. The experiments described here demonstrate that Dyn1 has the added cellular function of working collaboratively with the kinesin-5 motor, Kip1, to facilitate spindle elongation. We also showed that simultaneous loss of Kip1 and Dyn1 activity was lethal and appeared to stem from the cell's inability to initiate anaphase. This suggests that Kip1 and Dyn1 overlap for an essential function that other motors or spindle-associated factors cannot provide. When Kip1 activity was inhibited or eliminated in otherwise wild-type *C. albicans* cells, Dyn1 motors and aMTs became more abundant. We propose that the additional Dyn1 and aMTs afford increased pulling force from the cell cortex to compensate for the loss of outward pushing forces from the spindle midzone, helping anaphase spindle elongation to occur.

Similar to the findings of Finley *et al.*[202], we also demonstrated that Dyn1-deficient *C. albicans* cells remained in anaphase for up to three times as long as wild-type. Although this delay in anaphase completion was often due to mis-localization of the spindle into the mother cell, which reflects Dyn1's role in spindle positioning, many of the *dyn1Δ/Δ* cells that succeeded in elongating the spindle across the mother-bud junction cell contained persistent anaphase spindles. These findings show that Dyn1 activity is important for assisting in spindle elongation after anaphase onset and that the protracted anaphase of *dyn1Δ/Δ* yeast cells cannot be fully accounted for by activation of a Bub2p-mediated checkpoint, which monitors spindle position and spindle orientation until proper nuclear segregation occurs[202]. Finley *et al.* also show that Dyn1 is important but not

essential for spindle positioning in *C. albicans*. Correct spindle positioning in Dyn1-deficient cells is most likely enabled by chance interactions between dynamic aMTs and the cell cortex that guide movement of the daughter SPB toward and through the mother-bud junction[130]. Our observation that loss of aMTs by nocodazole addition or cold temperatures was lethal to *dyn1* Δ/Δ cells, but not to wild-type or even *kip1* Δ/Δ cells, supports this type of collaborative action between Dyn1 and aMT dynamics in both spindle positioning and anaphase spindle elongation.

Interestingly, in eukaryotes where kinesin-5 motors are essential for viability, these motors also predominantly mediate spindle elongation by ipMT sliding at the spindle midzone[82]. For instance, in *Drosophila* embryos, kinesin-5 Klp61F, induces ipMT sliding to push poles apart[234, 248]. Similarly, in budding yeast, Cin8 and Kip1 slide ipMTs apart, resulting in a five-fold increase in spindle length[77, 114]. Although Dyn1 also facilitates spindle elongation in budding yeast, it is unclear the extent of its pulling force compared to the pushing forces generated by both kinesin-5 motors[135].

In contrast, kinesin-5 is not essential in *C. elegans* and *D. discoideum*[81, 201]. Here, external pulling forces from aMT depolymerization or dynein are dominant, while kinesin-5 restricts sliding. However, in some systems, both motor families are essential for spindle elongation. In the filamentous fungi, *U. maydis*, although kinesin-5 is not essential, but is important in the slow phase of anaphase while dynein contributes to the fast phase[136].

We show that *C. albicans* uses both dynein and kinesin-5 for spindle elongation. In the absence of Dyn1, some spindles elongated at similar rates as wild-type cells. A possible reason for this is based on how *C. albicans* compensates force-balance mechanisms in lieu

of one motor. Outward pushing forces by kinesin-5-mediated anti-parallel ipMT sliding or polymerization of spindle MTs have previously been established as a critical mechanism for spindle elongation[222, 249]. Cells can likely employ both intra-spindle polymerization and Kip1-mediated ipMT sliding forces to elongate the spindles during anaphase. In some cases, this sliding force may not be sufficient, and spindles succumb to buckling as compressive forces prevail[250].

In addition, members of the kinesin-4, -6, -8, and -12 families of plus-end motors have been shown to contribute to antiparallel sliding of ipMTs during anaphase B[231, 251, 252]. Previous studies indicate that kinesin-8 motors are length-dependent MT depolymerizing motors [253]. In budding yeast, a complex interplay exists between MT depolymerization and ipMT sliding activity that contributes to spindle elongation and disassembly[252, 254]. *C. albicans* genome encodes one kinesin-8 motor, named Kip3, and it is conceivable that *C. albicans* could alter kinesin-8 function as a means of increasing the role of MT polymerization forces when needed.

Interestingly, both model yeasts, *S. pombe* and *S. cerevisiae*, predominantly use kinesin-5 based midzonal ipMT sliding to generate anaphase B force. So why was dynein function similar in *C. albicans* and *U. maydis*, but not as apparent in *S. cerevisiae* and *S. pombe*? A noticeable difference is the cell size, geometries, and distances over which the nucleus must be moved in each species. *C. albicans* is a polymorphic fungus that can switch between yeast, pseudohyphae and hyphal growth forms[255]. Dyn1's involvement in spindle elongation is likely more pronounced in hyphal spindles because the spindle lengths in these cells exceed that of yeast spindles[256]. Moreover, a MT pulling mechanism would be the preferred means of moving objects greater than 10 μm because

MT pushing could cause a high rate of MT buckling[222]. Thus, it is plausible that both kinesin-5 and dynein provide spindle elongation forces in *C. albicans* hyphae. Further research will be needed to investigate this possibility.

4.5 Materials and Methods

4.5.1 *C. albicans* Strains and Genetic Manipulations

A list of *C. albicans* strains used in this study is presented as **Table 4-1**. For a list of oligonucleotides used in *C. albicans* strain construction, please refer to **Table 4-2**. Gene disruption of the *C. albicans* *DYN1* open reading frame (Candida Genome Database: *orf19.5999*) was conducted by transformation and integration of a linear cassette containing a selectable marker. PCR amplification was used to generate disruption cassettes where a selectable marker was flanked by approximately 50 bp of *C. albicans* genomic sequence immediately 5' and 3' of the *DYN1*⁺ coding region. Disruption of *DYN1*⁺ in a wild type background (CF027) was conducted sequentially. First a *dyn1::LEU2*⁺ cassette was amplified from *pSN40*[212] using P304 and P305 and transformed into CF027. Correct *dyn1::LEU2*⁺ cassette integration was confirmed using primers P306 and P13. Second, a *dyn1::HIS1*⁺ cassette was amplified from *pSN52*[212] using primers P304 and P305 and transformed into *dyn1::LEU2* to create CF495. Integration of the disruption cassette at the correct location was confirmed by PCR amplification across the junctions of integration using primers P306 and P12.

Strains expressing fluorescently labeled β -tubulin were constructed using the plasmid pGAL:TUB2-GFP-NEUT5L and pGAL:TUB2-mScarlet-NEUT5L and linearized by *KPN1* to target to the neutral NEUT5L locus, as previously described[113]. Correct integration for pGAL vectors was confirmed by PCR using primers P16 and P107. To visualize the nucleus, the nucleolar protein Nop1 was fluorescently labeled using the plasmid pSFS2A-mScarlet (pRB897) (kindly provided by Dr. Richard Bennett) and amplified by primers P243 and P244[257]. Correct integration was confirmed using P312

and P245. Strains expressing fluorescently labeled spindle pole body component, SPC98, were constructed using a pGFP(3X) with primers P236 and P239. Correct integration as confirmed using primers P107 and P110.

Fluorescent tagging of *DYNI*⁺ in a wild type and *kip1*Δ/Δ background was accomplished using the method described by Gerami-Nejad *et al.*[215]. Briefly, long-tailed primers P310 and P311 and the plasmids pSFS2A-mNeonGreen-SAT1 (pRB895) as a template to create an integration cassette bearing approximately 50 base pairs of *DYNI*⁺ ORF immediately before the stop codon, and of sequence 3' to the ORF. Correct integration was confirmed by PCR using primers P309, P312 and P313.

Table 4-1. Names, genotypes, mating types, and sources of the strains used in this study

Strain	Genotype (Brief)	Genotype (Full)	Mating type	Source/parent
CF027	Wild type	<i>his1⁺/his1⁻ leu2⁺/leu2⁻ arg4⁺/arg4⁻</i>	α/α	RBY1133 ^[168]
CF024	<i>kar3Δ/Δ</i>	<i>kar3Δ::LEU2⁺/kar3Δ::HIS1⁺</i>	α/α	RSY11 ^[168]
CF311	<i>kip1Δ/Δ</i>	<i>kip1Δ::LEU2⁺/kip1Δ::HIS1⁺</i>	α/α	CF236 ^[242]
CF429	<i>kip1Δ/Δ</i> (CR)	<i>kip1Δ::gRNA</i>	α/α	AHY940 ^[211]
CF436	<i>tetO-KIP1/kip1Δ</i>	<i>tetO-KIP1-SAT1^R/kip1Δ::LEU2⁺</i>	α/α	CF236 ^[242]
CF495	<i>dyn1Δ/Δ</i>	<i>dyn1Δ::LEU2⁺/dyn1Δ::HIS1⁺</i>	α/α	CF027
CF546	<i>pGAL-TUB2-mScarlet</i> <i>DYN1-mNeonGreen</i>	<i>NEUT5L::[pGAL-TUB2-mScarlet-ARG4⁺]/NEUT5L⁺,</i> <i>DYN1-mNeonGreen-SAT1^R</i>	α/α	CF475 (This study)
CF543	<i>pGAL-TUB2-mScarlet</i> <i>DYN1-mNeonGreen</i>	<i>NEUT5L::[pGAL-TUB2-mScarlet-ARG4⁺]/NEUT5L⁺,</i> <i>DYN1-mNeonGreen-SAT1^R, kip1Δ::LEU2⁺/kip1Δ::HIS1⁺</i> <i>kip1Δ/Δ</i>	α/α	CF311 ^[242]
CF488	<i>pGAL-TUB2-GFP</i> <i>dyn1Δ/Δ</i>	<i>NEUT5L::[pGAL-TUB2-GFP-ARG4⁺]/NEUT5L⁺,</i> <i>dyn1Δ::LEU2⁺/dyn1Δ::HIS1⁺</i>	α/α	CF405
CF486	<i>pGAL-TUB2-GFP</i> <i>NOPI-mScarlet</i> <i>dyn1Δ/Δ</i>	<i>NEUT5L::[pGAL-TUB2-GFP-ARG4⁺]/NEUT5L⁺,</i> <i>NOPI-mScarlet-SAT1^R, dyn1Δ::LEU2⁺/dyn1Δ::HIS1⁺</i>	α/α	CF417 (This study)
CF405	<i>pGAL-TUB2-GFP</i>	<i>NEUT5L::[pGAL-TUB2-GFP-ARG4⁺]/NEUT5L⁺</i>	α/α	CF027
CF417	<i>pGAL-TUB2-GFP</i> <i>NOPI-mScarlet</i>	<i>NEUT5L::[pGAL-TUB2-GFP-ARG4⁺]/NEUT5L⁺,</i> <i>NOPI-mScarlet-SAT1^R</i>	α/α	CF405
CF542	<i>pGAL-TUB2-mCherry</i> <i>SPC98(3X)GFP-</i> <i>dyn1Δ/Δ</i>	<i>NEUT5L::[pGAL-TUB2-mCherry-ARG4⁺]/NEUT5L⁺,</i> <i>SPC98(3X)GFP-SAT1^R, dyn1Δ::LEU2⁺/dyn1Δ::HIS1⁺</i>	α/α	CF401 (This study)

^a Strains are in the *white* phase unless otherwise noted

^b All strains are derived from SN152 (Nobel and Johnson 2005). Full genotype at auxotrophic markers: *his1::hisG/his1::hisG leu2::hisG/leu2::hisG arg4::hisG/arg4::hisG ura3::imm434::URA3/ura3::imm434 iro1::IRO1/iro1::imm434*.

Table 4-2. Oligonucleotide primers used in strain construction

Primer	Name	Sequence (5' to 3')
P304	Long homologous tail knockout primer <i>DYN1::HIS1/LEU2/ARG4</i> 5'	GAAGGCTTTCAAAAATAGTGATCCAGAATATTTAAAAACA GAATCTTTATTTGAAATTTAATTCAACACA <i>ACCAGTGTGATGGATATCTGC</i>
P305	Long homologous tail knockout primer <i>DYN1::HIS1/LEU2/ARG4</i> 3'	TATCAAATCTTGTAAAAAGTAATATACAAATACAATTAT CTTTCTTTCATTAATAATAAACTAAAAAT <i>AGCTCGGATCCACTAGTAACG</i>
P306	-500bp <i>DYN1</i> check 5'	TCAAGTAGGTATTGTGCTTGTATTTTG
P309	<i>DYN1</i> ORF confirmation primer 5'	TTGGAACCATAACTTATGGTGGTAAAG
P12	<i>HIS1</i> check left 5'	ATTAGATACGTTGGTGGTTCAGTT
P13	<i>LEU2</i> check left 3'	AGAATTCCCAACTTTGTCTGTTC
P16	<i>ARG4</i> check left 3'	TTCCATTTAGAGAACTCATCATATTT
P310	<i>DYN1-mScarlet/mNeonGreen</i> localization long-tail 5'	TAGTGAAAAACAACCTGGATTAGAAATCGTGGAATCTG TACTTGATCTATCTGAAGATTTA <i>GGTGGTAGTGGTATGGTTCTAAAG</i>
P311	<i>DYN1-mScarlet/mNeon</i> localization long- tail 3'	CGGTCAAAGAGATTTGGACCGTATTGCTGCCAAACTTT GGAAGAAGATGACGAATAAATTA <i>GGCGGCCGCTCTAGAACTAGTGGATC</i>
P312	<i>mScarlet</i> check 3'	CTTGAACCATACATGAATTGTGGTGA
P313	<i>mNeonGreen</i> check 3'	CAGCTTGAAATGGTGACATTCCA
P107	<i>pGAL-TUB2-</i> <i>GFP/mCherry/mNeonGreen/mScarlet</i> downstream check 3'	TATTATCTATATTGTCAAGCCAAGACAAGCCCATT
P243	<i>NOPI-mScarlet</i> long-tail 5'	ACCTTATGAAAGAGACCATTGTATTGTTGTTGGTAGATAC ATGAGAAGCGGAATAAAGAAA GGTGGTAGTGGTATGGTTTCTAAAG
P244	<i>NOPI-mScarlet</i> long-tail 3'	AAGGTCAAAGTGCCATCAAAGGTGTGTTATTGGGTTTCAT TATCAAATTATTTGGTGACAA <i>GGCGGCCGCTCTAGAACTAGTGGATC</i>
P245	<i>NOPI</i> check 5'	GTTGATGCCGAACTGTGTTCG
P236	<i>SPC98(3X)-GFP</i> long-tail 5'	TTTGAAAAATGATTTGAATAGAGATTATAATTTAAAGGA TCTTAGTAAGTTGTTA <i>GGTTCAGTGATCCACCAGTTG</i>
P239	<i>SPC98(3X)-GFP</i> long-tail 3'	GGTTGGATATGCTACAGTATCAATTCGCATTTAGTTGCTA ATTTGTTACACAATATCTTCT <i>ATTCAGGACCACCTTGATTGTAAATAG</i>
P110	<i>SPC98(3X)-GFP</i> check 3'	GCAGCGTCCACCCTTTGTAAAAGTG

Bold and italic: portion of primer homologous to plasmid template

underline: restriction enzyme cut site.

4.5.2 *C. albicans* Transformation

C. albicans transformations were done using the lithium acetate-polyethylene glycol (PEG) heat shock method as previously described with minor modifications[216]. Transformations involving selection using the SAT1 gene were recovered in YPD (1% yeast extract, 2% peptone and 2% glucose) at 30°C for 4 h to allow expression of the ClonNAT resistance gene before plating on Nourseothricin selection medium.

4.5.3 *C. albicans* Growth Media and Chemical Reagents

All strains were maintained on YPD plates. YPD was supplemented with 200 µg/ml nourseothricin (clonNat; Werner BioAgents) for selection of positive SAT1 gene integration. Selection for auxotrophic markers was conducted using synthetic dropout (SD) medium containing 0.66% yeast nitrogen base, 0.2% yeast dropout mix lacking uracil, arginine, leucine, and histidine, 2% glucose, and 200 mg/L uridine and supplemented with 200 mg/L histidine, leucine, and/or arginine where required. Experimental cultures were grown to mid-logarithmic phase in YPD unless otherwise indicated. To create dilutions for spot assays, logarithmically growing cells were diluted to 1.0×10^6 cells/ml in phosphate-buffered saline (PBS). Serial dilutions of 10^5 , 10^4 , and 10^3 cells/ml were made. Five µL of cell culture dilutions was pipetted for each spot, and plates were incubated at 30°C for 2 days, unless otherwise indicated.

4.5.4 Microscopic Imaging of Spindle and Nuclear Morphologies and Motor Localization

Static images of cells were captured using a Zeiss Axio Observer epifluorescence microscope with a 100X (1.40 NA) oil objective AxioCam hRM camera controlled by Axiovision software. Time-lapse imaging and some static images were recorded using the

Olympus IX83 with a 100X oil objective (1.4 NA), and Andor Zyla 4.2 Plus camera controlled by the cellSens software. For time-lapse and static imaging, logarithmically growing cells were immobilized between an agarose pad and a glass coverslip, as previously described[113]. For time-lapses, images were captured in five z-slices 0.8 μm apart. Spindle length measurements were analyzed using ImageJ (NIH). Analysis was done with GraphPad Software. Figures were constructed in Adobe Photoshop and Adobe Illustrator.

Chapter 5

***Candida albicans* may actively downregulate spindle-associated kinesins to promote aneuploidy as part of a stress adaptation mechanism**

5.1 Abstract

C. albicans generates aneuploidy rapidly as a well-tolerated means of adaptation to environmental stresses. A classic example of this is observed when *C. albicans* is exposed to fluconazole (FLC). FLC disrupts chromosomal and cytoplasmic division synchronization, resulting in defective nuclear divisions and tetraploid cells. These cells often contain abnormal numbers of mitotic spindles. Attempts to return to a diploid state can produce viable aneuploid progeny that can tolerate and/or resist FLC stress. We previously showed that Kip1-depleted cells often contain two short spindles and multiple nuclei within the same cell compartment, as observed in tetraploid FLC-treated cells. This study shows that Kip1-depleted cells are genetically heterogeneous and have decreased susceptibility to FLC compared to wild-type cells. Their FLC survival phenotype appears to stem from selecting beneficial aneuploidies under FLC pressure that originated randomly (i.e., as random aneuploidies) in *kip1* Δ/Δ cells. Further, we show that aneuploidy generation in *kip1* Δ/Δ cells is transient and that they readily form new aneuploidies as surviving cells propagate. Lastly, gene expression analysis of FLC-treated wild-type *C. albicans* cells showed that levels of *KIP1* RNA, and a few other mitotic motor protein genes, are reduced compared to untreated cells. These findings suggest that Kip1 and some other mitotic kinesins may be critical parts of a stress-adaption mechanism used by *C.*

albicans to actively promote mitotic errors that lead to beneficial aneuploidies. These findings shed new light on how this human fungal pathogen generates genome plasticity.

5.2 Introduction

Candida albicans is an opportunistic fungal pathogen that can adapt to changing environmental conditions by transiently changing ploidy[258-261]. For *C. albicans*, these genome changes result in gene copy number variation which can affect protein abundance and be selected for to gain a fitness advantage[207, 262, 263]. The appearance of aneuploidy in other human fungal pathogens suggests that variations in chromosome organization and copy number are a common mechanism used by pathogenic fungi to rapidly generate diversity in response to changing growth conditions, including, but not limited to, antifungal drug exposure[264, 265]. In *C. albicans*, several forms of aneuploidy are formed under fluconazole (FLC) stress. The basis for this is accounted for by altered copy number of one or more genes that confer tolerance or resistance to FLC[10, 145, 161, 162, 258, 266, 267]. For instance, some FLC-resistant isolates exhibit an isochromosome 5L that provides extra copies of the drug resistance genes *ERG11* and *TAC1*[148]. Others showed a trisomy of chromosome 3, which carries at least two genes encoding efflux pumps, *CDR1* and *CDR2*, important in facilitating FLC efflux from the cell[162]. Although the reason these genetic rearrangements are selected is somewhat well understood, a comprehensive understanding of factors that precipitate these genome rearrangements remains largely unexplored.

One area worth investigating involves the machinery that *C. albicans* uses to perform the chromosome segregation process. The accuracy of chromosome segregation relies on the correct organization of MTs into a bipolar structure, proper chromosome

attachment to spindle MTs at kinetochores, and an appropriate length of time in mitosis to ensure that all chromosomes are correctly attached. Defects in any of these processes can lead to chromosome segregation errors and aneuploidy[138]. Recent work highlights the intimate association between mitotic spindle-associated motor proteins that regulate spindle structure and move DNA, and the quantity of DNA that is transported. These motor proteins help ensure that each chromosome is correctly tethered to, appropriately positioned, and later released by kinetochore MTs. Therefore, understanding the roles and regulation of motor proteins in mitosis is vital to identifying mechanisms by which chromosome segregation can be distorted, leading to gross chromosomal rearrangements that contribute to aneuploidy generation.

C. albicans encodes six kinesin motor families, of which four are known mitotic motors[113, 242]. Our previous studies have been instrumental in delineating the roles of some of these motor proteins in bipolar spindle formation and elongation[113, 242]. We also showed that *C. albicans* uses some motors differently from other eukaryotes. For example, in almost all eukaryotes, spindle assembly mechanisms rely on kinesin-5 motors to provide pushing forces that separate SPBs. We have previously shown that the *C. albicans* kinesin-14 Kar3 is needed for spindle assembly and that the partner protein Cik1 regulates its role. In absence of either subunit, cells often have short, monopolar pre-anaphase spindles, or two monopolar half-spindles that get pulled apart, fragmenting the nucleus[113]. On the other hand, our work, along with previous studies, demonstrates that *C. albicans* kinesin-5 Kip1 is important for chromosome congression and maintaining spindle integrity[33, 167, 242]. The absence of Kip1 function results in short bipolar spindles that sometimes break apart and form two bipolar spindles in one cell compartment.

Both spindles undergo coordinated nuclear division, dividing either across the bud neck or within one cellular compartment yielding four nuclear patches. After some time, nuclear patches in each cell appear to merge or collapse onto one another. *kip1* Δ/Δ mutants are viable, suggesting that these aberrant spindle defects and abnormal DNA content may sustain cell growth.

The mitotic and nuclear defects observed in the absence of these motor proteins establish their importance in being physical drivers of chromosome attachment and movement. In this study, we show that Kip1 mutants readily generate random aneuploidies. These aneuploidies are short-lived and readily change as the cells are propagated. Rapid aneuploidy turnover is also observed under FLC treatment. However, the aneuploidies selected resemble ones previously shown to confer a fitness advantage in FLC-treated wild-type cells. Furthermore, the addition of FLC to wild-type cells elicits changes in RNA expression levels of motor proteins and spindle apparatus components. We propose that *C. albicans* cells actively regulate its mitotic kinesins, like Kip1, to promote spindle errors that foster aneuploidy under stress.

5.3 Results

5.3.1 *kip1* Δ/Δ mutants are less sensitive to FLC exposure compared to wild-type

The analysis of the cell cycle events that occur in *C. albicans* during FLC exposure by Harrison *et al.* demonstrated that FLC-resistant isolates likely arise from cells that failed to divide and then experienced mitotic collapse to form tetraploid cells with multiple spindles[155]. They found that unequal chromosome segregation in these cells produced aneuploid progeny that were FLC-resistant (**Figure 5-1A**). Intrigued by how the mitotic defects in these FLC-treated wild-type cells were similar to untreated cells lacking Kip1

activity, we wondered if Kip1-depleted cells are readily able to produce FLC-resistant aneuploid progeny. In other words, the prevalence of abnormal number of spindles in *kip1Δ/Δ* cells could result in an abundance of unequal DNA segregation events that increase the odds of developing drug resistant/tolerant populations. To begin to address this question, we first assessed the effect of two concentrations of FLC on growth of wild-type cells and cells lacking activity of three confirmed mitotic kinesins, Kip1, Kar3/Cik1, and Kip3, using a dilution spot assay (**Figure 5-1B**). At 30°C, the *kip1Δ/Δ* and *cik1Δ/Δ* mutants grew almost equally well as untreated cells, while wild type and *kip3Δ/Δ* cells showed no growth. At 37°C, *kip1Δ/Δ* was the only kinesin deletion strain that survived FLC. Survival of wild-type cells in the presence of FLC at this temperature is likely accounted for by heat shock growth response[268, 269]. Both *cik1Δ/Δ* and *kip3Δ/Δ* exhibit a temperature-sensitive growth defect.

Close inspection of the wild type and *kip1Δ/Δ* spots revealed heterogeneity in the sizes of the colonies (not shown). To elucidate mechanisms contributing to survival of the *kip1Δ/Δ* cells during FLC exposure, we microscopically imaged spindle structures in these cells using fluorescent-tubulin and SPC98 and monitored chromosome segregation using DAPI staining. Stereotypical cell cycle dynamics, including budding, bipolar spindle formation, and chromosome segregation, were observed for wild-type cells in the “no drug” condition (**Figure 5-1C**). Addition of FLC to wild-type cells resulted in large cells (reminiscent of tetraploid cells) with two individual nuclear patches, each associated with a bipolar spindle. These alterations in cell size and spindle structures in FLC-treated wild-type cells are consistent with the observations by Harrison *et al*[155]. As previously observed, a subpopulation of *kip1Δ/Δ* cells have two spindles in one cell

compartment[242]. FLC-treated *kip1Δ/Δ* cells form multiple spindles and multinucleate cells as well, but they also form binucleate trimers (i.e., cells composed of three compartments -mother, daughter, and granddaughter). These cells share a single contiguous cytoplasm in which subcellular structures were able to pass through the two bud necks. Notably, trimers also formed in *kar3Δ/Δ* cells[155]. As previously shown by Harrison *et al.*, nuclei with more than two SPBs are much more likely to undergo unequal nuclear segregation and the majority of trimers form at least one tetraploid or 4N cell with two spindles. Thus *kip1Δ/Δ* cells have a high likelihood of undergoing unequal DNA segregation to produce aneuploids.

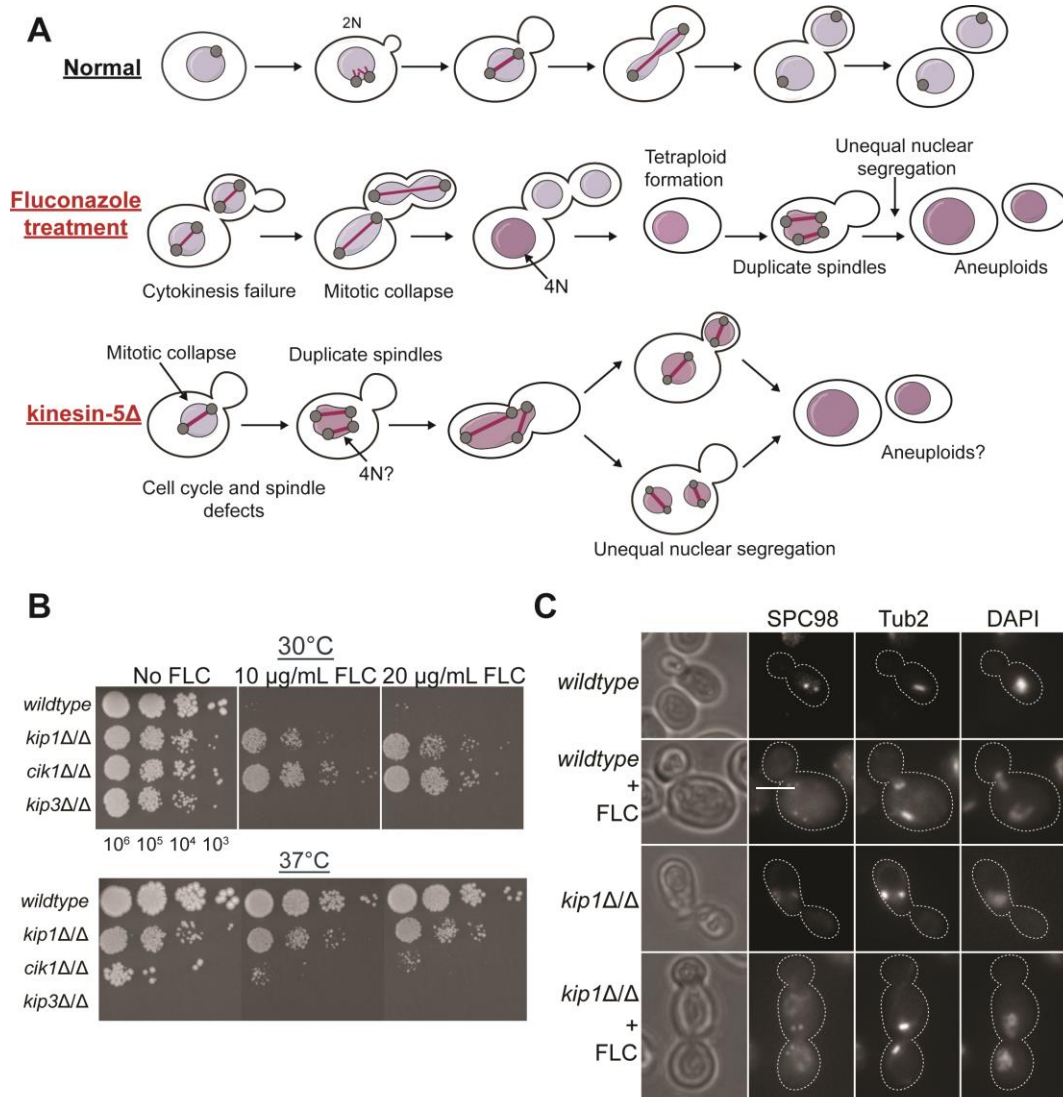


Figure 5-1. *kip1Δ/Δ* mutants survive better in the presence of FLC compared to wild-type. (A). Cartoon model of the cell cycle defects exhibited in FLC-treated wild type cells and *kip1Δ/Δ* mutants. (B) Wild type (CF027), *kip1Δ/Δ* (CF311), *cik1Δ/Δ* (CF016) *kip3Δ/Δ* (CF381) cells were plated on YPD or YPD + 10 μg/mL or 20 μg/mL FLC. Cells were serially diluted to the indicated concentrations and 5 μL drops were plated and incubated for 2 days at 30°C and 37°C. (C) Images of wild type (CF363) and *kip1Δ/Δ* (CF368) cells expressing SPC98-GFP, Tub2-mCherry, with DAPI-stained nuclei. All cells were obtained from logarithmically growing, unsynchronized cultures in SDC-sucrose medium at 30°C. Cells were incubated with 10 μg/mL FLC for 8 h before imaging. Scale bars, 5 μm.

5.3.2 *kip1* Δ/Δ cell population is genetically heterogeneous.

To investigate prevalence of aneuploidy in *kip1* Δ/Δ cells before and after FLC-exposure (10 μ g/ml), we measured the DNA content of log-phase yeast cell populations using flow cytometry (**Figure 5-2A**). Wild-type cells not exposed to FLC consistently appeared in two peaks corresponding to the G1 phase (2N DNA content) and G2-phase (4N DNA content) of the cell cycle, respectively. In contrast, wild-type cells that were exposed to FLC for 8h had a much larger G2-phase peak as a greater proportion of cells become 4N. Multiple aneuploid peaks in the region between 2N and 4N also appeared in FLC-treated wild-type cell population, coinciding with the S-phase region[270]. In the “no drug” condition, *kip1* Δ/Δ mutants already possessed multiple peaks between 2N and 4N, indicating the presence of aneuploids. The prevalence of these peaks, along with the G2-phase peak, increased with FLC addition. Thus, FLC addition increases the number of cells with 4N DNA content as well as DNA content between 2N and 4N (i.e., aneuploids).

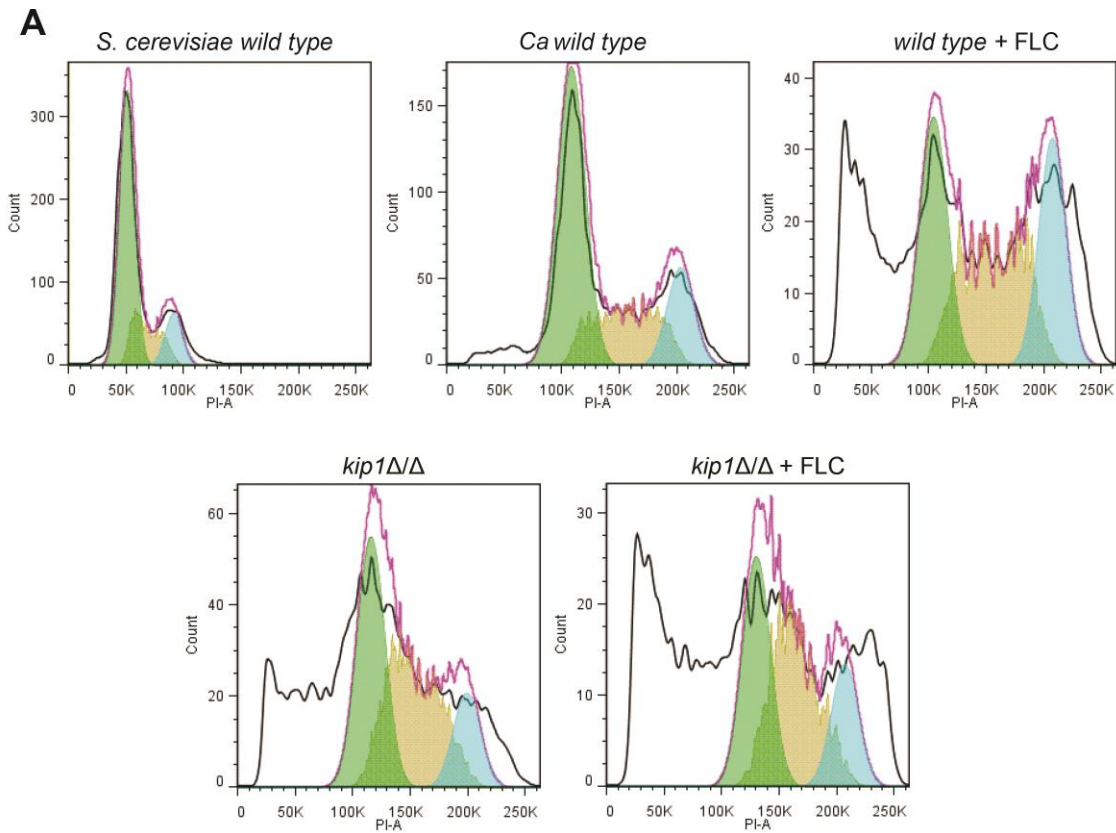


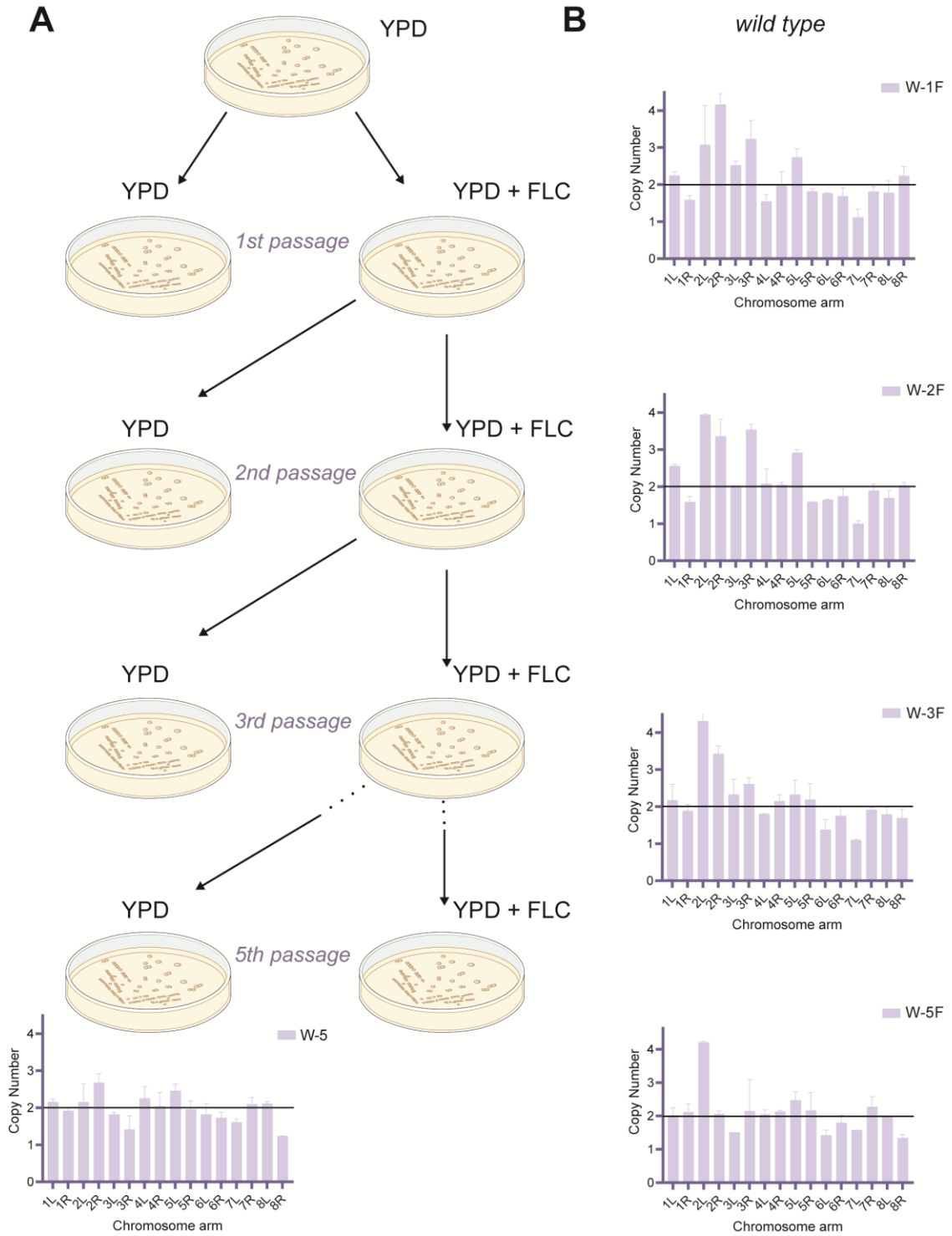
Figure 5-2. Flow Cytometry analysis of *kip1Δ/Δ* mutants demonstrates aneuploid peaks. (A) Flow cytometry analysis of DNA content of wild type (CF027) and *kip1Δ/Δ* (CF311) cells in the presence and absence of FLC incubation. Cells were incubated with 10 $\mu\text{g}/\text{mL}$ of FLC. *S. cerevisiae* wild-type strain was used as a haploid control. Black lines, raw data; pink lines, sum of the curves. Coloured peaks (green, yellow, blue) are G1, S and G2 phases, respectively, calculated using the Watson (Pragmatic) model in FlowJo.

5.3.3 Absence of Kip1 readily generates non-specific aneuploidies

To more directly investigate the types of aneuploidies that develop in *kip1* Δ/Δ cells before and after FLC exposure, we performed short-term cell evolution experiments (**Figure 5-3A**). Wild type and *kip1* Δ/Δ cells were cultured and plated on YPD medium and then individual colonies were selected and passaged on plates with and without FLC every 2 days for a total of 5 passages. Total DNA was extracted from 6 of the colonies that grew on the final plate and qPCR was performed to determine their ploidy genotypes. Analysis of chromosome copy number in a control wild-type colony revealed no aneuploidy on the initial “no drug” plate. After the first passage under FLC pressure, aneuploidy of several chromosome arms (2L, 2R, 3R, 5L) was present. The second passage under FLC pressure had a similar aneuploidy indicating that the aneuploidies (2L, 2R, 3R, 5L) were selected for under FLC. However, in the third passage, chromosome arms 3L and 5L returned to a diploid state. In the final passage under FLC pressure, only aneuploidy of chromosome arm 2L remained stable while 2R became diploid (**Figure 5-3B**).

In contrast, analysis of chromosome copy number in *kip1* Δ/Δ colonies that formed on the initial “no drug” plate revealed that all isolates (n=6) had a different aneuploidy (**Figure 5-3C, initial state**). This confirms that random viable aneuploid cells emerge in the absence of Kip1 activity. When cells from these six “no drug” *kip1* Δ/Δ colonies were passaged five times under FLC pressure, new aneuploidies emerged for all of them (**Figure 5-3C, final passage**), indicating that FLC also increases the rate of aneuploid formation, in addition to selecting in FLC-resistant aneuploids, and that the aneuploidy states are not stable.

To understand when the new FLC-resistant *kip1* Δ/Δ aneuploids arose during the evolution experiment, we analyzed the ploidy status of one colony from the first three passages and the final fifth passage (**Figure 5-3D**). At the start of the experiment, the *kip1* Δ/Δ colony had aneuploidy of several chromosome arms (4L, 6L, 6R). When these cells were passaged once on YPD plates only (i.e., no FLC pressure), a different aneuploidy was observed (3L). Similarly, the first passage under FLC stress had a different aneuploidy (2R, 3R, 4L) that the starting *kip1* Δ/Δ colony. The second passage under FLC pressure again had a different aneuploidy (2L, 2R, 4L, 6L). The third passage under FLC pressure had a different aneuploidy (2L, 2R, 3L, 3R, 4R, 7L). The final pressure under FLC pressure again had a different aneuploidy (2L, 2R, 3R, 4L, 6L). Interestingly, in each passage under FLC exhibited a unique aneuploidy that harbored chromosomes previously shown to provide a fitness benefit for FLC resistance or tolerance due to changes in dosage of certain resistance-conferring genes[271]. For example, the right arm of chromosome 3 harbors genes for the efflux pump, *CDR1* or efflux pump regulators such as *MRR1*[272]. Chromosome 3 also encodes stress response proteins (*PBS2*) or proteins important in membrane and cell wall integrity (*RHB1* and *KRE6*)[273] that mediate FLC tolerance. Taken together, we show that *kip1* Δ/Δ mutants are heterogeneous and readily develop new aneuploidies, likely due to the mitotic defects they experience. Under FLC pressure, aneuploid progenies that provide a fitness benefit seem to be predominant.



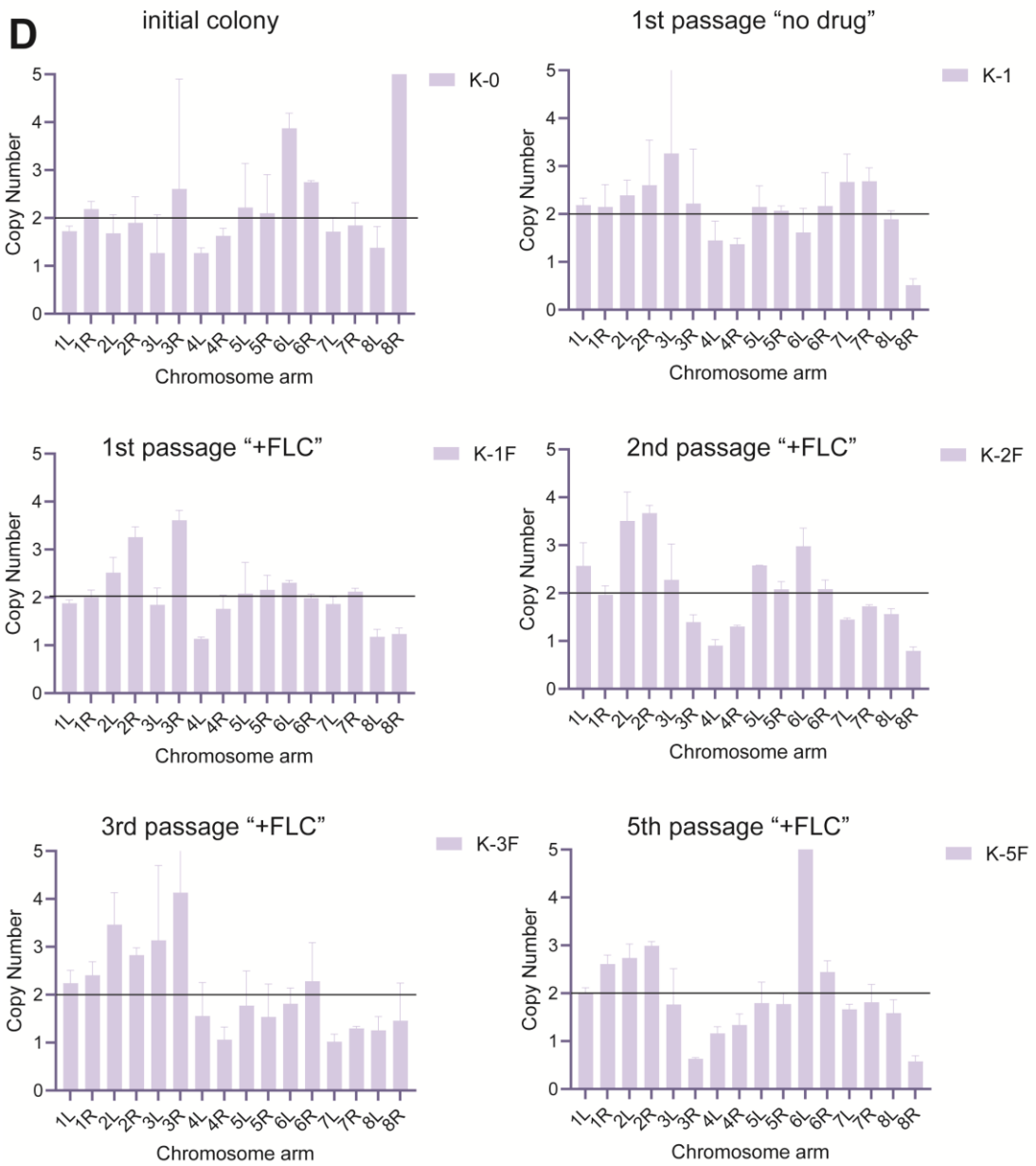
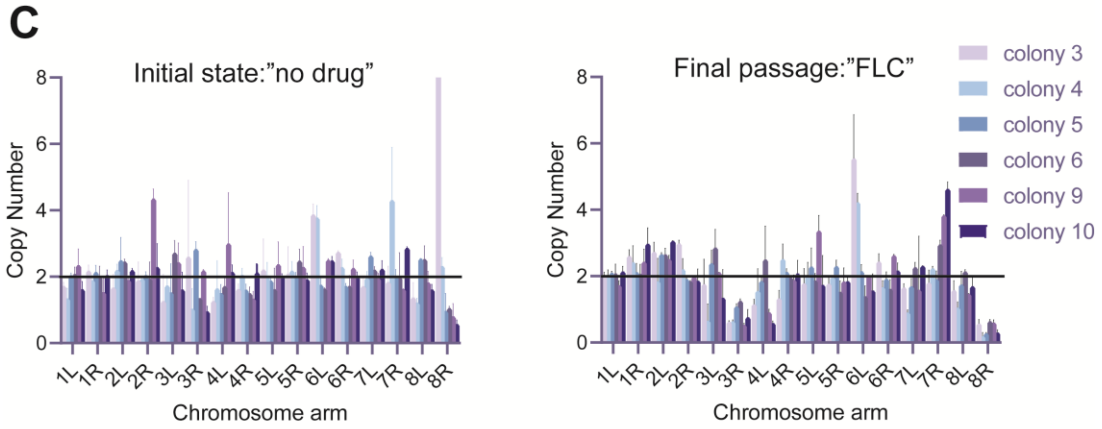


Figure 5-3. Kip1 mutants exhibit non-specific aneuploidies. (A) Cell evolution experiment where cells from liquid cultures of both wild type (CF027) and *kip1* $\Delta\Delta$ (CF311) were plated on YPD plates. Single colonies were selected and plated on both YPD and YPD + 10 μ g/mL FLC plates. Colonies were passaged every two days for a total of five passages. (B) Karyotype of a wild type colony during the course of the cell evolution experiment. gDNA was extracted as described in Materials and Methods and karyotypes was determined by quantitative PCR (qPCR). PCR assays[274] were designed with primers to non-coding regions proximal to the centromere on each *C. albicans* chromosome arm. All PCR reactions were performed in technical triplicates. Chromosome copy numbers were determined using the $2^{-\Delta\Delta C_t}$ method[275]. (C) Karyotype of six *kip1* Δ/Δ colonies at the start (no drug) and end (under FLC pressure) of the experiment. Experiment was carried out as (B) (D). Karyotype of one *kip1* Δ/Δ colony during the first three and last passage of cell evolution experiment.

5.3.4 Wild-type cells treated with FLC downregulate motor protein gene expression

Increasing evidence implicates aneuploidy and genome instability in tumor cells to result from genome doubling or amplification[276, 277]. When genome size increases, cells tend to form multipolar spindles likely to ensure attachment and separation of all genome content[209]. In tetraploid cells, multipolar divisions are lethal because genomic material is distributed among three or more daughter cells, causing massive loss of genome content[278]. To mitigate this problem, tetraploid cells cluster their centrosomes to prevent aberrant multipolar spindle structures and form bipolar-like spindles that divide into only two daughter cells[279]. Changes in kinesin motor protein expression is one way for cells to control centrosome clustering in these cells[209, 280]. Given the ability of *kip1Δ/Δ* cells to readily form aneuploids, we were curious if regulation of motors could be a way to encourage aneuploid formation when wild-type cells are under FLC stress. To address this question, we performed transcriptomic analysis using RNA-sequencing on FLC-treated wild-type cells and *kip1Δ/Δ* mutants. 10 μg/mL of FLC was added to wild-type cells and incubated for 4 hours until cells reached mid-logarithmic phase. Both FLC-treated wild-type and *kip1Δ/Δ* cell cultures were snap frozen in Liquid N₂ and RNA was extracted using Qiagen RNA extraction kit (see Materials and Methods). Total RNA was sent to the National Research Council of Canada DNA Sequencing Technologies Facility where sequencing was performed on an Illumina HiSeq 2500 platform.

Following RNA expression analysis with a log₂fold cutoff of 1 and -1 for up and down regulated genes, respectively, we identified 735 up-regulated genes and 595 down-regulated genes (**Figure 5-4A**). In line with previous studies, addition of FLC to wild-type cells resulted in an increase in RNA levels of *ERG11*, which encodes for lanosterol 14α-

demethylase. Overexpression of lanosterol 14 α -demethylase contributes to the maintenance of cell membrane integrity as a response to ergosterol depletion from FLC addition[281, 282]. *CDR11*, a member of the ATP-binding cassette (ABC) transporters, was also upregulated in FLC-treated wild-type cells[283]. These changes are expected outcomes of FLC-resistant aneuploidies but do not explain how the aneuploidy arose. Few studies have carefully examined expression changes in genes that could generate mitotic errors and chromosome segregation defects, such as mitotic motor proteins[124].

To look for genes important in mitosis, we input up- and down- regulated genes into the Candida Genome Database (CGD) Gene Ontology (GO) Slim Mapper tool to filter based on cellular components related to cell division/mitosis (**Figure 5-4B**). Kinesin-5, *KIP1*, kinesin-14 subunit, *CIK1*, kinesin-8, *KIP3*, and kinesin-7, *KIP2* were all found to be downregulated in wild-type cells treated with FLC. However, we did not observe significant changes in dynein or the uncharacterized kinesin-3. We next used the CGD GO Term Finder tool to identify cellular processes affected by mis-regulation of these motors. Changes in RNA expression levels of these motors affects spindle assembly, organization, elongation, along with MT organization and nuclear migration when cells experience FLC stress.

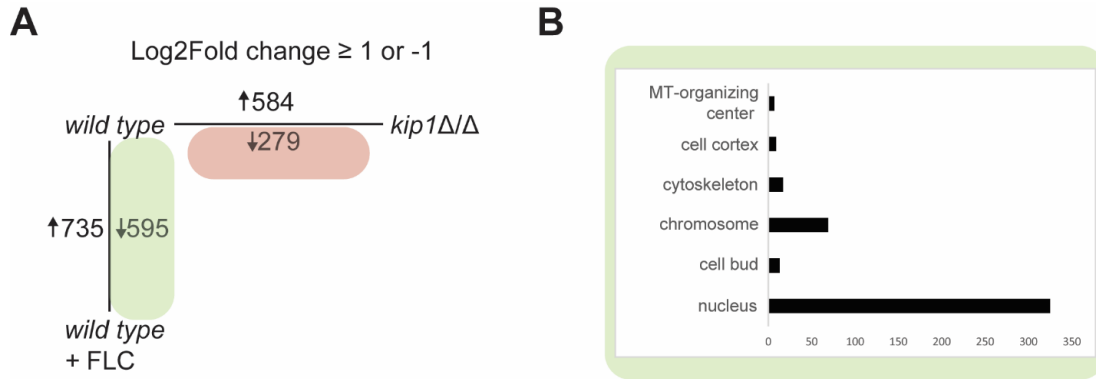


Figure 5-4. Differential gene expression profiles of wild-type cells treated with FLC.

(A) The number of up/down regulated genes remaining after log₂fold cut-off of 1 and -1 respectively. 10 μ g/mL FLC was added to overnight wild type (CF027) cell cultures and incubated for 4 hours. (B) GO term enrichment analysis of gene expression levels measured by RNA-seq for spindle and chromosome components.

5.3.5 Addition of FLC alters expression levels of many spindle-related proteins

In addition to the gene expression changes of motor proteins, we also observed altered regulation of genes related to spindle function (**Table 5-1**). Two uncharacterized genes, *C7_01830W_A* and *CR_02680W_A*, whose orthologs in *S. cerevisiae* are kinetochore proteins were downregulated. *C7_01830W_A* is orthologous to Nls1 in *S. cerevisiae* and is part of the central kinetochore complex that acts as a bridge in joining kinetochore subunits contacting DNA to those contacting MTs[284]. Adjacent to the central kinetochore complex is the outer kinetochore complex containing Ndc80 (orthologous to *CR_02680W_A*), a conserved coiled coil protein that interacts with spindle MTs[285]. Both Nls1 and Ndc80 have a negative genetic interaction and are essential parts of the kinetochore[285]. Additionally, the unique site-specific protease, *ESPI*, also known as Separase, and two putative cohesion proteins (*SMC1* and *SMC2*) were also downregulated. Separase is activated during anaphase where it cleaves subunits of the cohesion complex to dissolve the association between sister chromatids and initiate their poleward movement[286, 287]. Separase activity further leads to a stabilization of the anaphase spindle midzone, which is a prerequisite for timely exit from mitosis[286, 287]. Spindle midzone stabilization is typically provided by MT-crosslinking proteins. Expression of *ASE1*, the MT-crosslinker, and *NUD1*, a core SPB protein, was downregulated. Ase1 crosslinking of interpolar MTs provides stabilization of the anaphase midzone as the spindle elongates, consecutively stimulating the mitotic exit network (MEN), a GTPase signaling pathway[288]. Nud1 acts as a scaffold to recruit MEN components[288]. Activation of MEN promotes exit from mitosis by inducing spindle breakdown, cyclin degradation and cytokinesis[288, 289].

BIR1 (yeast homologue of survivin), a key component of the chromosomal passenger complex (CPC) was also downregulated. The spatial and temporal regulation of CPC dictates its dynamic localization pattern during mitosis and cytokinesis[290-292]. For example, CPC localization to the centromeres in early mitosis is important for the regulation of chromosome structure, kinetochore–MT attachments and the spindle assembly checkpoint. In late mitosis, CPC localizes to the spindle midzone where it initiates spindle disassembly and contractile ring formation[290-292]. Disturbance of CPC function results in chromosome congression and segregation defects that range from aneuploid to complete tetraploid progeny, the latter associated with the absence of a functional CPC[293].

Lastly, cortical proteins *INT1* and *NUM1* were downregulated. Int1 genetically interacts with the Sep7 septin, and both work together in maintaining the diffusion barrier at the bud neck for the mitotic exit protein Lte1[294]. In the absence of both Int1 and Sep7, cells undergo a premature activation of mitotic exit prior to correct spindle alignment, yielding multinucleated cells[294]. Similarly, Num1 is distributed along the cortex onto which dynein offloads and can mediate spindle positioning[295]. When the spindle is misaligned, mitotic exit is delayed due to inhibition of MEN, a process that is spatially controlled by Lte1[296]. It is therefore not surprising that *LTE1* was also downregulated. Reduced Lte1 levels would activate MEN regardless of spindle alignment, giving rise to mispositioned spindles and asymmetric cell division[297].

Table 5-1. Downregulated genes related to spindle function when FLC is added to wild-type *C. albicans* cells

Component	Gene	Log₂fold	Function
MT-organizing center	<i>KIP1</i>	-1.39	Kinesin-5 - MT-crosslinking; important in spindle integrity and elongation
	<i>NUD1</i>	-1.145	SPB outer plaque component; acts through the mitotic exit network to specify asymmetric SPB inheritance
	<i>CIK1</i>	-1.154	Kinesin-associated protein; non-catalytic subunit of Kinesin-14, Kar3
Cytoskeleton	<i>KIP3</i>	-1.514	Kinesin-8; important in MT depolymerization
	<i>KIP2</i>	-1.319	Kinesin-7 - important in mitotic spindle positioning
	<i>ASE1</i>	-1.171	Interpolar MT crosslinker
	<i>INT1</i>	-1.007	Anillin-related protein; important in assembly and organization of the AMR
	<i>CR_05100W_A</i>	-1.451	Uncharacterized; ortholog is a subunit of chromosomal passenger complex (CPC) (BIR1)
	<i>C5_03170C_A</i>	-1.144	Uncharacterized; ortholog is important in axial bud site selection;
	<i>MYO1</i>	-2.353	Component of actomyosin ring at neck of newly emerged bud
	<i>MLP1</i>	-1.466	Myosin-like protein associated with the nuclear envelope
Chromosome	<i>SMC3</i>	-1.931	Uncharacterized; ortholog is a subunit of the multiprotein cohesin complex
	<i>SMC2</i>	-1.863	Uncharacterized; ortholog is a subunit of the multiprotein cohesin complex
	<i>SMC1</i>	-1.858	Uncharacterized; ortholog is a subunit of the multiprotein cohesin complex
	<i>SCM3</i>	-1.145	Nonhistone component of centromeric chromatin; required for kinetochore assembly and G2/M progression
	<i>CR_02680W_A</i>	-1.642	Uncharacterized; ortholog is a component of the kinetochore associated Ndc80 complex (NDC80)
	<i>C1_01070C_A</i>	-1.108	Uncharacterized; ortholog may be part of MIS12/MIND kinetochore complex
	<i>C7_01830W_A</i>	-1.034	Uncharacterized; ortholog is an essential component of the MIND kinetochore complex
	<i>ESP1</i>	-1.266	Separase, caspase-like cysteine protease that cleaves cohesins to allow chromatid separation during anaphase
Cell cortex/bud	<i>BEM2</i>	-1.581	Actin cytoskeleton organization
	<i>C4_07080C_A</i>	-1.36	Uncharacterized; ortholog is a protein required for nuclear migration; mediates interactions of dynein and cytoplasmic microtubules with the cell cortex (NUM1)
	<i>AMN1</i>	-1.46	Uncharacterized; putative negative regulator of exit from mitosis

5.3.6 *kip1*Δ/Δ mutants exhibit similar gene expression changes for spindle proteins as FLC-treated wild-type cells

We next asked what effect Kip1 loss had on gene expression in *C. albicans*. Absence of Kip1 resulted in 584 upregulated and 279 downregulated genes (**Figure 5-5A**). Again, we filtered the gene set to include genes involved in the cell cycle/mitosis (**Figure 5-5B**). Interestingly, complete absence of Kip1 invokes very similar changes in expression of spindle-related proteins as that observed in FLC-treated wild-type cells, where 179 downregulated genes were common between FLC-treated wild-type cells and *kip1*Δ/Δ (**Figure 5-5C**). Apart from *KIP2*, *NLS1*, *ASE1*, and *INT1*, all other genes were downregulated in *kip1*Δ/Δ cells (**Table 5-2**). It is important to note that log₂fold change values of *KIP2* (-0.903), *ASE1* (-0.825) and *INT1* (-0.943) which were just outside our cut-off threshold of -1. In addition, unlike FLC-treated wild-type cells, absence of Kip1 upregulated the spindle assembly checkpoint *MAD1*. Mad1 monitors unattached kinetochores of misaligned chromosomes and generates a ‘wait anaphase’ signal by inhibiting the anaphase promoting complex/cyclosome (APC/C)[186]. Protein-protein interaction screening in *S. pombe* revealed that Mad1 interacts with kinesin-5 at kinetochores of misaligned chromosomes and promotes chromosome gliding towards the spindle equator[177].

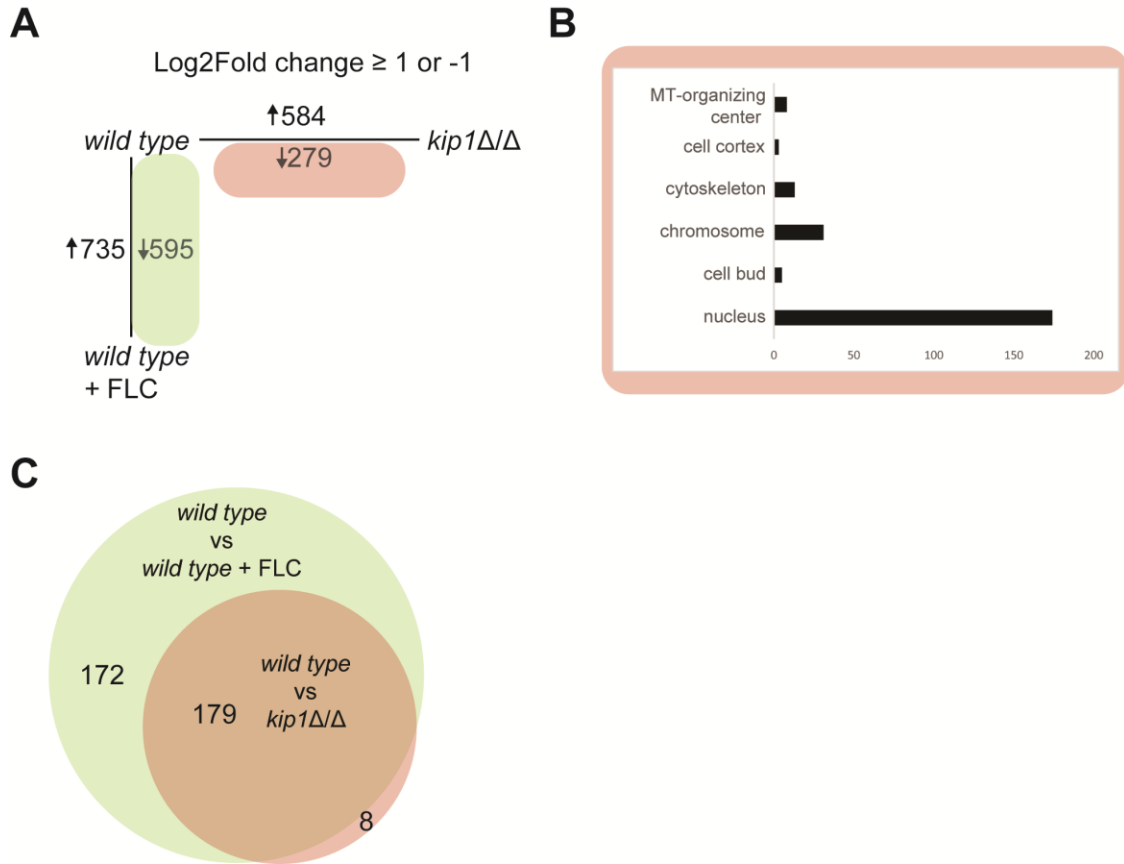


Figure 5-5. Differential gene expression profiles of wild-type cells vs *kip1* Δ/Δ . (A) The number of up/down regulated genes remaining after log₂fold cut-off of 1 and -1 respectively. (B) GO term enrichment analysis of gene expression levels measured by RNA-seq for spindle and chromosome components. (C) Comparison of common versus unique downregulated genes in FLC-treated wild-type cells and *kip1* Δ/Δ cells (B).

Table 5-2. Downregulated spindle component genes in *kip1Δ/Δ*

Component	Gene	Log₂Fold	Function
MT-organizing center	<i>KIP1</i>	-5.554	Kinesin-5 - MT-crosslinking; important in spindle integrity and elongation
	<i>CIK1</i>	-1.225	Kinesin-associated protein; non-catalytic subunit of Kinesin-14, Kar3
	<i>NUD1</i>	-1.938	SPB outer plaque component; acts through the mitotic exit network to specify asymmetric SPB inheritance
	<i>MYO1</i>	-1.735	Component of actomyosin ring at neck of newly emerged bud
	<i>CI_12660W_A</i>	-1.638	Uncharacterized; ortholog is MAD1 – a protein important in the spindle assembly checkpoint (SAC)
	<i>MLP1</i>	-1.018	Myosin-like protein associated with the nuclear envelope
Cytoskeleton	<i>KIP3</i>	-1.163	Kinesin-8; important in MT depolymerization
	<i>ESP1</i>	-1.037	Separase, caspase-like cysteine protease that cleaves cohesins to allow chromatid separation during anaphase
	<i>CR_05100W_A</i>	-1.174	Uncharacterized; ortholog is a subunit of chromosomal passenger complex (CPC)
	<i>MTW1</i>	-1.1	Kinetochore component
Chromosome	<i>CI_01070C_A</i>	-1.061	Uncharacterized; ortholog may be part of MIS12/MIND kinetochore complex
	<i>SMC3</i>	-1.654	Uncharacterized; ortholog is a subunit of the multiprotein cohesin complex
	<i>SMC2</i>	-1.409	Uncharacterized; ortholog is a subunit of the multiprotein cohesin complex
	<i>SMC1</i>	-1.476	Uncharacterized; ortholog is a subunit of the multiprotein cohesin complex
	<i>CR_02680W_A</i>	-1.627	Uncharacterized; ortholog is a component of the kinetochore associated Ndc80 complex (NDC80)
Cell cortex/bud	<i>AMN1</i>	-1.171	Uncharacterized; putative negative regulator of exit from mitosis
	<i>C4_07080C_A</i>	-1.189	Uncharacterized; ortholog is a protein required for nuclear migration; mediates interactions of dynein and cytoplasmic microtubules with the cell cortex (NUM1)

5.4 Discussion

Accurate chromosome segregation is critical for cell function, survival, and propagation. As such, deciphering the mechanics that govern chromosome segregation are vital. Molecular motors play important roles in chromosome stability, alignment, and movement[87, 185, 203, 298-300]. We previously showed that in the absence of *C. albicans* kinesin-5 Kip1, the mitotic spindle experiences defects that lead to multiple spindle components and nuclear patches[167, 242]. In this study, we show that cells devoid of Kip1 function are genetically heterogeneous. Our data show that a subpopulation of *kip1* Δ/Δ cells is aneuploid and that the aneuploidy formed is both random and transient. Furthermore, aneuploidy in these cells enables survival under FLC exposure. Based on these results and the importance of Kip1 in spindle integrity/maintenance, we propose that *C. albicans* may have developed the ability to actively regulate motor activity under stress as a mechanism to facilitate aneuploidy formation. In support of this, we found that Kip1 gene expression and several other motors were reduced in wild-type cells treated with FLC. Interestingly, altered gene expression of several spindle proteins was also detected.

Under FLC treatment, trimeras arise due to cytokinesis failure between the mother-daughter cells and provide a route to producing tetraploids[155]. Cytokinesis failure could be a result of gradual depletion of cell membrane protein, ergosterol (Erg11p), and/or accumulation of 14 α -Methyl-ergosta 8,24(28)-dien-3,6-diol, the toxic sterol produced by Erg3p when Erg11p is inhibited[155]. Alternatively, and not mutually exclusive, cytokinesis failure may be a consequence of changes in cell cycle coordination as a response to FLC stress. Under FLC, spindles form but experience mitotic collapse, causing two daughter nuclei to re-fuse. This occurs in ~ 75% of trimeras and was previously

postulated to result from spindle elongation occurring within a single cell compartment, or by cross-talk between spindle disassembly signals in one nucleus to cause early spindle disassembly of the spindle in the other nucleus[155]. Although it is unclear why mitotic collapse occurs, changes in motor protein expression or regulation could be a triggering factor. Evidence of this can be seen in the spindle phenotypes of *kip1* Δ/Δ cells [242]. Loss of Kip1 led to frequent mitotic defects in which cells failed to complete anaphase and then formed abnormal numbers of spindles that often experience additional rounds of mitotic collapse. Moreover, it is well documented that forces acting on the nucleus change throughout mitosis[134-136]. As cells undergo anaphase, the separation of sister chromatids by forces generated by kinesin-5 proteins pushes SPBs and associated DNA apart. This can be coupled to, or spatially regulated by, inward compressive forces from kinesin-14 motors and outward pulling forces on aMTs from dynein[134-136]. When such forces are imbalanced, cells can experience a range of phenotypes, including spindle collapse[105, 301].

Anaphase spindles can also be prone to collapse if the spindle midzone has poor structural stability[112]. Our previous studies of *C. albicans* cells that lacked both Kip1 and Kar3Cik1 indicated that these motors work together to stabilize the spindle, presumably by forming crosslinks between parallel and antiparallel spindle MTs [242]. Therefore, the observed decrease in expression of these motors, along with the passive MT-crosslinkers like Ase1, in FLC-treated wild-type cells could decrease spindle midzone structural stability of the elongating spindle in anaphase and contribute to the spindle collapse.

In tetraploid FLC-treated wild-type cells and *kip1* Δ/Δ mutants, nuclei are associated with extra spindle components. Mitoses with extra spindle components increases the level of chromosomal instability events such as recombination, a process that can elicit loss of heterozygosity (LOH) events as well as generate aneuploidies including isochromosome formation[155, 279]. Furthermore, extra spindle components can be prone to unequal chromosome segregation possibly because of incorrect alignment or attachment of sister chromatids and/or by the failure of one of the spindles to elongate across the bud neck both of which are controlled/influenced by motor protein function.

FLC-treated wild-type and *kip1* Δ/Δ cells exhibited downregulation of essential kinetochore proteins which could disrupt proper attachment of chromosomes to kinetochores. A number of studies have shown how altered regulation of these motors can contribute to unstable MT-kinetochore attachment or movement. For example, localization of the kinesin-5 Cin8 to kinetochores was observed in *S. cerevisiae*[185] where it provides sufficient tension of the kinetochore MT to the SPB. The recruitment of Cin8 to the kinetochores was further dependent on the MT-binding domains of the kinetochore protein Ndc80. Insufficient levels of Cin8 or mutations in Ndc80 both led to loss of tension and a major delay in mitotic progression. In addition, Cin8 motors at the kinetochore MT plus-ends promote net plus-end disassembly and influence chromosome congression[163]. Similarly, recent work in *C. albicans* linked Kip1 function at the kinetochore to a length-dependent depolymerase activity that organizes chromosomes at the spindle equator[33]. When one copy of Kip1 is missing, kinetochore MTs are longer and more disorganized compared to wild-type[33]. Whether Kip1 interacts with Ndc80 in *C. albicans* has yet to be determined. However, our observation of decreased Kip1 and Ndc80 in FLC-treated

wild-type cells suggests that these cells could experience some form of kinetochore malfunction and ploidy changes[302].

Additionally, FLC-treated wild-type and *kip1* Δ/Δ cells exhibited downregulation of the putative separase, *ESP1*. Separase facilitates cohesion cleavage during sister chromatid separation thereby triggering anaphase. However, emerging studies highlight Separase function in diverse cellular processes including nuclear positioning, spindle formation, and spindle midzone assembly and stability [303]. Separase is important in targeting the CPC/C to the midzone where it can provide additional spindle stabilization factors. Esp1 functional regulation could be attributed to its different proteolytic or non-proteolytic targets which determine its function during mitosis [304, 305]. In *C. albicans*, Esp1 thus far has a more canonical role in chromosome segregation, where it operates as a conventional separase to initiate spindle elongation[306-308]. In its absence, cells become large-budded with short G2/M or early anaphase spindles and extra SPBs in an unsegregated DNA mass[306-308]. It is worth investigating how changes in Esp1 expression levels control non-disjunction events in *C. albicans* mitosis and whether motor proteins could be a direct or indirect target for Esp1.

Altered motor protein function in tetraploid cells is highly reminiscent to certain human cancer cells. For instance, high expression of the kinesin-5 Eg5 was observed in gastric cancer cells where tetraploidy and aneuploidy are apparent[280, 309, 310]. Overexpression of Eg5 has also been observed in other cancer cells such as oral, breast and lung cancers, and is associated with a poor prognosis[280, 311, 312]. A recent study conducted in HeLa cells concluded that spindle polarity and tetraploid cell behaviour was determined by the balance of forces stemming from changes in Eg5 expression. Whereas

high levels of Eg5 correlated with tetraploid cells undergoing multipolar mitosis and generating aneuploid progeny, low levels of Eg5 dictated bipolar mitosis, where centrosomes clustered together in a “bipolar-like” structure and generated near-tetraploid progeny[280]. Therefore, regulation of kinesin-5 could control tumor heterogeneity and drive resistance to cancer therapies[280, 313, 314].

Aneuploidy can also advance other diseased states in humans. For example, in Alzheimer’s disease, defective mitoses accumulate aneuploid cells that are prone to neurodegeneration. The mechanistic processes that enable aneuploidy generation are linked to an excess of human Tau protein in the brain and cerebrospinal fluid of affected individuals. Interestingly, Tau-induced mitotic defects mimicked Eg5 loss-of-function defects[315]. Mechanistic analysis revealed that MT-bound Tau inhibits Eg5 movement along MTs, promoting Eg5 detachment and cell cycle defects, including aneuploidy.

Kinesin-5 activity influencing aneuploid formation is also apparent in other eukaryotic systems. In fission yeast, aneuploidy is generated due to kinesin-14 Pkl1 loss. When spindle MTs are unfocused due to the absence of Pkl1 (i.e., reduced MT crosslinking at the spindle poles), outward sliding forces by the kinesin-5 Cut7 result in long MT minus-end protrusions. As a result, post-anaphase segregated chromosomes get pushed to the site of cell division, which can lead to chromosome cut and aneuploidy during cytokinesis[124]. Changes in motor protein regulation to induce genome plasticity may be a property that cells employ under stress exposure, including changing cell environments or drug addition.

C. albicans exhibits a high tolerance for aneuploidy. This likely stems from an absence of a conventional meiotic cycle. Instead, they employ a cryptic parasexual cycle

that undergoes ploidy reduction via an uncoordinated process of concerted chromosome loss to produce diploid or near diploid cells[157]. Alternatively, cells may require spindle flexibility during morphological changes from yeast, pseudohyphal, and hyphal cells to respond to changing environments. Therefore, active control of motor protein expression may be a way to regulate spindle and chromosome organization and contribute to mitotic errors that foster genomic plasticity. Whether *C. albicans* and other human fungal pathogens evolutionarily adapted changes in motor protein expression as a general or specific stress-response mechanism remains to be investigated.

5.5 Materials and Methods

5.5.1 *C. albicans* Cell Culture and Growth Assays

A list of *C. albicans* strains used in this study is presented as **Table 5-3**. Strains were maintained on YPD plates. Experimental cultures were grown to mid-logarithmic phase in completely supplemented dropout medium (SDC) unless otherwise indicated. To create dilutions for spot assays, logarithmically growing cells were diluted to 1.0×10^6 cells/ml in phosphate-buffered saline (PBS). Serial dilutions of 10^5 , 10^4 , and 10^3 cells/ml were made. Five microliters of cell culture dilutions were pipetted for each spot, and plates were incubated at 30°C for 2 days, unless otherwise indicated.

For the cell evolution experiment, cultures were grown to mid-logarithmic phase and plated on YPD. 12 colonies were picked and passaged on YPD and YPD + 10 µg/mL Fluconazole every 48 hours, for a total of five passages.

Table 5-3. Names, genotypes, mating types, and sources of the strains used in this study

Strain	Genotype (Brief)	Genotype (Full)	Mating type	Source/parent
CF027	Wild type	<i>his1⁻/his1⁻ leu2⁻/leu2⁻ arg4⁻/arg4⁻</i>	α/α	RB1133 ^[168]
CF024	<i>kar3</i> Δ/Δ	<i>kar3</i> $\Delta::LEU2^+/kar3$ $\Delta::HIS1^+$	α/α	RSY11 ^[168]
CF016	<i>cik1</i> Δ/Δ	<i>cik1</i> $\Delta::LEU2^+/cik1$ $\Delta::HIS1^+$	α/α	CF027 ^[113]
CF311	<i>kip1</i> Δ/Δ	<i>kip1</i> $\Delta::LEU2^+/kip1$ $\Delta::HIS1^+$	α/α	CF236 ^[242]
CF381	<i>kip3</i> Δ/Δ	<i>kip3</i> $\Delta::LEU2^+/kip1$ $\Delta::HIS1^+$	α/α	CF027
CF429	<i>kip1</i> Δ/Δ (CR)	<i>kip1</i> $\Delta::gRNA$	α/α	AHY940 ^[211]
CF436	<i>tetO-KIP1/kip1</i> Δ	<i>tetO-KIP1-SAT1^R/kip1</i> $\Delta::LEU2^+$	α/α	CF236 ^[242]
CF495	<i>dyn1</i> Δ/Δ	<i>dyn1</i> $\Delta::LEU2^+/dyn1$ $\Delta::HIS1^+$	α/α	CF027
CF363	pGAL-TUB2-mCherry SPC98-GFP	<i>NEUT5L::[pGAL-TUB2-mCherry-ARG4⁺]/NEUT5L⁺, SPC98-GFP-SAT1^R</i>	α/α	CF156
CF368	pGAL-TUB2-mCherry SPC98-GFP <i>kip1</i> Δ/Δ	<i>NEUT5L::[pGAL-TUB2-mCherry-ARG4⁺]/NEUT5L⁺, SPC98-GFP-SAT1^R, <i>kip1</i>$\Delta::LEU2^+/kip1$$\Delta::HIS1^+$</i>	α/α	CF286 ^[242]

^a Strains are in the *white* phase unless otherwise noted

^b All strains are derived from SN152 (Nobel and Johnson 2005). Full genotype at auxotrophic markers: *his1::hisG/his1::hisG leu2::hisG/leu2::hisG arg4::hisG/arg4::hisG ura3::imm434::URA3/ura3::imm434 iro1::IRO1/iro1::imm434*.

5.5.2 Light Microscopy

Microscopy for static images was conducted using a Zeiss Axio Observer epifluorescence microscope with a 100X (1.40 NA) oil objective AxioCam hRM camera controlled by Axiovision software. Time-lapse imaging and some static imaging was conducted using the Olympus IX83 with a 100X oil objective (1.4 NA), Andor Zyla 4.2 Plus camera controlled by the cellSens software. Logarithmically growing cells were immobilized between an agarose pad and a glass coverslip, as previously described[113]. Images were captured in five z-slices 0.8 μm apart. Image stacks were compiled and analyzed using ImageJ (NIH) software. Final figures were compiled in Adobe Photoshop and Adobe Illustrator.

5.5.3 Flow Cytometry

Cells were grown to a density of 1×10^7 in liquid medium and gently spun down (500 x g) for 3 min. The supernatant was removed, and cells were fixed with 70% (v/v) ethanol for at least 1 h at room temperature. Cells were then washed twice with 50 mM sodium citrate and sonicated for 20-30 s at 30% power to separate the cells. Following sonication, cells were centrifuged and resuspended with 50 mM sodium citrate and incubated for at least 3 h at 37°C in 0.5 mg ml⁻¹ RNase A (Bioshop RNA675) in 50 mM sodium citrate. Cells were stained with 25 $\mu\text{g ml}^{-1}$ propidium iodide overnight in the dark at 37°C. Cells were sonicated for 5–10 s at 15% power, and 30,000 cells were analyzed on BD FACsAria 3 Cell Sorter (Becton Dickenson Biosciences). Data were analyzed in FlowJo. We thank Anna Selmecki for the detailed Flow Cytometry protocol and Matthew Gordon for Flow Cytometry experimental runs and analysis.

5.5.4 qPCR Ploidy Assay

Chromosome copy number was determined by qPCR ploidy assays according to the protocol of Pavelka et al[274]. Primers in non-coding regions on each chromosome arm were kindly provided by Judith Berman. DNA samples were prepared as previously described[316], with a 3 h RNase incubation period. Triplicate qPCR reactions were performed using the SYBR PowerUp Green Master mix kit in a QuantStudio5 instrument, and the qPCR results were analyzed by the modified Ct method[274]. Ct values for each chromosome were normalized to the control sample and $\Delta\Delta\text{Ct}$ was calculated using the median Ct value for each strain.

5.5.5 RNA Sequencing

Logarithmically growing yeast cells were harvested and centrifuged at 4,000 X g for 10 min at 4°C. Cell pellets were flash frozen in liquid nitrogen, and genomic DNA-free total RNA was extracted from each pellet by grinding the fungal mass to a fine powder and resuspending it in 1 ml TRIzol (Ambion) solution and using the RNeasy mini-spin columns (Qiagen) following the manufacturer's protocol. RNA quantification was carried out spectrophotometrically at 260 nm and 280 nm, and RNA integrity was evaluated by NanoDrop2000 (Thermo Scientific). Total RNA (1µg/sample) was shipped to the National Research Council of Canada DNA Sequencing Technologies Facility (Saskatoon, Canada), where further quality check was performed using a BioAnalyzer. Following short cDNA fragment synthesis using the TruSeq Stranded RNALT kit, the cDNA was sequenced on an Illumina HiSeq 2500 platform according to the manufacturer's guidelines (Illumina, USA). The DESeq2-based SARTools (v1.5.1) pipeline was adopted for differential analysis of mapped *C. albicans* Assembly 22 RNA-seq count data as previously

described[217]. A BH *p-value* adjustment was performed[218, 219], and the false-discovery rate was set at $P < 0.05$.

Chapter 6

General Discussion and Future Directions

6.1 *C. albicans* as a model system for studying mitotic motors

The work in this thesis embarked on characterizing the function of the kinesin-5 family motor, Kip1, in *C. albicans*. Although most eukaryotes require this motor to form their mitotic spindle, it was found that *C. albicans* does not. This discovery aligns with the earlier finding that spindle assembly from newly separated SPBs in *C. albicans* relies heavily on the kinesin-14, Kar3Cik1, which is also unprecedented in eukaryotes that have been studied[70-74]. When both kinesins are unavailable due to deletion or inhibition, *C. albicans* cells cannot survive. It therefore seems that this fungus has not developed mechanisms to implement other spindle force producers in the way that budding and fission yeast have to compensate for kinesin-5 and -14 loss[67, 111, 195]. Altogether, these findings provide a sound rationale for investigating the entire mechanism of mitosis in *C. albicans*, rather than rely on model eukaryotes like *S. cerevisiae* or *S. pombe* as proxies. Combined with emerging data showing that polyploidization, ploidy reduction, and the parasexual cycle of *C. albicans* can mimic fates of cancer cells, there is substantial knowledge to be gained from using *C. albicans* as a model system to study the molecular drivers of mitosis.

6.2 An apparent lack of force-balance

Typically, when inward spindle forces (toward the spindle midzone) are excessive due to ablation of kinesin-5 activity, only monopolar spindles will form[64-69]. Excessive outward forces, through loss of kinesin-14, will result in unstable spindles with

unfocused spindle poles[107]. Given the noncanonical spindle defects that arise in *C. albicans* cells lacking kinesin-14 or kinesin-5 activity, a critical question is: How does this fungus control the force-balance equilibrium that assembles the bipolar spindle and maintains its proper architecture during each stage of mitosis? This question is difficult to answer because spindles usually have redundant force-generating systems operating conjointly and cells can compensate for loss of individual spindle-associated proteins by up- or down-regulating others[121, 123]. The lethal phenotype produced when kinesin-14 and kinesin-5 are both absent implies that they have synergistic or cooperative roles in the *C. albicans* spindle, which contrasts their antagonistic roles in other eukaryotes. Kip1's localization near the spindle poles during the early stages of spindle assembly may mean that it crosslinks and stabilizes the first few antiparallel MT overlaps that form when the SPBs begin to separate. Primary sequence analysis shows that *C. albicans* Kip1 harbors the conserved "BASS" domain that enables kinesin-5 motors to form homotetramers. This architecture places a motor domain pair at each end of the motor complex, where they can each crosslink and slide a separate MT. Thus, Kip1 motors could capture and crosslink the MTs that initially form high-angle interactions with their counterparts from the other SPB[113]. The minus-end directed motility of Kar3/Cik1 could then re-angle these MTs into an antiparallel configuration, leading to a bipolar architecture. In this regard, the MT crosslinking activity of either motor may suffice to establish enough ipMT overlaps that a bipolar spindle can form. This idea is supported by modeling simulations by Blackwell R., *et al.* who demonstrated that as long as sufficient antiparallel MT overlaps from adjacent SPBs are maintained, forces from MT polymerization or other motors can construct a bipolar spindle[98]. This type of mechanism may explain why *kar3Δ/Δ* mutants were still

able to form bipolar spindles when the Kip1 inhibitor, ABT, was included in the growth media. Although incapable of sliding MTs, Kip1 motors that became locked onto the MTs near SPBs by ABT could, in principle, still stabilize the initial antiparallel MT overlaps. This illuminating finding hints at the possibility that *C. albicans* Kip1 may play a more passive role than its homologs in the early stages of mitosis by functioning exclusively as a MT crosslinker rather than a crosslinker and outward force producer.

Later in mitosis, the need for plus-end directed motility of Kip1 appears to be more critical. ABT addition would prevent Kip1 from re-localizing from the spindle poles to the midzone. In this regard, both Kip1 and Kar3/Cik1 depletion would result in insufficient crosslinks to stabilize MTs, especially at the spindle midzone, compromising spindle integrity and leading to cell death. These outcomes demonstrate that the roles of kinesin-5 and -14 motors in *C. albicans* do not conform to the classic force-balance paradigm observed in other eukaryotes, including related yeasts.

In other yeasts, the consequences of force imbalances have been well-characterized[68, 119, 120, 317]. When opposing motors are both absent, the spindle can still form and function, albeit with subpar integrity. This raises another important question: why are energy-consuming motor activities needed if essentially the same spindle structure can form without them? The answer may lie in the robustness of spindle MT dynamics and function. Although opposing motors may not be required, their presence could allow the spindle to tolerate mechanical and biochemical fluctuations of these MTs while maintaining integrity and accuracy of kinetochore attachments and chromosome segregation. For example, Neahring *et al.*, demonstrated that spindles form in the absence of opposing motors but are more fragile and mechanically unstable in metaphase and

exhibit lagging chromosomes (i.e., error-prone) in anaphase[318]. Moreover, MT-associated motors broadly regulate the properties of MT networks, such as their elasticity and viscosity, MT polymerization dynamics, and MT cytoskeleton organization[318-320]. Therefore, opposing motor activity could also help the spindle's ability to distribute and dissipate forces from internal and external pushes, pulls or torques on spindle MTs. Perhaps *C. albicans*' unique use of its mitotic motors permits this fungus to more readily experience error-prone mitosis, enhancing its genome plasticity. Alternatively, spindle force-balance could exist in other formats in *C. albicans* that are less dependent on these motor proteins. For example, cells may use extensile and compressive forces from MT assembly dynamics, elastic elements such as chromosomes, and the nuclear envelope to help control spindle assembly and architectural fluctuations[321].

6.3 Kip1 and Dyn1 collaborate in spindle elongation

The data presented in Chapters 3 and 4 show that anaphase spindle elongation is largely dependent on pushing forces from Kip1 motors located in the spindle midzone and pulling forces on aMTs from Dyn1 motors at the cell cortex. Each motor can partially compensate for loss of the other to complete anaphase, but different defects are often evident when one motor is missing. The absence of Kip1 delays anaphase onset, produces shorter spindles, and cells generally exhibit growth defects. In Dyn1-depleted cells, anaphase onset is not delayed, but the time cells spend in anaphase is significantly longer. These cells also experience major growth defects and spindle mispositioning and buckling. We propose that both motors provide spindle elongation forces but do so by different mechanisms and at different times during anaphase. Buckling of late anaphase spindles in Dyn1-depleted cells suggests that the bulk of the extensile force likely comes from Dyn1 at this stage, while

Kip1's force contribution is maximal at the start of anaphase. In this scenario, inward, compressive forces from the spindle (i.e., inward forces from motors, nucleus, chromosomes etc.) would exceed Kip1's outward, extensile forces and cause spindle buckling/bending[250].

Additionally, we envision that each motor's role(s) may differ in the other growth forms of *C. albicans*. Indeed, *kip1* Δ/Δ mutants exhibited more significant growth defects in hypha-inducing conditions. Compared to wild-type, *kip1* Δ/Δ cells had fewer septa after 6 h. When we looked at DAPI-stained *kip1* Δ/Δ hyphae, we saw that nuclear division occurred but was significantly slower than wild-type. These phenotypes may stem from a delay in anaphase, like that observed in the yeast growth form. Images of *kip1* Δ/Δ hyphae expressing fluorescent tubulin showed bipolar spindles with long astral MTs that extended the length of the germ tube. In hyphae, timely regulation of motor activity may be further exaggerated where Kip1 provides initial pushing forces, followed by Dyn1 pulling forces as the spindle elongates. We propose that in the absence of Kip1, spindles that formed in hyphae cannot reach the minimum length needed to trigger Dyn1 pulling forces. To compensate this, the cell produces long aMTs that span the length of the germ tube (**Figure 6-1A**). This process would considerably delay the entry into anaphase, most likely contributing to the extremely slow growth of *kip1* Δ/Δ hyphal cells (**Figure 6-1B**). In filamentous fungi, this model of kinesin-5 mediated initial spindle elongation, followed by powerful Dyn1 pulling forces, is needed to limit the duration of anaphase[136]. Solely relying on kinesin-5 forces would prolong anaphase 5-6-times longer than if both Kip1 and Dyn1 coordinated anaphase forces[136, 322], limiting the cell's ability to compete for resources.

6.4 Can tuning motor activity induce tetraploidy?

Cytokinesis is the final step in mitosis. This process is initiated during chromosome segregation, when the ingressing cleavage furrow begins to partition the cytoplasm between the mother and daughter cells. However, cytokinesis is not complete until much later when the final cytoplasmic bridge connecting the mother and daughter cell is severed. Cytokinesis is a highly-ordered process, where cytoskeletal, chromosomal, and cell cycle regulatory pathways are all coordinated and proteins can participate in multiple steps. As such, it is not surprising that cytokinesis can sometimes fail. Cytokinesis failure leads to both centrosome/SPB amplification and production of tetraploid cells[323].

C. albicans cells exposed to FLC experience cytokinesis failure. Soon after, budding ensues and cells form trimers (mother, daughter, and granddaughter cells) that contain multiple bipolar spindles. Often, one set of bipolar spindles experiences a mitotic collapse, resulting in tetraploid cells. Unequal segregation of the chromosomes in these tetraploid nuclei can result in aneuploid progeny capable of cell survival[155]. The work presented in this thesis highlights that a subpopulation of cells devoid of Kip1 function also experience a mitotic collapse, form multiple spindle components, and then to attempt to segregate their abnormal nuclei, sometimes erroneously, leading to genetically heterogeneous cells. The similarity in spindle phenotypes of both conditions (i.e., FLC-treated wild-type cells and *kip1* Δ/Δ mutants) led us to investigate whether altered Kip1 function could induce mitotic errors that lead to aneuploidy generation in FLC-treated cells. In support of this, we found that Kip1 gene expression, as well as several other motors,

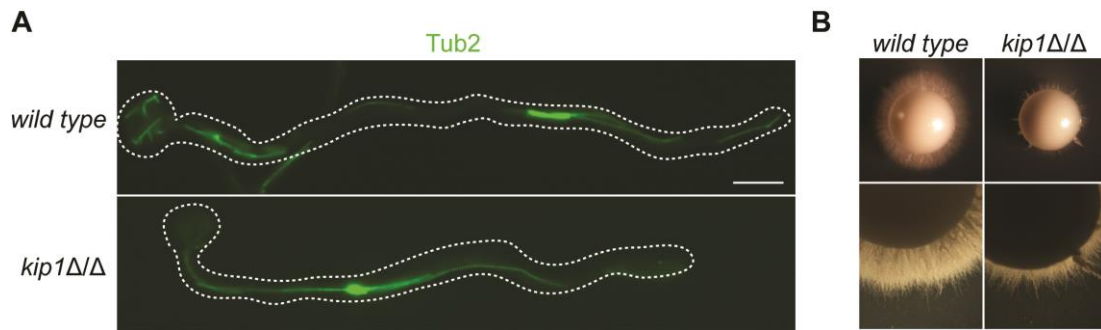


Figure 6-1. Hyphal defects in *kip1Δ/Δ* mutants. (A) Images of wild type (CF289) and *kip1Δ/Δ* (CF226) cells expressing Tub2-GFP. Stationary-phase cultures of wild type and *kip1Δ/Δ* strains were diluted into fresh SDC-sucrose medium and incubated at 37°C for 5 h to induce hyphae. Scale bars, 5 μm. (B) Wild type and *kip1Δ/Δ* mutants were grown on solid media containing mannitol (Spider media) to stimulate hyphal growth.

was reduced in wild-type cells treated with FLC.

Interestingly, FLC-treated wild-type cells also had altered expression of several genes encoding proteins that are important for spindle disassembly and cytokinesis including motor proteins such as Kip1, and chromosomal passenger complex (CPC) proteins. In Chapter 5, we discussed that budding yeast kinesin-5 (Kip1) and kinesin-8 (Kip3) recruit CPC to the midzone to ensure timely spindle disassembly[290]. Both motors trap CPC at the spindle midzone where CPC phosphorylates MT-stabilizing proteins such as Bim1 to promote their dissociation from the midzone[324], and to activate MT-destabilizing proteins like She1[325] to promote spindle disassembly. In FLC-treated wild-type cells, reduced Kip1 and CPC protein expression could affect CPC localization to the spindle midzone, directly impacting spindle disassembly mechanisms and cytokinesis.

We were also intrigued by the downregulation of proteins important in the mitotic exit network (MEN). MEN is a Ras-like GTPase signaling pathway that integrates both spatial and temporal cues to ensure that cytokinesis occurs only after chromosomes have partitioned between the mother and daughter cell during anaphase. In wild-type cells treated with FLC, Nud1 was downregulated. Nud1 acts as a scaffold to recruit and activate the Dbf2-Mob1 kinase complex, which promotes the release of the protein phosphatase Cdc14[326]. The released phosphatase triggers exit from mitosis by reversing mitotic phosphorylation on various proteins, including the major mitotic regulator, Cdk1 (Cdc28 yeast equivalent) and thus allowing exit from mitosis and preparation for a new G1 phase[327, 328]. Downregulation of mitotic exit proteins could disrupt normal cell cycle progression and lead to cytokinesis and/or re-initiation of cell cycle resulting in the

emergence of another cell compartment (i.e., granddaughter cells observed in FLC-treated wild-type cells).

6.5 Future studies to delineate the links between cell stress and spindle motor regulation

The work presented in this thesis has underscored the importance of Kip1 and Dyn1 in maintaining spindle integrity and as drivers of spindle elongation. It has also shown that the absence of Kip1 results in the appearance of random aneuploidies, some of which may be selected if they afford resistance to FLC or other stresses. However, several questions remain unanswered. Does Kip1 have any functional domains that specifically interact with regulator factors induced to act under stressful growth conditions? If so, what are these binding partners of Kip1, and how do they regulate Kip1's activities? To identify Kip1 regulatory binding partners and determine how they may alter the activity of this kinesin to generate mitotic defects under stress in *C. albicans*, N- and C-terminally TAP-tagged (tandem affinity purification) versions of Kip1 could be designed. Cells expressing these proteins could then be grown in cultures under conditions that activate stress-specific pathways. Capturing the TAP-tagged kinesins by affinity purification followed by mass spectrometry analysis will enable characterization of the bound fraction components and identification of kinesin binding proteins that change Kip1 localization or function under stress. To verify that identified proteins are forming specific associations with Kip1, a fluorescent tag could be fused to their respective genes, allowing use of fluorescence microscopy to assess cell cycle stage-dependent co-localization with Kip1. For proteins associated with Kip1 under stress conditions specifically, transcriptomic analyses could be

used to determine how each stress condition regulates their genes, thus providing new links between condition-specific gene regulation and downstream mitotic effects.

6.6 Significance of this research

By addressing central questions about how kinesins and dynein control the assembly and function of the mitotic spindle in *C. albicans*, this thesis offers important new insight into a process that can generate chromosome aberrations in fungal genomes that lead to drug resistance. With this knowledge, we may become better equipped to develop new antifungal agents that target these mitotic factors, yet do not cross-react with their counterparts in humans. We could also apply this knowledge to emerging fungal threats, such as *Candida auris*. This pathogen has caused outbreaks of deadly invasive infections worldwide because of its ability to survive all clinically available antifungal medications[329]. Similar to *C. albicans*, *C. auris* undergoes significant genome reorganization within a short time frame when exposed to antifungals[330]. As antifungal drug resistance continues to emerge among these pathogens[331, 332], infection-related deaths will undoubtedly escalate. Thus, *C. albicans* is an excellent model yeast for studying how mitotic motors function and how they could play critical roles in generating genetic diversity as an adaptive mechanism in other clinically important pathogens.

References

1. McManus, B.A. and D.C. Coleman, *Molecular epidemiology, phylogeny and evolution of Candida albicans*. Infect Genet Evol, 2014. **21**: p. 166-78.
2. Kumamoto, C.A., *Inflammation and gastrointestinal Candida colonization*. Curr Opin Microbiol, 2011. **14**(4): p. 386-91.
3. Rosenbach, A., et al., *Adaptations of Candida albicans for growth in the mammalian intestinal tract*. Eukaryot Cell, 2010. **9**(7): p. 1075-86.
4. Kim, J. and P. Sudbery, *Candida albicans, a major human fungal pathogen*. Journal of microbiology, 2011. **49**(2): p. 171-7.
5. Odds, F.C., *Candida infections: an overview*. Critical reviews in microbiology, 1987. **15**(1): p. 1-5.
6. Finkel, J.S. and A.P. Mitchell, *Genetic control of Candida albicans biofilm development*. Nat Rev Microbiol, 2011. **9**(2): p. 109-18.
7. Berman, J. and P.E. Sudbery, *Candida Albicans: a molecular revolution built on lessons from budding yeast*. Nat Rev Genet, 2002. **3**(12): p. 918-30.
8. Jones, T., et al., *The diploid genome sequence of Candida albicans*. Proc Natl Acad Sci U S A, 2004. **101**(19): p. 7329-34.
9. Kabir, M.A., M.A. Hussain, and Z. Ahmad, *Candida albicans: A Model Organism for Studying Fungal Pathogens*. ISRN Microbiol, 2012. **2012**: p. 538694.
10. Selmecki, A., A. Forche, and J. Berman, *Genomic plasticity of the human fungal pathogen Candida albicans*. Eukaryot Cell, 2010. **9**(7): p. 991-1008.
11. Selmecki, A.M., et al., *Acquisition of aneuploidy provides increased fitness during the evolution of antifungal drug resistance*. PLoS Genet, 2009. **5**(10): p. e1000705.
12. Wickes, B.L. and R. Petter, *Genomic variation in C. albicans*. Curr Top Med Mycol, 1996. **7**(1): p. 71-86.
13. Schneider, A., *Untersuchungen über Plathelminthen*. Upper-Hessian Society for Natural and Medical Science, 1873. **14**.
14. Strasburger, *Zellbildung und Zelltheilung "Cell Formation and Cell Division*. Gustav Fischer, 1880.
15. Van Beneden, E., *Recherches sur les Dicyemides*. Bull. Acad, 1876. **41**: p. 1-111.
16. Flemming, W., *Zur Kenntniss der Zelle und ihre Lebenserscheinungen*. Arch. Mike. Anat, 1878. **16**: p. 302-436.
17. Mayzel, W., *Ueber eigenthümliche Vorgänge bei der Theilung der Kerne in Epithelialzellen*. Zentralbl. Med. Wiss, 1885. **13**: p. 849-852.
18. Weissmann, A., *Die Continuität des Keimplasma's als Grundlage einer Theorie der Vererbung*. Fischer, 1885.
19. Lauterborn, R., *Untersuchungen ueber Bau, Kernteilung und Bewegung der Diatomeen*. Wilhelm Engelmann., 1896.
20. Rozsa, G. and R.W. Wyckoff, *The electron microscopy of dividing cells*. Biochim Biophys Acta, 1950. **6**(2): p. 334-9.
21. Roth, L.E. and E.W. Daniels, *Electron microscopic studies of mitosis in amebae. II. The giant ameba Pelomyxa carolinensis*. J Cell Biol, 1962. **12**: p. 57-78.
22. Brinkley, B.R. and E. Stubblefield, *The fine structure of the kinetochore of a mammalian cell in vitro*. Chromosoma, 1966. **19**(1): p. 28-43.
23. Fuge, H., *Ultrastructure and function of the spindle apparatus. Microtubules and chromosomes during nuclear division*. Protoplasma, 1974. **82**(4): p. 289-320.
24. Wade, R.H., D. Chretien, and D. Job, *Characterization of microtubule protofilament numbers. How does the surface lattice accommodate?* J Mol Biol, 1990. **212**(4): p. 775-86.

25. Zhang, R., et al., *Mechanistic Origin of Microtubule Dynamic Instability and Its Modulation by EB Proteins*. Cell, 2015. **162**(4): p. 849-59.
26. Thawani, A., et al., *Molecular mechanism of microtubule nucleation from gamma-tubulin ring complex*. 2019: p. 853010.
27. Prosser, S.L. and L. Pelletier, *Mitotic spindle assembly in animal cells: a fine balancing act*. Nat Rev Mol Cell Biol, 2017. **18**(3): p. 187-201.
28. Morgan, D.O., *The Cell Cycle*, ed. E. Lawrence. 2007, London: New Science Press Ltd 297.
29. Jaspersen, S.L. and M. Winey, *The budding yeast spindle pole body: structure, duplication, and function*. Annu Rev Cell Dev Biol, 2004. **20**: p. 1-28.
30. Ruthnick, D., et al., *Characterization of spindle pole body duplication reveals a regulatory role for nuclear pore complexes*. J Cell Biol, 2017. **216**(8): p. 2425-2442.
31. Meunier, S. and I. Vernos, *Microtubule assembly during mitosis - from distinct origins to distinct functions?* J Cell Sci, 2012. **125**(Pt 12): p. 2805-14.
32. McDonald, K.L., M.K. Edwards, and J.R. McIntosh, *Cross-sectional structure of the central mitotic spindle of *Diatoma vulgare*. Evidence for specific interactions between antiparallel microtubules*. J Cell Biol, 1979. **83**(2 Pt 1): p. 443-61.
33. McCoy, K.M., et al., *Physical limits on kinesin-5-mediated chromosome congression in the smallest mitotic spindles*. Mol Biol Cell, 2015. **26**(22): p. 3999-4014.
34. van het Hoog, M., et al., *Assembly of the *Candida albicans* genome into sixteen supercontigs aligned on the eight chromosomes*. Genome Biol, 2007. **8**(4): p. R52.
35. Tyson, J.J., K.C. Chen, and B. Novák, *Cell Cycle, Budding Yeast*, in *Encyclopedia of Systems Biology*, W. Dubitzky, et al., Editors. 2013, Springer New York: New York, NY. p. 337-341.
36. Huang, B. and T.C. Huffaker, *Dynamic microtubules are essential for efficient chromosome capture and biorientation in *S. cerevisiae**. J Cell Biol, 2006. **175**(1): p. 17-23.
37. Rudner, A.D. and A.W. Murray, *The spindle assembly checkpoint*. Curr Opin Cell Biol, 1996. **8**(6): p. 773-80.
38. Straight, A.F. and A.W. Murray, *The spindle assembly checkpoint in budding yeast*. Methods Enzymol, 1997. **283**: p. 425-40.
39. Morgan, D.O., *SnapShot: cell-cycle regulators I*. Cell, 2008. **135**(4): p. 764-764 e1.
40. Maddox, P.S., K.S. Bloom, and E.D. Salmon, *The polarity and dynamics of microtubule assembly in the budding yeast *Saccharomyces cerevisiae**. Nat Cell Biol, 2000. **2**(1): p. 36-41.
41. Clarke DJ, S.A., Gimenez-Abian JF., *DNA Damage-Independent Checkpoints from Yeast to Man*. Madame Curie Bioscience Database. 2000-2013, Austin TX: Landes Bioscience.
42. Rozelle, D.K., S.D. Hansen, and K.B. Kaplan, *Chromosome passenger complexes control anaphase duration and spindle elongation via a kinesin-5 brake*. J Cell Biol, 2011. **193**(2): p. 285-94.
43. Wordeman, L., *How kinesin motor proteins drive mitotic spindle function: Lessons from molecular assays*. Semin Cell Dev Biol, 2010. **21**(3): p. 260-8.
44. Yang, T., X.B. Zhang, and Z.M. Zheng, *Suppression of KIF14 expression inhibits hepatocellular carcinoma progression and predicts favorable outcome*. Cancer Sci, 2013. **104**(5): p. 552-7.
45. Wang, Q., et al., *Kinesin family member 14 is a candidate prognostic marker for outcome of glioma patients*. Cancer Epidemiol, 2013. **37**(1): p. 79-84.
46. Theriault, B.L., et al., *Kinesin family member 14: an independent prognostic marker and potential therapeutic target for ovarian cancer*. Int J Cancer, 2012. **130**(8): p. 1844-54.

47. Huszar, D., et al., *Kinesin motor proteins as targets for cancer therapy*. *Cancer Metastasis Rev*, 2009. **28**(1-2): p. 197-208.
48. Rath, O. and F. Kozielski, *Kinesins and cancer*. *Nat Rev Cancer*, 2012. **12**(8): p. 527-39.
49. Yu, Y. and Y.M. Feng, *The role of kinesin family proteins in tumorigenesis and progression: potential biomarkers and molecular targets for cancer therapy*. *Cancer*, 2010. **116**(22): p. 5150-60.
50. Brady, S.T., *A novel brain ATPase with properties expected for the fast axonal transport motor*. *Nature*, 1985. **317**(6032): p. 73-5.
51. Hirokawa, N. and R. Takemura, *Kinesin superfamily proteins and their various functions and dynamics*. *Exp Cell Res*, 2004. **301**(1): p. 50-9.
52. Miki, H., Y. Okada, and N. Hirokawa, *Analysis of the kinesin superfamily: insights into structure and function*. *Trends Cell Biol*, 2005. **15**(9): p. 467-76.
53. Woehlke, G. and M. Schliwa, *Walking on two heads: the many talents of kinesin*. *Nat Rev Mol Cell Biol*, 2000. **1**(1): p. 50-8.
54. Hackney, D.D., *Evidence for alternating head catalysis by kinesin during microtubule-stimulated ATP hydrolysis*. *Proc Natl Acad Sci U S A*, 1994. **91**(15): p. 6865-9.
55. Hancock, W.O. and J. Howard, *Kinesin's processivity results from mechanical and chemical coordination between the ATP hydrolysis cycles of the two motor domains*. *Proc Natl Acad Sci U S A*, 1999. **96**(23): p. 13147-52.
56. Yount, A.L., H. Zong, and C.E. Walczak, *Regulatory mechanisms that control mitotic kinesins*. *Exp Cell Res*, 2015. **334**(1): p. 70-7.
57. Yildiz, A., et al., *Kinesin walks hand-over-hand*. *Science*, 2004. **303**(5658): p. 676-8.
58. Endres, N.F., et al., *A lever-arm rotation drives motility of the minus-end-directed kinesin Ncd*. *Nature*, 2006. **439**(7078): p. 875-8.
59. Rank, K.C., et al., *Kar3Vik1, a member of the kinesin-14 superfamily, shows a novel kinesin microtubule binding pattern*. *J Cell Biol*, 2012. **197**(7): p. 957-70.
60. Kashina, A.S., G.C. Rogers, and J.M. Scholey, *The bimC family of kinesins: essential bipolar mitotic motors driving centrosome separation*. *Biochim Biophys Acta*, 1997. **1357**(3): p. 257-71.
61. Scholey, J.E., et al., *Structural basis for the assembly of the mitotic motor Kinesin-5 into bipolar tetramers*. *Elife*, 2014. **3**: p. e02217.
62. Miyamoto, D.T., et al., *The kinesin Eg5 drives poleward microtubule flux in Xenopus laevis egg extract spindles*. *J Cell Biol*, 2004. **167**(5): p. 813-8.
63. Kapitein, L.C., et al., *The bipolar mitotic kinesin Eg5 moves on both microtubules that it crosslinks*. *Nature*, 2005. **435**(7038): p. 114-8.
64. Kapoor, T.M., et al., *Probing spindle assembly mechanisms with monastrol, a small molecule inhibitor of the mitotic kinesin, Eg5*. *J Cell Biol*, 2000. **150**(5): p. 975-88.
65. Cochran, J.C., et al., *Monastrol inhibition of the mitotic kinesin Eg5*. *J Biol Chem*, 2005. **280**(13): p. 12658-67.
66. Sharp, D.J., et al., *The bipolar kinesin, KLP61F, cross-links microtubules within interpolar microtubule bundles of Drosophila embryonic mitotic spindles*. *J Cell Biol*, 1999. **144**(1): p. 125-38.
67. Hoyt, M.A., et al., *Loss of function of Saccharomyces cerevisiae kinesin-related CIN8 and KIP1 is suppressed by KAR3 motor domain mutations*. *Genetics*, 1993. **135**(1): p. 35-44.
68. Saunders, W.S. and M.A. Hoyt, *Kinesin-related proteins required for structural integrity of the mitotic spindle*. *Cell*, 1992. **70**(3): p. 451-8.
69. Hoyt, M.A., et al., *Two Saccharomyces cerevisiae kinesin-related gene products required for mitotic spindle assembly*. *J Cell Biol*, 1992. **118**(1): p. 109-20.
70. Cochran, J.C., et al., *Mechanistic analysis of the mitotic kinesin Eg5*. *J Biol Chem*, 2004. **279**(37): p. 38861-70.

71. van den Wildenberg, S.M., et al., *The homotetrameric kinesin-5 KLP61F preferentially crosslinks microtubules into antiparallel orientations*. *Curr Biol*, 2008. **18**(23): p. 1860-4.
72. Tao, L., et al., *A homotetrameric kinesin-5, KLP61F, bundles microtubules and antagonizes Ncd in motility assays*. *Curr Biol*, 2006. **16**(23): p. 2293-302.
73. Gordon, D.M. and D.M. Roof, *The kinesin-related protein Kip1p of Saccharomyces cerevisiae is bipolar*. *J Biol Chem*, 1999. **274**(40): p. 28779-86.
74. Hildebrandt, E.R., et al., *Homotetrameric form of Cin8p, a Saccharomyces cerevisiae kinesin-5 motor, is essential for its in vivo function*. *J Biol Chem*, 2006. **281**(36): p. 26004-13.
75. Winey, M., et al., *Three-dimensional ultrastructural analysis of the Saccharomyces cerevisiae mitotic spindle*. *J Cell Biol*, 1995. **129**(6): p. 1601-15.
76. Mann, B.J. and P. Wadsworth, *Kinesin-5 Regulation and Function in Mitosis*. *Trends Cell Biol*, 2019. **29**(1): p. 66-79.
77. Straight, A.F., J.W. Sedat, and A.W. Murray, *Time-lapse microscopy reveals unique roles for kinesins during anaphase in budding yeast*. *J Cell Biol*, 1998. **143**(3): p. 687-94.
78. Roostalu, J., E. Schiebel, and A. Khmelinskii, *Cell cycle control of spindle elongation*. *Cell Cycle*, 2010. **9**(6): p. 1084-90.
79. Bishop, J.D., Z. Han, and J.M. Schumacher, *The Caenorhabditis elegans Aurora B kinase AIR-2 phosphorylates and is required for the localization of a BimC kinesin to meiotic and mitotic spindles*. *Mol Biol Cell*, 2005. **16**(2): p. 742-56.
80. Miki, T., et al., *Endogenous localizome identifies 43 mitotic kinesins in a plant cell*. *Proc Natl Acad Sci U S A*, 2014. **111**(11): p. E1053-61.
81. Tikhonenko, I., et al., *Kinesin-5 is not essential for mitotic spindle elongation in Dictyostelium*. *Cell Motil Cytoskeleton*, 2008. **65**(11): p. 853-62.
82. Ferenz, N.P., A. Gable, and P. Wadsworth, *Mitotic functions of kinesin-5*. *Semin Cell Dev Biol*, 2010. **21**(3): p. 255-9.
83. Sawin, K.E., et al., *Mitotic spindle organization by a plus-end-directed microtubule motor*. *Nature*, 1992. **359**(6395): p. 540-3.
84. Kajtez, J., et al., *Overlap microtubules link sister k-fibres and balance the forces on bi-oriented kinetochores*. *Nat Commun*, 2016. **7**: p. 10298.
85. Ma, N., et al., *TPX2 regulates the localization and activity of Eg5 in the mammalian mitotic spindle*. *J Cell Biol*, 2011. **195**(1): p. 87-98.
86. Chen, H., et al., *The non-motor adaptor HMMR dampens Eg5-mediated forces to preserve the kinetics and integrity of chromosome segregation*. *Mol Biol Cell*, 2018.
87. Tytell, J.D. and P.K. Sorger, *Analysis of kinesin motor function at budding yeast kinetochores*. *J Cell Biol*, 2006. **172**(6): p. 861-74.
88. Uteng, M., et al., *Poleward transport of Eg5 by dynein-dynactin in Xenopus laevis egg extract spindles*. *J Cell Biol*, 2008. **182**(4): p. 715-26.
89. Gable, A., et al., *Dynamic reorganization of Eg5 in the mammalian spindle throughout mitosis requires dynein and TPX2*. *Mol Biol Cell*, 2012. **23**(7): p. 1254-66.
90. Edamatsu, M., *Bidirectional motility of the fission yeast kinesin-5, Cut7*. *Biochem Biophys Res Commun*, 2014. **446**(1): p. 231-4.
91. Shapira, O., et al., *A potential physiological role for bi-directional motility and motor clustering of mitotic kinesin-5 Cin8 in yeast mitosis*. *J Cell Sci*, 2017. **130**(4): p. 725-734.
92. Roostalu, J., et al., *Directional switching of the kinesin Cin8 through motor coupling*. *Science*, 2011. **332**(6025): p. 94-9.
93. Gerson-Gurwitz, A., et al., *Directionality of individual kinesin-5 Cin8 motors is modulated by loop 8, ionic strength and microtubule geometry*. *Embo J*, 2011. **30**(24): p. 4942-54.
94. Fridman, V., et al., *Kinesin-5 Kip1 is a bi-directional motor that stabilizes microtubules and tracks their plus-ends in vivo*. *J Cell Sci*, 2013. **126**(Pt 18): p. 4147-59.

95. Thiede, C., et al., *Regulation of bi-directional movement of single kinesin-5 Cin8 molecules*. Bioarchitecture, 2012. **2**(2): p. 70-74.
96. Kapitein, L.C., et al., *Microtubule cross-linking triggers the directional motility of kinesin-5*. J Cell Biol, 2008. **182**(3): p. 421-8.
97. Kwok, B.H., et al., *Allosteric inhibition of kinesin-5 modulates its processive directional motility*. Nat Chem Biol, 2006. **2**(9): p. 480-5.
98. Blackwell, R., et al., *Physical determinants of bipolar mitotic spindle assembly and stability in fission yeast*. Sci Adv, 2017. **3**(1): p. e1601603.
99. Barrett, J.G., B.D. Manning, and M. Snyder, *The Kar3p kinesin-related protein forms a novel heterodimeric structure with its associated protein Cik1p*. Mol Biol Cell, 2000. **11**(7): p. 2373-85.
100. Duan, D., et al., *Neck rotation and neck mimic docking in the noncatalytic Kar3-associated protein Vik1*. J Biol Chem, 2012. **287**(48): p. 40292-301.
101. Joshi, M., et al., *Kar3Vik1 mechanochemistry is inhibited by mutation or deletion of the C terminus of the Vik1 subunit*. J Biol Chem, 2013. **288**(52): p. 36957-70.
102. Matulienė, J., et al., *Function of a minus-end-directed kinesin-like motor protein in mammalian cells*. Journal of Cell Science, 1999. **112** (Pt 22): p. 4041-50.
103. Karabay, A. and R.A. Walker, *Identification of microtubule binding sites in the Ncd tail domain*. Biochemistry, 1999. **38**(6): p. 1838-49.
104. She, Z.Y. and W.X. Yang, *Molecular mechanisms of kinesin-14 motors in spindle assembly and chromosome segregation*. J Cell Sci, 2017. **130**(13): p. 2097-2110.
105. Fink, G., et al., *The mitotic kinesin-14 Ncd drives directional microtubule-microtubule sliding*. Nature cell biology, 2009. **11**(6): p. 717-23.
106. Ambrose, J.C., et al., *A minus-end-directed kinesin with plus-end tracking protein activity is involved in spindle morphogenesis*. Molecular Biology of the Cell, 2005. **16**(4): p. 1584-92.
107. Hepperla, A.J., et al., *Minus-end-directed Kinesin-14 motors align antiparallel microtubules to control metaphase spindle length*. Dev Cell, 2014. **31**(1): p. 61-72.
108. Civelekoglu-Scholey, G., et al., *Prometaphase spindle maintenance by an antagonistic motor-dependent force balance made robust by a disassembling lamin-B envelope*. J Cell Biol, 2010. **188**(1): p. 49-68.
109. Sharp, D.J., et al., *Functional coordination of three mitotic motors in Drosophila embryos*. Mol Biol Cell, 2000. **11**(1): p. 241-53.
110. Saunders, W., et al., *The Saccharomyces cerevisiae kinesin-related motor Kar3p acts at preanaphase spindle poles to limit the number and length of cytoplasmic microtubules*. J Cell Biol, 1997. **137**(2): p. 417-31.
111. Troxell, C.L., et al., *pk11(+) and klp2(+): Two kinesins of the Kar3 subfamily in fission yeast perform different functions in both mitosis and meiosis*. Mol Biol Cell, 2001. **12**(11): p. 3476-88.
112. Gardner, M.K., et al., *The microtubule-based motor Kar3 and plus end-binding protein Bim1 provide structural support for the anaphase spindle*. J Cell Biol, 2008. **180**(1): p. 91-100.
113. Frazer, C., et al., *Candida albicans Kinesin Kar3 Depends on a Cik1-Like Regulatory Partner Protein for Its Roles in Mating, Cell Morphogenesis, and Bipolar Spindle Formation*. Eukaryot Cell, 2015. **14**(8): p. 755-74.
114. Saunders, W., V. Lengyel, and M.A. Hoyt, *Mitotic spindle function in Saccharomyces cerevisiae requires a balance between different types of kinesin-related motors*. Molecular Biology of the Cell, 1997. **8**(6): p. 1025-33.

115. Mountain, V., et al., *The kinesin-related protein, HSET, opposes the activity of Eg5 and cross-links microtubules in the mammalian mitotic spindle*. J Cell Biol, 1999. **147**(2): p. 351-66.
116. Yeh, E., et al., *Spindle dynamics and cell cycle regulation of dynein in the budding yeast, Saccharomyces cerevisiae*. J Cell Biol, 1995. **130**(3): p. 687-700.
117. Maliga, Z., T.M. Kapoor, and T.J. Mitchison, *Evidence that monastrol is an allosteric inhibitor of the mitotic kinesin Eg5*. Chem Biol, 2002. **9**(9): p. 989-96.
118. Syrovatkina, V., C. Fu, and P.T. Tran, *Antagonistic spindle motors and MAPs regulate metaphase spindle length and chromosome segregation*. Curr Biol, 2013. **23**(23): p. 2423-9.
119. Sharp, D.J., et al., *Antagonistic microtubule-sliding motors position mitotic centrosomes in Drosophila early embryos*. Nat Cell Biol, 1999. **1**(1): p. 51-4.
120. Rincon, S.A., et al., *Kinesin-5-independent mitotic spindle assembly requires the antiparallel microtubule crosslinker Ase1 in fission yeast*. Nat Commun, 2017. **8**: p. 15286.
121. Yukawa, M., Y. Yamada, and T. Toda, *Suppressor Analysis Uncovers That MAPs and Microtubule Dynamics Balance with the Cut7/Kinesin-5 Motor for Mitotic Spindle Assembly in Schizosaccharomyces pombe*. G3 (Bethesda), 2019. **9**(1): p. 269-280.
122. Toso, A., et al., *Kinetochore-generated pushing forces separate centrosomes during bipolar spindle assembly*. J Cell Biol, 2009. **184**(3): p. 365-72.
123. Yukawa, M., et al., *A microtubule polymerase cooperates with the kinesin-6 motor and a microtubule cross-linker to promote bipolar spindle assembly in the absence of kinesin-5 and kinesin-14 in fission yeast*. Mol Biol Cell, 2017. **28**(25): p. 3647-3659.
124. Syrovatkina, V. and P.T. Tran, *Loss of kinesin-14 results in aneuploidy via kinesin-5-dependent microtubule protrusions leading to chromosome cut*. Nat Commun, 2015. **6**: p. 7322.
125. Yamamoto, A. and Y. Hiraoka, *Cytoplasmic dynein in fungi: insights from nuclear migration*. J Cell Sci, 2003. **116**(Pt 22): p. 4501-12.
126. Moore, J.K., M.D. Stuchell-Brereton, and J.A. Cooper, *Function of dynein in budding yeast: mitotic spindle positioning in a polarized cell*. Cell Motil Cytoskeleton, 2009. **66**(8): p. 546-55.
127. Li, Y., et al., *Kinetochore dynein generates a poleward pulling force to facilitate congression and full chromosome alignment*. Cell Res, 2007. **17**(8): p. 701-12.
128. Tran, P.T., et al., *A mechanism for nuclear positioning in fission yeast based on microtubule pushing*. J Cell Biol, 2001. **153**(2): p. 397-411.
129. Heil-Chapdelaine, R.A., N.K. Tran, and J.A. Cooper, *Dynein-dependent movements of the mitotic spindle in Saccharomyces cerevisiae Do not require filamentous actin*. Mol Biol Cell, 2000. **11**(3): p. 863-72.
130. Martin, R., A. Walther, and J. Wendland, *Deletion of the dynein heavy-chain gene DYN1 leads to aberrant nuclear positioning and defective hyphal development in Candida albicans*. Eukaryot Cell, 2004. **3**(6): p. 1574-88.
131. Liakopoulos, D., et al., *Asymmetric loading of Kar9 onto spindle poles and microtubules ensures proper spindle alignment*. Cell, 2003. **112**(4): p. 561-74.
132. Vaisberg, E.A., M.P. Koonce, and J.R. McIntosh, *Cytoplasmic dynein plays a role in mammalian mitotic spindle formation*. J Cell Biol, 1993. **123**(4): p. 849-58.
133. Robinson, J.T., et al., *Cytoplasmic dynein is required for the nuclear attachment and migration of centrosomes during mitosis in Drosophila*. J Cell Biol, 1999. **146**(3): p. 597-608.
134. Gerson-Gurwitz, A., et al., *Mid-anaphase arrest in S. cerevisiae cells eliminated for the function of Cin8 and dynein*. Cell Mol Life Sci, 2009. **66**(2): p. 301-13.

135. Saunders, W.S., et al., *Saccharomyces cerevisiae kinesin- and dynein-related proteins required for anaphase chromosome segregation*. J Cell Biol, 1995. **128**(4): p. 617-24.
136. Fink, G., et al., *Dynein-mediated pulling forces drive rapid mitotic spindle elongation in Ustilago maydis*. EMBO J, 2006. **25**(20): p. 4897-908.
137. Musacchio, A. and E.D. Salmon, *The spindle-assembly checkpoint in space and time*. Nat Rev Mol Cell Biol, 2007. **8**(5): p. 379-93.
138. Compton, D.A., *Mechanisms of aneuploidy*. Curr Opin Cell Biol, 2011. **23**(1): p. 109-13.
139. Orr, B., K.M. Godek, and D. Compton, *Aneuploidy*. Curr Biol, 2015. **25**(13): p. R538-42.
140. Wenzel, E.S. and A.T.K. Singh, *Cell-cycle Checkpoints and Aneuploidy on the Path to Cancer*. In Vivo, 2018. **32**(1): p. 1-5.
141. Chunduri, N.K. and Z. Storchova, *The diverse consequences of aneuploidy*. Nat Cell Biol, 2019. **21**(1): p. 54-62.
142. Torres, E.M., B.R. Williams, and A. Amon, *Aneuploidy: cells losing their balance*. Genetics, 2008. **179**(2): p. 737-46.
143. Duesberg, P., R. Stindl, and R. Hehlmann, *Origin of multidrug resistance in cells with and without multidrug resistance genes: chromosome reassortments catalyzed by aneuploidy*. Proc Natl Acad Sci U S A, 2001. **98**(20): p. 11283-8.
144. Gordon, D.J., B. Resio, and D. Pellman, *Causes and consequences of aneuploidy in cancer*. Nat Rev Genet, 2012. **13**(3): p. 189-203.
145. Selmecki, A., A. Forche, and J. Berman, *Aneuploidy and isochromosome formation in drug-resistant Candida albicans*. Science, 2006. **313**(5785): p. 367-70.
146. Berman, J., *Ploidy plasticity: a rapid and reversible strategy for adaptation to stress*. FEMS Yeast Res, 2016. **16**(3).
147. Selmecki, A.M., et al., *Polyploidy can drive rapid adaptation in yeast*. Nature, 2015. **519**(7543): p. 349-52.
148. Coste, A., et al., *Genotypic evolution of azole resistance mechanisms in sequential Candida albicans isolates*. Eukaryot Cell, 2007. **6**(10): p. 1889-904.
149. Rosenberg, S.M., *Stress-induced loss of heterozygosity in Candida: a possible missing link in the ability to evolve*. MBio, 2011. **2**(5).
150. Legrand, M., et al., *Candida albicans: An Emerging Yeast Model to Study Eukaryotic Genome Plasticity*. Trends Genet, 2019. **35**(4): p. 292-307.
151. Hose, J., et al., *The genetic basis of aneuploidy tolerance in wild yeast*. Elife, 2020. **9**.
152. Forche, A., et al., *The parasexual cycle in Candida albicans provides an alternative pathway to meiosis for the formation of recombinant strains*. PLoS Biol, 2008. **6**(5): p. e110.
153. Todd, R.T., et al., *Genome plasticity in Candida albicans is driven by long repeat sequences*. Elife, 2019. **8**.
154. Dunn, M.J. and M.Z. Anderson, *To Repeat or Not to Repeat: Repetitive Sequences Regulate Genome Stability in Candida albicans*. Genes (Basel), 2019. **10**(11).
155. Harrison, B.D., et al., *A tetraploid intermediate precedes aneuploid formation in yeasts exposed to fluconazole*. PLoS Biol, 2014. **12**(3): p. e1001815.
156. Magee, B.B. and P.T. Magee, *Induction of mating in Candida albicans by construction of MTL α and MTL α strains*. Science, 2000. **289**(5477): p. 310-3.
157. Bennett, R.J. and A.D. Johnson, *Completion of a parasexual cycle in Candida albicans by induced chromosome loss in tetraploid strains*. EMBO J, 2003. **22**(10): p. 2505-15.
158. Miller, M.G. and A.D. Johnson, *White-opaque switching in Candida albicans is controlled by mating-type locus homeodomain proteins and allows efficient mating*. Cell, 2002. **110**(3): p. 293-302.

159. Shapiro, R.S., N. Robbins, and L.E. Cowen, *Regulatory circuitry governing fungal development, drug resistance, and disease*. Microbiol Mol Biol Rev, 2011. **75**(2): p. 213-67.
160. Tsai, H.J. and A. Nelli, *A Double-Edged Sword: Aneuploidy is a Prevalent Strategy in Fungal Adaptation*. Genes (Basel), 2019. **10**(10).
161. Selmecki, A., et al., *An isochromosome confers drug resistance in vivo by amplification of two genes, ERG11 and TAC1*. Mol Microbiol, 2008. **68**(3): p. 624-41.
162. Perepnikhatka, V., et al., *Specific chromosome alterations in fluconazole-resistant mutants of Candida albicans*. J Bacteriol, 1999. **181**(13): p. 4041-9.
163. Gardner, M.K., et al., *Chromosome congression by Kinesin-5 motor-mediated disassembly of longer kinetochore microtubules*. Cell, 2008. **135**(5): p. 894-906.
164. Maddox, P., et al., *Direct observation of microtubule dynamics at kinetochores in Xenopus extract spindles: implications for spindle mechanics*. J Cell Biol, 2003. **162**(3): p. 377-82.
165. Skibbens, R.V. and E.D. Salmon, *Micromanipulation of chromosomes in mitotic vertebrate tissue cells: tension controls the state of kinetochore movement*. Exp Cell Res, 1997. **235**(2): p. 314-24.
166. Skibbens, R.V., C.L. Rieder, and E.D. Salmon, *Kinetochore motility after severing between sister centromeres using laser microsurgery: evidence that kinetochore directional instability and position is regulated by tension*. J Cell Sci, 1995. **108 (Pt 7)**: p. 2537-48.
167. Chua, P.R., et al., *Effective killing of the human pathogen Candida albicans by a specific inhibitor of non-essential mitotic kinesin Kip1p*. Mol Microbiol, 2007. **65**(2): p. 347-62.
168. Sherwood, R.K. and R.J. Bennett, *Microtubule motor protein Kar3 is required for normal mitotic division and morphogenesis in Candida albicans*. Eukaryot Cell, 2008. **7**(9): p. 1460-74.
169. Roof, D.M., P.B. Meluh, and M.D. Rose, *Kinesin-related proteins required for assembly of the mitotic spindle*. J Cell Biol, 1992. **118**(1): p. 95-108.
170. Heck, M.M., et al., *The kinesin-like protein KLP61F is essential for mitosis in Drosophila*. J Cell Biol, 1993. **123**(3): p. 665-79.
171. Kashina, A.S., et al., *A bipolar kinesin*. Nature, 1996. **379**(6562): p. 270-2.
172. Blangy, A., et al., *Phosphorylation by p34cdc2 regulates spindle association of human Eg5, a kinesin-related motor essential for bipolar spindle formation in vivo*. Cell, 1995. **83**(7): p. 1159-69.
173. Enos, A.P. and N.R. Morris, *Mutation of a Gene That Encodes a Kinesin-Like Protein Blocks Nuclear Division in Aspergillus-Nidulans*. Cell, 1990. **60**(6): p. 1019-1027.
174. Gaglio, T., et al., *Opposing motor activities are required for the organization of the mammalian mitotic spindle pole*. J Cell Biol, 1996. **135**(2): p. 399-414.
175. Geiser, J.R., et al., *Saccharomyces cerevisiae genes required in the absence of the CIN8-encoded spindle motor act in functionally diverse mitotic pathways*. Mol Biol Cell, 1997. **8**(6): p. 1035-50.
176. Hagan, I. and M. Yanagida, *Novel potential mitotic motor protein encoded by the fission yeast cut7+ gene*. Nature, 1990. **347**(6293): p. 563-6.
177. Akera, T., et al., *Mad1 promotes chromosome congression by anchoring a kinesin motor to the kinetochore*. Nat Cell Biol, 2015. **17**(9): p. 1124-33.
178. Fridman, V., et al., *Midzone organization restricts interpolar microtubule plus-end dynamics during spindle elongation*. EMBO Rep, 2009. **10**(4): p. 387-93.
179. Movshovich, N., et al., *Slk19-dependent mid-anaphase pause in kinesin-5-mutated cells*. J Cell Sci, 2008. **121**(Pt 15): p. 2529-39.
180. Yukawa, M., et al., *Kinesin-6 Klp9 plays motor-dependent and -independent roles in collaboration with Kinesin-5 Cut7 and the microtubule crosslinker Ase1 in fission yeast*. Sci Rep, 2019. **9**(1): p. 7336.

181. Manning, B.D., et al., *Differential regulation of the Kar3p kinesin-related protein by two associated proteins, Cik1p and Vik1p*. J Cell Biol, 1999. **144**(6): p. 1219-33.
182. Yukawa, M., et al., *Two spatially distinct kinesin-14 proteins, Pkl1 and Klp2, generate collaborative inward forces against kinesin-5 Cut7 in S. pombe*. J Cell Sci, 2018. **131**(1).
183. Drummond, D.R. and I.M. Hagan, *Mutations in the bimC box of Cut7 indicate divergence of regulation within the bimC family of kinesin related proteins*. J Cell Sci, 1998. **111** (Pt 7): p. 853-65.
184. Hoyt, M.A., *Cellular roles of kinesin and related proteins*. Curr Opin Cell Biol, 1994. **6**(1): p. 63-8.
185. Suzuki, A., et al., *A Kinesin-5, Cin8, Recruits Protein Phosphatase 1 to Kinetochores and Regulates Chromosome Segregation*. Curr Biol, 2018. **28**(17): p. 2697-2704 e3.
186. Akera, T. and Y. Watanabe, *The spindle assembly checkpoint promotes chromosome bi-orientation: A novel Mad1 role in chromosome alignment*. Cell Cycle, 2016. **15**(4): p. 493-7.
187. Segal, E.S., et al., *Gene Essentiality Analyzed by In Vivo Transposon Mutagenesis and Machine Learning in a Stable Haploid Isolate of Candida albicans*. MBio, 2018. **9**(5).
188. Leach, M.D. and L.E. Cowen, *Membrane fluidity and temperature sensing are coupled via circuitry comprised of Ole1, Rsp5, and Hsf1 in Candida albicans*. Eukaryot Cell, 2014. **13**(8): p. 1077-84.
189. Nakayama, H., et al., *Tetracycline-regulatable system to tightly control gene expression in the pathogenic fungus Candida albicans*. Infect Immun, 2000. **68**(12): p. 6712-9.
190. Markus, S.M. and W.L. Lee, *Microtubule-dependent path to the cell cortex for cytoplasmic dynein in mitotic spindle orientation*. Bioarchitecture, 2011. **1**(5): p. 209-215.
191. Carminati, J.L. and T. Stearns, *Microtubules orient the mitotic spindle in yeast through dynein-dependent interactions with the cell cortex*. J Cell Biol, 1997. **138**(3): p. 629-41.
192. Shaw, S.L., et al., *Astral microtubule dynamics in yeast: a microtubule-based searching mechanism for spindle orientation and nuclear migration into the bud*. J Cell Biol, 1997. **139**(4): p. 985-94.
193. Eshel, D., et al., *Cytoplasmic dynein is required for normal nuclear segregation in yeast*. Proc Natl Acad Sci U S A, 1993. **90**(23): p. 11172-6.
194. O'Connell, M.J., et al., *Suppression of the bimC4 mitotic spindle defect by deletion of klpA, a gene encoding a KAR3-related kinesin-like protein in Aspergillus nidulans*. J Cell Biol, 1993. **120**(1): p. 153-62.
195. Pidoux, A.L., M. LeDizet, and W.Z. Cande, *Fission yeast pkl1 is a kinesin-related protein involved in mitotic spindle function*. Mol Biol Cell, 1996. **7**(10): p. 1639-55.
196. Wang, B., et al., *The Aspergillus nidulans bimC4 mutation provides an excellent tool for identification of kinesin-14 inhibitors*. Fungal Genet Biol, 2015. **82**: p. 51-5.
197. Fu, C., et al., *Phospho-regulated interaction between kinesin-6 Klp9p and microtubule bundler Ase1p promotes spindle elongation*. Dev Cell, 2009. **17**(2): p. 257-67.
198. Cole, D.G., et al., *A "slow" homotetrameric kinesin-related motor protein purified from Drosophila embryos*. J Biol Chem, 1994. **269**(37): p. 22913-6.
199. Storchova, Z., et al., *Genome-wide genetic analysis of polyploidy in yeast*. Nature, 2006. **443**(7111): p. 541-7.
200. Truong, T., et al., *Comparative Ploidy Proteomics of Candida albicans Biofilms Unraveled the Role of the AHP1 Gene in the Biofilm Persistence Against Amphotericin B*. Mol Cell Proteomics, 2016. **15**(11): p. 3488-3500.
201. Saunders, A.M., et al., *Kinesin-5 acts as a brake in anaphase spindle elongation*. Curr Biol, 2007. **17**(12): p. R453-4.
202. Finley, K.R., et al., *Dynein-dependent nuclear dynamics affect morphogenesis in Candida albicans by means of the Bub2p spindle checkpoint*. J Cell Sci, 2008. **121**(Pt 4): p. 466-76.

203. Tubman, E., et al., *Kinesin-5 mediated chromosome congression in insect spindles*. Cell Mol Bioeng, 2018. **11**(1): p. 25-36.
204. Barton, N.R., A.J. Pereira, and L.S. Goldstein, *Motor activity and mitotic spindle localization of the Drosophila kinesin-like protein KLP61F*. Mol Biol Cell, 1995. **6**(11): p. 1563-74.
205. Cytrynbaum, E.N., J.M. Scholey, and A. Mogilner, *A force balance model of early spindle pole separation in Drosophila embryos*. Biophys J, 2003. **84**(2 Pt 1): p. 757-69.
206. Brown, A.J., et al., *Stress adaptation in a pathogenic fungus*. J Exp Biol, 2014. **217**(Pt 1): p. 144-55.
207. Forche, A., et al., *Stress alters rates and types of loss of heterozygosity in Candida albicans*. MBio, 2011. **2**(4).
208. Mary, H., et al., *Fission yeast kinesin-8 controls chromosome congression independently of oscillations*. J Cell Sci, 2015. **128**(20): p. 3720-30.
209. Chen, S., et al., *Transient endoreplication down-regulates the kinesin-14 HSET and contributes to genomic instability*. Mol Biol Cell, 2016. **27**(19): p. 2911-23.
210. van Ree, J.H., et al., *Pten regulates spindle pole movement through Dlg1-mediated recruitment of Eg5 to centrosomes*. Nat Cell Biol, 2016. **18**(7): p. 814-21.
211. Nguyen, N., M.M.F. Quail, and A.D. Hernday, *An Efficient, Rapid, and Recyclable System for CRISPR-Mediated Genome Editing in Candida albicans*. Msphere, 2017. **2**(2).
212. Noble, S.M. and A.D. Johnson, *Strains and strategies for large-scale gene deletion studies of the diploid human fungal pathogen Candida albicans*. Eukaryot Cell, 2005. **4**(2): p. 298-309.
213. Murad, A.M., et al., *Cip10, an efficient and convenient integrating vector for Candida albicans*. Yeast, 2000. **16**(4): p. 325-7.
214. Gola, S., et al., *New modules for PCR-based gene targeting in Candida albicans: rapid and efficient gene targeting using 100 bp of flanking homology region*. Yeast, 2003. **20**(16): p. 1339-47.
215. Gerami-Nejad, M., J. Berman, and C.A. Gale, *Cassettes for PCR-mediated construction of green, yellow, and cyan fluorescent protein fusions in Candida albicans*. Yeast, 2001. **18**(9): p. 859-64.
216. Walther, A. and J. Wendland, *An improved transformation protocol for the human fungal pathogen Candida albicans*. Curr Genet, 2003. **42**(6): p. 339-43.
217. Varet, H., et al., *SARTools: A DESeq2- and EdgeR-Based R Pipeline for Comprehensive Differential Analysis of RNA-Seq Data*. PLoS One, 2016. **11**(6): p. e0157022.
218. Benjamini, Y. and Y. Hochberg, *Controlling the False Discovery Rate - a Practical and Powerful Approach to Multiple Testing*. Journal of the Royal Statistical Society Series B-Statistical Methodology, 1995. **57**(1): p. 289-300.
219. Benjamini, Y. and D. Yekutieli, *The control of the false discovery rate in multiple testing under dependency*. Annals of Statistics, 2001. **29**(4): p. 1165-1188.
220. Cheerambathur, D.K., et al., *Quantitative analysis of an anaphase B switch: predicted role for a microtubule catastrophe gradient*. J Cell Biol, 2007. **177**(6): p. 995-1004.
221. Yukawa, M., Y. Teratani, and T. Toda, *How Essential Kinesin-5 Becomes Non-Essential in Fission Yeast: Force Balance and Microtubule Dynamics Matter*. Cells, 2020. **9**(5).
222. Vukusic, K. and I.M. Tolic, *Anaphase B: Long-standing models meet new concepts*. Semin Cell Dev Biol, 2021.
223. Maiato, H. and M. Lince-Faria, *The perpetual movements of anaphase*. Cell Mol Life Sci, 2010. **67**(13): p. 2251-69.
224. Walczak, C.E., S. Cai, and A. Khodjakov, *Mechanisms of chromosome behaviour during mitosis*. Nat Rev Mol Cell Biol, 2010. **11**(2): p. 91-102.

225. McIntosh, J.R., *Motors or dynamics: what really moves chromosomes?* Nat Cell Biol, 2012. **14**(12): p. 1234.
226. Scholey, J.M., G. Civelekoglu-Scholey, and I. Brust-Mascher, *Anaphase B*. Biology (Basel), 2016. **5**(4).
227. Shimamoto, Y., S. Forth, and T.M. Kapoor, *Measuring Pushing and Braking Forces Generated by Ensembles of Kinesin-5 Crosslinking Two Microtubules*. Dev Cell, 2015. **34**(6): p. 669-81.
228. Aist, J.R., et al., *Direct experimental evidence for the existence, structural basis and function of astral forces during anaphase B in vivo*. J Cell Sci, 1991. **100** (Pt 2): p. 279-88.
229. Inoue, S. and E.D. Salmon, *Force generation by microtubule assembly/disassembly in mitosis and related movements*. Mol Biol Cell, 1995. **6**(12): p. 1619-40.
230. Masuda, H. and W.Z. Cande, *The role of tubulin polymerization during spindle elongation in vitro*. Cell, 1987. **49**(2): p. 193-202.
231. Brust-Mascher, I., et al., *Model for anaphase B: role of three mitotic motors in a switch from poleward flux to spindle elongation*. Proc Natl Acad Sci U S A, 2004. **101**(45): p. 15938-43.
232. Tolic-Norrelykke, I.M., et al., *Positioning and elongation of the fission yeast spindle by microtubule-based pushing*. Curr Biol, 2004. **14**(13): p. 1181-6.
233. Avunie-Masala, R., et al., *Phospho-regulation of kinesin-5 during anaphase spindle elongation*. J Cell Sci, 2011. **124**(Pt 6): p. 873-8.
234. Brust-Mascher, I., et al., *Kinesin-5-dependent poleward flux and spindle length control in Drosophila embryo mitosis*. Mol Biol Cell, 2009. **20**(6): p. 1749-62.
235. Hagan, I. and M. Yanagida, *Kinesin-related cut7 protein associates with mitotic and meiotic spindles in fission yeast*. Nature, 1992. **356**(6364): p. 74-6.
236. Grill, S.W., et al., *Polarity controls forces governing asymmetric spindle positioning in the Caenorhabditis elegans embryo*. Nature, 2001. **409**(6820): p. 630-3.
237. Waters, J.C., R.W. Cole, and C.L. Rieder, *The force-producing mechanism for centrosome separation during spindle formation in vertebrates is intrinsic to each aster*. J Cell Biol, 1993. **122**(2): p. 361-72.
238. Aist, J.R. and M.W. Berns, *Mechanics of chromosome separation during mitosis in Fusarium (Fungi imperfecti): new evidence from ultrastructural and laser microbeam experiments*. J Cell Biol, 1981. **91**(2 Pt 1): p. 446-58.
239. Li, Y.Y., et al., *Disruption of mitotic spindle orientation in a yeast dynein mutant*. Proc Natl Acad Sci U S A, 1993. **90**(21): p. 10096-100.
240. Grava, S., et al., *Asymmetric recruitment of dynein to spindle poles and microtubules promotes proper spindle orientation in yeast*. Dev Cell, 2006. **10**(4): p. 425-39.
241. Tame, M.A., et al., *Astral microtubules control redistribution of dynein at the cell cortex to facilitate spindle positioning*. Cell Cycle, 2014. **13**(7): p. 1162-70.
242. Shoukat, I., C. Frazer, and J.S. Allingham, *Kinesin-5 Is Dispensable for Bipolar Spindle Formation and Elongation in Candida albicans, but Simultaneous Loss of Kinesin-14 Activity Is Lethal*. mSphere, 2019. **4**(6).
243. Barral, Y., *Mitosis: FEAR pulls them apart*. Dev Cell, 2004. **6**(5): p. 608-10.
244. Tolic-Norrelykke, I.M., *Push-me-pull-you: how microtubules organize the cell interior*. Eur Biophys J, 2008. **37**(7): p. 1271-8.
245. Drechsler, H. and A.D. McAinsh, *Kinesin-12 motors cooperate to suppress microtubule catastrophes and drive the formation of parallel microtubule bundles*. Proc Natl Acad Sci U S A, 2016. **113**(12): p. E1635-44.

246. van Heesbeen, R.G., M.E. Tanenbaum, and R.H. Medema, *Balanced activity of three mitotic motors is required for bipolar spindle assembly and chromosome segregation*. Cell Rep, 2014. **8**(4): p. 948-56.
247. Li, G. and J.K. Moore, *Microtubule dynamics at low temperature: evidence that tubulin recycling limits assembly*. Mol Biol Cell, 2020. **31**(11): p. 1154-1166.
248. Civelekoglu-Scholey, G. and J.M. Scholey, *Mitotic force generators and chromosome segregation*. Cell Mol Life Sci, 2010. **67**(13): p. 2231-50.
249. Dogterom, M., et al., *Force generation by dynamic microtubules*. Curr Opin Cell Biol, 2005. **17**(1): p. 67-74.
250. Ward, J.J., et al., *Mechanical design principles of a mitotic spindle*. Elife, 2014. **3**: p. e03398.
251. Nislow, C., et al., *A plus-end-directed motor enzyme that moves antiparallel microtubules in vitro localizes to the interzone of mitotic spindles*. Nature, 1992. **359**(6395): p. 543-7.
252. Su, X., et al., *Microtubule-sliding activity of a kinesin-8 promotes spindle assembly and spindle-length control*. Nat Cell Biol, 2013. **15**(8): p. 948-57.
253. Varga, V., et al., *Yeast kinesin-8 depolymerizes microtubules in a length-dependent manner*. Nat Cell Biol, 2006. **8**(9): p. 957-62.
254. Rizk, R.S., et al., *The kinesin-8 Kip3 scales anaphase spindle length by suppression of midzone microtubule polymerization*. J Cell Biol, 2014. **204**(6): p. 965-75.
255. Odds, F.C., *Morphogenesis in Candida albicans*. Crit Rev Microbiol, 1985. **12**(1): p. 45-93.
256. Finley, K.R. and J. Berman, *Microtubules in Candida albicans hyphae drive nuclear dynamics and connect cell cycle progression to morphogenesis*. Eukaryot Cell, 2005. **4**(10): p. 1697-711.
257. Frazer, C., A.D. Hernday, and R.J. Bennett, *Monitoring Phenotypic Switching in Candida albicans and the Use of Next-Gen Fluorescence Reporters*. Curr Protoc Microbiol, 2019. **53**(1): p. e76.
258. Rustchenko, E., *Chromosome instability in Candida albicans*. FEMS Yeast Res, 2007. **7**(1): p. 2-11.
259. Enjalbert, B., et al., *Role of the Hog1 stress-activated protein kinase in the global transcriptional response to stress in the fungal pathogen Candida albicans*. Mol Biol Cell, 2006. **17**(2): p. 1018-32.
260. Enjalbert, B., A. Nantel, and M. Whiteway, *Stress-induced gene expression in Candida albicans: absence of a general stress response*. Mol Biol Cell, 2003. **14**(4): p. 1460-7.
261. Hromatka, B.S., S.M. Noble, and A.D. Johnson, *Transcriptional response of Candida albicans to nitric oxide and the role of the YHB1 gene in nitrosative stress and virulence*. Mol Biol Cell, 2005. **16**(10): p. 4814-26.
262. Bennett, R.J., A. Forche, and J. Berman, *Rapid mechanisms for generating genome diversity: whole ploidy shifts, aneuploidy, and loss of heterozygosity*. Cold Spring Harb Perspect Med, 2014. **4**(10).
263. Lephart, P.R. and P.T. Magee, *Effect of the major repeat sequence on mitotic recombination in Candida albicans*. Genetics, 2006. **174**(4): p. 1737-44.
264. Polakova, S., et al., *Formation of new chromosomes as a virulence mechanism in yeast Candida glabrata*. Proc Natl Acad Sci U S A, 2009. **106**(8): p. 2688-93.
265. Hu, G., et al., *Comparative hybridization reveals extensive genome variation in the AIDS-associated pathogen Cryptococcus neoformans*. Genome Biol, 2008. **9**(2): p. R41.
266. Rancati, G., et al., *Aneuploidy underlies rapid adaptive evolution of yeast cells deprived of a conserved cytokinesis motor*. Cell, 2008. **135**(5): p. 879-93.
267. Rosenberg, A., et al., *Antifungal tolerance is a subpopulation effect distinct from resistance and is associated with persistent candidemia*. Nat Commun, 2018. **9**(1): p. 2470.

268. Cowen, L.E. and S. Lindquist, *Hsp90 potentiates the rapid evolution of new traits: drug resistance in diverse fungi*. *Science*, 2005. **309**(5744): p. 2185-9.
269. Cowen, L.E., et al., *Genetic architecture of Hsp90-dependent drug resistance*. *Eukaryot Cell*, 2006. **5**(12): p. 2184-8.
270. Eudey, T.L., *Statistical considerations in DNA flow cytometry*. *Statistical Science*, 1996. **11**(4): p. 320-334, 15.
271. Liang, S.H. and R.J. Bennett, *The Impact of Gene Dosage and Heterozygosity on The Diploid Pathobiont Candida albicans*. *J Fungi (Basel)*, 2019. **6**(1).
272. Nishimoto, A.T., C. Sharma, and P.D. Rogers, *Molecular and genetic basis of azole antifungal resistance in the opportunistic pathogenic fungus Candida albicans*. *J Antimicrob Chemother*, 2020. **75**(2): p. 257-270.
273. Todd, R.T. and A. Selmecki, *Expandable and reversible copy number amplification drives rapid adaptation to antifungal drugs*. *Elife*, 2020. **9**.
274. Pavelka, N., et al., *Aneuploidy confers quantitative proteome changes and phenotypic variation in budding yeast*. *Nature*, 2010. **468**(7321): p. 321-5.
275. Livak, K.J. and T.D. Schmittgen, *Analysis of relative gene expression data using real-time quantitative PCR and the 2(-Delta Delta C(T)) Method*. *Methods*, 2001. **25**(4): p. 402-8.
276. Zack, T.I., et al., *Pan-cancer patterns of somatic copy number alteration*. *Nat Genet*, 2013. **45**(10): p. 1134-40.
277. Dewhurst, S.M., et al., *Tolerance of whole-genome doubling propagates chromosomal instability and accelerates cancer genome evolution*. *Cancer Discov*, 2014. **4**(2): p. 175-185.
278. Vitale, I., et al., *Multipolar mitosis of tetraploid cells: inhibition by p53 and dependency on Mos*. *EMBO J*, 2010. **29**(7): p. 1272-84.
279. Ganem, N.J., S.A. Godinho, and D. Pellman, *A mechanism linking extra centrosomes to chromosomal instability*. *Nature*, 2009. **460**(7252): p. 278-82.
280. Shu, S., et al., *The balance of forces generated by kinesins controls spindle polarity and chromosomal heterogeneity in tetraploid cells*. *J Cell Sci*, 2019. **132**(24).
281. Kelly, S.L., et al., *Benzo(a)pyrene hydroxylase activity in yeast is mediated by P450 other than sterol 14 alpha-demethylase*. *Biochem Biophys Res Commun*, 1993. **197**(2): p. 428-32.
282. Kelly, D.E., D.C. Lamb, and S.L. Kelly, *Genome-wide generation of yeast gene deletion strains*. *Comp Funct Genomics*, 2001. **2**(4): p. 236-42.
283. Morschhauser, J., *The genetic basis of fluconazole resistance development in Candida albicans*. *Biochim Biophys Acta*, 2002. **1587**(2-3): p. 240-8.
284. Euskirchen, G.M., *Nnf1p, Dsn1p, Mtw1p, and Nsl1p: a new group of proteins important for chromosome segregation in Saccharomyces cerevisiae*. *Eukaryot Cell*, 2002. **1**(2): p. 229-40.
285. Costanzo, M., et al., *A global genetic interaction network maps a wiring diagram of cellular function*. *Science*, 2016. **353**(6306).
286. Sullivan, M. and F. Uhlmann, *A non-proteolytic function of separase links the onset of anaphase to mitotic exit*. *Nat Cell Biol*, 2003. **5**(3): p. 249-54.
287. D'Amours, D., F. Stegmeier, and A. Amon, *Cdc14 and condensin control the dissolution of cohesin-independent chromosome linkages at repeated DNA*. *Cell*, 2004. **117**(4): p. 455-69.
288. Gordon, O., et al., *Nud1p, the yeast homolog of Centriolin, regulates spindle pole body inheritance in meiosis*. *EMBO J*, 2006. **25**(16): p. 3856-68.
289. Sullivan, M., L. Holt, and D.O. Morgan, *Cyclin-specific control of ribosomal DNA segregation*. *Mol Cell Biol*, 2008. **28**(17): p. 5328-36.

290. Ibarlucea-Benitez, I., et al., *Kinesins relocate the chromosomal passenger complex to the midzone for spindle disassembly*. J Cell Biol, 2018. **217**(5): p. 1687-1700.
291. Carmena, M., et al., *The chromosomal passenger complex (CPC): from easy rider to the godfather of mitosis*. Nat Rev Mol Cell Biol, 2012. **13**(12): p. 789-803.
292. Carmena, M., *A mitosis-specific AMPK trimer?* Cell Cycle, 2012. **11**(7): p. 1269.
293. van der Horst, A. and S.M. Lens, *Cell division: control of the chromosomal passenger complex in time and space*. Chromosoma, 2014. **123**(1-2): p. 25-42.
294. Orellana-Munoz, S., et al., *The anillin-related Int1 protein and the Sep7 septin collaborate to maintain cellular ploidy in Candida albicans*. Sci Rep, 2018. **8**(1): p. 2257.
295. Lammers, L.G. and S.M. Markus, *The dynein cortical anchor Num1 activates dynein motility by relieving Pac1/LIS1-mediated inhibition*. J Cell Biol, 2015. **211**(2): p. 309-22.
296. Markus, S.M., K.A. Kalutkiewicz, and W.L. Lee, *Astral microtubule asymmetry provides directional cues for spindle positioning in budding yeast*. Exp Cell Res, 2012. **318**(12): p. 1400-6.
297. Bertazzi, D.T., B. Kurtulmus, and G. Pereira, *The cortical protein Lte1 promotes mitotic exit by inhibiting the spindle position checkpoint kinase Kin4*. J Cell Biol, 2011. **193**(6): p. 1033-48.
298. Edzuka, T. and G. Goshima, *Drosophila kinesin-8 stabilizes the kinetochore-microtubule interaction*. J Cell Biol, 2019. **218**(2): p. 474-488.
299. Middleton, K. and J. Carbon, *KAR3-encoded kinesin is a minus-end-directed motor that functions with centromere binding proteins (CBF3) on an in vitro yeast kinetochore*. Proc Natl Acad Sci U S A, 1994. **91**(15): p. 7212-6.
300. Liu, H., et al., *The coordination of centromere replication, spindle formation, and kinetochore-microtubule interaction in budding yeast*. PLoS Genet, 2008. **4**(11): p. e1000262.
301. Zheng, F., et al., *Klp2 and Ase1 synergize to maintain meiotic spindle stability during metaphase I*. J Biol Chem, 2020. **295**(38): p. 13287-13298.
302. Kozgunova, E., M. Nishina, and G. Goshima, *Kinetochore protein depletion underlies cytokinesis failure and somatic polyploidization in the moss Physcomitrella patens*. Elife, 2019. **8**.
303. Kumar, R., *Separase: Function Beyond Cohesion Cleavage and an Emerging Oncogene*. J Cell Biochem, 2017. **118**(6): p. 1283-1299.
304. Rahal, R. and A. Amon, *The Polo-like kinase Cdc5 interacts with FEAR network components and Cdc14*. Cell Cycle, 2008. **7**(20): p. 3262-72.
305. Uhlmann, F., et al., *Cleavage of cohesin by the CD clan protease separin triggers anaphase in yeast*. Cell, 2000. **103**(3): p. 375-86.
306. Sparapani, S. and C. Bachewich, *Characterization of a novel separase-interacting protein and candidate new securin, Eip1p, in the fungal pathogen Candida albicans*. Mol Biol Cell, 2019. **30**(19): p. 2469-2489.
307. Baum, P., et al., *A yeast gene essential for regulation of spindle pole duplication*. Mol Cell Biol, 1988. **8**(12): p. 5386-97.
308. McGrew, J.T., et al., *Requirement for ESP1 in the nuclear division of Saccharomyces cerevisiae*. Mol Biol Cell, 1992. **3**(12): p. 1443-54.
309. Abarbanel, J., et al., *Cytogenetic studies in patients with gastric cancer*. World J Surg, 1991. **15**(6): p. 778-82.
310. Tsushima, K., et al., *Correlation of DNA ploidy, histopathology, stage and clinical outcome in gastric carcinoma*. Surg Oncol, 1992. **1**(1): p. 17-25.
311. Daigo, K., et al., *Characterization of KIF11 as a novel prognostic biomarker and therapeutic target for oral cancer*. Int J Oncol, 2018. **52**(1): p. 155-165.

312. Jin, Q., et al., *High Eg5 expression predicts poor prognosis in breast cancer*. *Oncotarget*, 2017. **8**(37): p. 62208-62216.
313. Fisher, R., L. Pusztai, and C. Swanton, *Cancer heterogeneity: implications for targeted therapeutics*. *Br J Cancer*, 2013. **108**(3): p. 479-85.
314. Heng, H.H., et al., *Chromosomal instability (CIN): what it is and why it is crucial to cancer evolution*. *Cancer Metastasis Rev*, 2013. **32**(3-4): p. 325-40.
315. Bouge, A.L. and M.L. Parmentier, *Tau excess impairs mitosis and kinesin-5 function, leading to aneuploidy and cell death*. *Dis Model Mech*, 2016. **9**(3): p. 307-19.
316. Hoffman, C.S., *Preparation of yeast DNA*. *Current protocols in molecular biology* / edited by Frederick M. Ausubel ... [et al.], 2001. **Chapter 13**: p. Unit13 11.
317. Mitchison, T.J., et al., *Roles of polymerization dynamics, opposed motors, and a tensile element in governing the length of Xenopus extract meiotic spindles*. *Mol Biol Cell*, 2005. **16**(6): p. 3064-76.
318. Neahring, L., N.H. Cho, and S. Dumont, *Opposing motors provide mechanical and functional robustness in the human spindle*. *Dev Cell*, 2021.
319. Oriola, D., F. Julicher, and J. Bruges, *Active forces shape the metaphase spindle through a mechanical instability*. *Proc Natl Acad Sci U S A*, 2020. **117**(28): p. 16154-16159.
320. Bruges, J. and D. Needleman, *Physical basis of spindle self-organization*. *Proc Natl Acad Sci U S A*, 2014. **111**(52): p. 18496-500.
321. Khodjakov, A., S. La Terra, and F. Chang, *Laser microsurgery in fission yeast; role of the mitotic spindle midzone in anaphase B*. *Curr Biol*, 2004. **14**(15): p. 1330-40.
322. Straube, A., I. Weber, and G. Steinberg, *A novel mechanism of nuclear envelope breakdown in a fungus: nuclear migration strips off the envelope*. *EMBO J*, 2005. **24**(9): p. 1674-85.
323. Normand, G. and R.W. King, *Understanding cytokinesis failure*. *Adv Exp Med Biol*, 2010. **676**: p. 27-55.
324. Zimniak, T., et al., *Phosphoregulation of the budding yeast EBI homologue Bim1p by Aurora/Ipl1p*. *J Cell Biol*, 2009. **186**(3): p. 379-91.
325. Woodruff, J.B., D.G. Drubin, and G. Barnes, *Mitotic spindle disassembly occurs via distinct subprocesses driven by the anaphase-promoting complex, Aurora B kinase, and kinesin-8*. *J Cell Biol*, 2010. **191**(4): p. 795-808.
326. Campbell, I.W., X. Zhou, and A. Amon, *The Mitotic Exit Network integrates temporal and spatial signals by distributing regulation across multiple components*. *Elife*, 2019. **8**.
327. Jaspersen, S.L., et al., *A late mitotic regulatory network controlling cyclin destruction in Saccharomyces cerevisiae*. *Mol Biol Cell*, 1998. **9**(10): p. 2803-17.
328. Visintin, R., et al., *The phosphatase Cdc14 triggers mitotic exit by reversal of Cdk-dependent phosphorylation*. *Mol Cell*, 1998. **2**(6): p. 709-18.
329. Chowdhary, A., A. Voss, and J.F. Meis, *Multidrug-resistant Candida auris: 'new kid on the block' in hospital-associated infections?* *J Hosp Infect*, 2016. **94**(3): p. 209-212.
330. Bing, J., et al., *Experimental Evolution Identifies Adaptive Aneuploidy as a Mechanism of Fluconazole Resistance in Candida auris*. *Antimicrob Agents Chemother*, 2020. **65**(1).
331. Pianalto, K.M. and J.A. Alspaugh, *New Horizons in Antifungal Therapy*. *J Fungi (Basel)*, 2016. **2**(4).
332. Robbins, N., T. Caplan, and L.E. Cowen, *Molecular Evolution of Antifungal Drug Resistance*. *Annu Rev Microbiol*, 2017. **71**: p. 753-775.